12-9-2013 12:00 AM

Regulation of eukaryotic Mcm2-7 activity

Lance F. DaSilva
The University of Western Ontario

Supervisor
Dr. David Edgell
The University of Western Ontario

Graduate Program in Biochemistry
A thesis submitted in partial fulfillment of the requirements for the degree in Doctor of Philosophy
© Lance F. DaSilva 2013

Recommended Citation

REGULATION OF EUKARYOTIC MCM2-7 ACTIVITY

(Thesis format: Integrated Article)

by

Lance F. DaSilva

Graduate Program in Biochemistry

A thesis submitted in partial fulfillment
of the requirements for the degree of
Doctor of Philosophy

The School of Graduate and Postdoctoral Studies
The University of Western Ontario
London, Ontario, Canada

© Lance F. DaSilva 2013

Abstract

The transfer of genetic material from one cell generation to the next requires precise genome duplication. Aberrant DNA replication can lead to genomic instability and contribute to diseases arising from an unregulated cell cycle, such as cancer. Replicative DNA polymerases require a single-stranded (ssDNA) template from which to produce newly synthesized DNA. In eukaryotes, ssDNA is generated by the heterohexameric minichromosome maintenance 2 through 7 (Mcm2-7) replicative helicase that unwinds duplex DNA. Strict temporal separation of helicase loading and activation at multiple replication origins ensures once per cell cycle replication. The processes involved in activating Mcm2-7 to unwind DNA during S phase are poorly understood. Through *in vivo* and *in vitro* analyses, the current study examines the factors involved in modulating *S. cerevisiae* Mcm2-7 activity.

Mec1, a member of the PIKK (phosphoinositide three-kinase-related kinase) family of proteins, is involved in the response to replicative stress and DNA damage. It also plays a role during an unperturbed cell cycle and is required to phosphorylate Mcm2-7 prior to helicase activation. We characterized alleles of *S. cerevisiae mec1* that alter the conserved FATC domain. Mutants of Mec1 resulted in temperature sensitive growth, sensitivity to hydroxyurea and reduced kinase activity *in vitro*. These mutants were also less stable than wild-type Mec1 and demonstrated reduced nuclear localization. We also identified *rpn3-L140P*, which encodes a component of the 19S proteasomal regulatory particle of the 26S proteasome, as a suppressor of the temperature-sensitive growth caused by *mec1-W2368A*.

As Cdt1 is required for the nuclear import and origin loading of Mcm2-7, we also sought to investigate the interaction between these two components in more detail. Using reconstituted Mcm2-7•Cdt1 complexes from bacterial-expressed proteins, we demonstrated that these complexes exhibit lower ATPase and helicase activity than Mcm2-7. We also showed that Mcm2-7 dissociates into subcomplexes, and that Mcm3, 5 and 7 bound origins in the absence of Cdt1. We propose that the reduced ATPase activity of Mcm2-7 by Cdt1 binding is induced by structural changes in the Mcm2-7 ring. We also suggest that Cdt1 helps to stabilize the Mcm2-7 hexamer.

To investigate the role of phosphorylation on Mcm2-7, we utilized a phosphomimetic mutant of Mcm4 that when incorporated into Mcm2-7 can bypass the requirement for DDK. While phosphomimetic Mcm4 demonstrated slightly lower ATPase activity than the wildtype protein, phosphomimetic Mcm2-7 complexes exhibited wildtype ATPase, helicase and DNA binding activity.

Taken together, our work identifies the functional role of the C-terminal residues of Mec1 and the protein's turnover by the proteosome. Our studies also provide new insights into the factors and processes involved in the activation of Mcm2-7 to unwind DNA.

Keywords

Co-Authorship Statement

In regards to the work presented in Chapter 2:

DaSilva, L.F., Pillon, S., Genereaux, J., Davey, MJ., Gloor, G.B., Karagiannis, J., and Brandl, C.J. The C-terminal residues of *Saccharomyces cerevisiae* Mec1 are required for its Localization, Stability and Function. *G3: Genes, Genomes, Genetics* 3(10): 1661-74 (2013)

L.F. DaSilva contributed to experimental design, performed experiments for Figures 2.1, 2.4, 2.5, 2.6, 2.7, 2.8, 2.9, 2.10 and wrote the manuscript with C. Brandl. S. Pillon and G. Gloor performed the genomic sequence analysis of suppressor strains and wrote the Perl script to identify polymorphisms in these strains. J. Genereaux contributed to experiments for Figures 2.2, 2.3 and 2.6. M.J. Davey contributed to experimental design and contributed to experiments for Figure 2.3. J. Karagiannis performed experiments for Figure 2.6. C.J. Brandl contributed to experimental design, and performed tetrad dissection to generate yeast strains.

In regards to the work presented in Chapter 3:

DaSilva, L.F., Kolaczyk, T., M., Langston, L., O'Donnell, M., Davey, M.J. and Edgell, D.R. Modulation of Mcm2-7 activity by Cdt1. Manuscript in preparation.

L.F. DaSilva contributed to experimental design, performed experiments for Figures 3.1, 3.2, 3.3, 3.4, 3.5, 3.6, 3.7, 3.8, 3.9 and 3.11, and wrote the manuscript with M.J. Davey. T. Kolaczyk contributed to experimental design, purified proteins and complexes and performed experiments for Figure 3.1, 3.2 and 3.4. L. Langston contributed to experimental design and performed the experiment for Figure 3.10. M. O'Donnell contributed to experimental design. M.J. Davey and D.R. Edgell supervised L.F. DaSilva during his thesis.

In regards to the work presented in Chapter 4:

DaSilva, L.F., Stead, B.E. and Davey, M.J. Investigating the role of phosphorylation on Mcm2-7 activity. Manuscript in preparation.

L.F. DaSilva contributed to experimental design, performed experiments for Figures 4.2, 4.3, 4.4, 4.5, 4.6, 4.7, and wrote the manuscript. B.E. Stead created the *mcm4pm* yeast strain and performed experiment for Figure 4.1. M.J. Davey contributed to experimental design and supervised L.F. DaSilva during his thesis.

Acknowledgments

A great deal of gratitude goes out to my late supervisor, Dr. Megan J. Davey, for her guidance and support throughout my PhD studies. I truly appreciated our many discussions and the encouragement you provided when my research seemed to be moving at a snail's pace.

I would also like to thank Dr. D.R. Edgell for his guidance and support. He played an invaluable role as both my supervisory committee member and also as my supervisor throughout my PhD studies.

I would also like to thank my supervisory committee members, Dr. Eric Ball and Dr. Chris Brandl for helpful discussions and suggestions during my PhD research.

Throughout my studies, I have had the pleasure to work and converse with many excellent colleagues. In particular, I thank Brent Stead, Tom Kolaczyk and Simon Lam for helpful discussions and insight. I would also like to thank Xiaoli Ma for her technical expertise throughout my PhD studies. I also thank my colleagues in the Edgell lab for their support.

I also thank Dr. Lance Langston and Dr. Mike O'Donnell from The Rockefeller University for reagents and helpful discussions and suggestions.

A tremendous amount of appreciation goes out to Dr. Dave Litchfield and Dr. Dave Edgell for their help and support following the loss of my mentor. I would also like to thank the numerous faculty, administrative and support staff in the Department of Biochemistry for creating an inspiring and collegial training environment.

I thank my parents for helping me to realize my true potential and encouraging me throughout my graduate studies.

I am especially thankful to my beautiful wife Darah and my sweet daughter Violet. You are my life and my inspiration.

Table of Contents

List of Tables

List of Figures

List of Abbreviations

AAA+   ATPases associated with a variety of cellular activities

ACL   Allosteric communication loop

APC/C   Anaphase promoting complex/cyclosome

ARS   Autonomously replicating sequence

ATM   Ataxia telangiectasia mutated

ATP   Adenosine triphosphate

ATPγS   Adenosine 5'-[γ-thio] triphosphate

ATR   Ataxia telangiectasia and Rad3-related

bp   Base pair

bob1   Bypass of block 1

BRCT   BRCA1 C-terminus

BSA   Bovine serum albumin

CBB   Coomassie brilliant blue

CDK   Cyclin-dependent kinase

Cdc   cell division cycle

Cdt1   Cdc10-dependent transcript 1

CEN   Centromeric

Chk1   Checkpoint kinase 1

Ci   Curie

CK2	Casein kinase 2
CMG	Cdc45/Mcm2-7/GINS complex
Csm3	Chromosome segregation in meiosis 3
Ctf4	Chromosome transmission fidelity 4
Dbf4	Dumbbell former 4
DDD	DDK docking domain
DDK	Dbf4-dependent kinase; Cdc7/Dbf4
DDK	DNA damage response
DNA	Deoxyribonucleic acid
DNA-PKcs	DNA-dependent protein kinase, catalytic subunit
dNTP	Deoxyribonucleotide triphosphate
Dpb11	DNA polymerase B 11
dsDNA	double-stranded DNA
dT	deoxythymidylates
DTT	Dithiothreitol
EDTA	Ethylenediaminetetraacetic acid
eGFP	Enhanced green fluorescent protein
EMSA	Electrophoretic mobility shift assay
EXT	Exterior
FACT	Facilitates chromatin transcription

FAT	FRAP-ATM-TRRAP
FATC	FAT C-terminal
FPLC	Fast protein liquid chromatography
H2i	Helix 2 insert
HAT	Histone acetyltransferase
HEAT	Huntington, Elongation Factor 3, PR65/A, TOR
HEPES	4-(2-hydroxyethyl)-1-piperazineethanesulfonic acid
G1	Gap 1
G1-CDK	Gap 1-specific Cyclin-dependent kinase
G2	Gap 2
GINS	Go Ichi Ni San; Five, one, two and three, in Japanese
HU	Hydroxyurea
Ies4	Ino80 subunit 4
Ino80	Inositol requiring 80
kD	Kilodalton
Lcd1	Lethal, checkpoint-defective, DNA damage sensitive 1
M	Mitosis phase
Mcm	Minichromosome maintenance
Mcm-BP	Minichromosome maintenance-binding protein
Mec1	Mitosis entry checkpoint 1

Mrc1	Mediator of the replication checkpoint 1
mTOR	mammalian target of rapamycin
Nic96	Nucleoporin-interacting component of 96 kDa
NP-40	Nonyl phenoxypolyethoxylethanol
NSD	N-terminal serine/threonine-rich domain
NT	N-terminal
NTP	Nucleotide triphosphate
ORC	Origin recognition complex
P-loop	Phosphate-binding loop
PAGE	Polyacrylamide gel electrophoresis
PCR	Polymerase chain reaction
PEG	Polyethylene glycol
PI3K	Phosphatidylinositol 3-kinase
PIKK	Phosphoinositide three-kinase related kinase
PKA	Protein kinase A
PM	Phosphomimetic
PRD	PIKK regulatory domain
Pre-IC	Pre-initiation complex
Pre-RC	Pre-replicative complex
PS1	Pre-sensor 1

PVDF	Polyvinylidene fluoride
Rad53	Radiation sensitive 53
RFP	Red fluorescent protein
Rnr	Ribonucleotide reductase
RPA	Replication protein A
Rpn3	Regulatory particle non-ATPase 3
Rpt	Regulatory Particle Triple-A
S	Synthesis phase
SI	Sensor I
SII	Sensor II
SAGA	Spt-Ada-Gcn5 Acetyltransferase
SC	Synthetic complete media
S-CDK	S-phase-specific Cyclin-dependent kinase
SDS	Sodium dodecyl sulfate
Sld	Synthetically lethal with *dpb11-1*
SMG-1	Suppressor with morphological effect on genitalia family member 1
Sml1	Suppressor of Mec1 lethality
ssDNA	Single-stranded DNA
TDP-43	Transactive response DNA binding protein 43 kDa
TLC	Thin layer chromatography

Tof1	Topoisomerase I-interacting factor
TOR	Target of rapamycin
TORC	TOR complex
TPR	Tetratricopeptide repeats
Tris	Tris(hydroxymethyl)aminomethane
TRRAP	Transformation/transcription domain-associated protein
Tti	Two Tel2-interacting protein
TTT	Tel2, Tti1 and Tti2 complex
UV	Ultraviolet
WH	Winged-helix
YPD	Yeast extract, peptone, dextrose; non-selective yeast growth medium

Chapter 1

1 Introduction

1.1 DNA replication in eukaryotes

The fidelity of DNA replication is essential to the maintenance of the genetic integrity of all organisms. Errors during DNA replication can lead to genomic instability, and contribute to disease processes such as cancer [1]. The initiation of DNA replication is a multifaceted and dynamic process initiated at hundreds, if not thousands, of discrete sites along DNA called origins of replication [2-4]. Eukaryotic organisms have developed highly conserved and tightly controlled mechanisms to ensure that DNA replication occurs once and only once from each origin of replication per cell division cycle. Fundamental to this control is the stringent temporal separation of replicative DNA helicase loading and DNA unwinding. A key factor during DNA replication, the minichromosome maintenance 2 through 7 (Mcm2-7) replicative DNA helicase is loaded onto origin DNA in late M and early G1 phases, but no unwinding occurs. In a poorly understood manner, Mcm2-7 is activated to unwind duplex DNA during S phase to permit DNA polymerases to use the separated strands as templates for newly synthesized DNA (Figure 1.1) [5-7]. The current study explores the protein factors and the cell cycle signals that dictate the timing of DNA unwinding by Mcm2-7. This knowledge will contribute significantly toward understanding the fundamental process of DNA replication which is of great importance to studying diseases caused by an unregulated cell cycle.

Much of our knowledge of eukaryotic DNA replication comes from studies on the model organism *Saccharomyces cerevisiae*. During G1 phase of the cell cycle, origin sequences direct the assembly of multiprotein complexes that ultimately create replication forks with opposite polarity at each origin [2, 6, 8]. While origins in most eukaryotes lack any consensus, those of *S. cerevisiae* are the best characterized [9-12]. In *S. cerevisiae*, the *cis*-acting DNA replication elements are known as autonomous replicating sequences (ARS) and were initially identified by their ability to promote stable transformation and the autonomous replication of plasmid DNA in yeast [13-18]. A
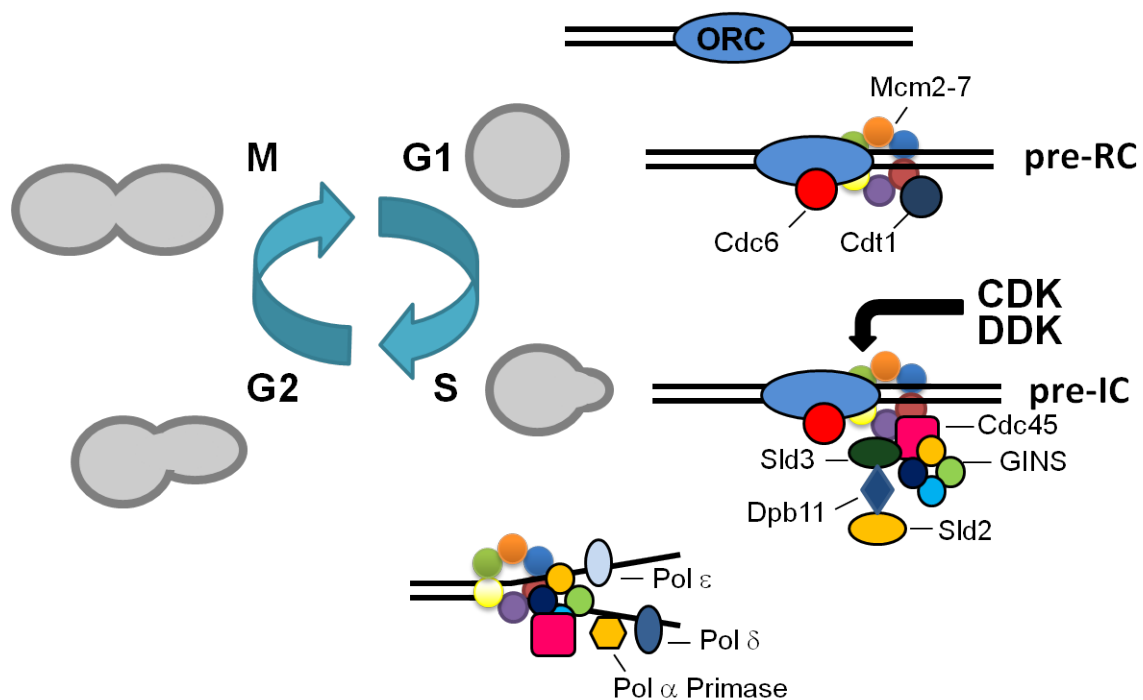
Figure 1.1: DNA replication is regulated with respect to the cell cycle

During the G1 phase, Mcm2-7 is loaded as a double hexamer onto origins in a Cdt1-dependent manner. Origins are licensed for DNA replication, but Mcm2-7 remains inactive in the pre-RC. In S phase, activation and conversion of the pre-RC to the pre-IC occurs from the collective action of CDK and DDK and the recruitment of other factors. DDK phosphorylates the N-terminal tails of Mcm2, 4 and 6. DDK is required for the early-firing origin recruitment of Sld3 and Cdc45 before S-CDK activity. S-CDK phosphorylates Sld2 and Sld3 which are bridged by Dpb11, and this in turn promotes the recruitment of GINS and DNA polymerase ε to origins. Together with Cdc45 and GINS, Mcm2-7 acts as the core in a large and stable CMG helicase complex to unwind duplex DNA. Priming of leading and lagging strands is carried out by DNA polymerase α. Ultimately, leading and lagging strand DNA synthesis is performed by DNA polymerase ε and δ, respectively. Adapted from 2, 6, 19, 20.

conserved eukaryotic initiator complex known as the origin recognition complex (ORC) binds these origins of replication [8, 21]. ORC is comprised of six subunits that together with Cdc6 and Cdt1, loads the replicative DNA helicase, consisting of a complex of the minichromosome maintenance 2 through 7 (Mcm2-7) proteins, into the pre-replicative complex (pre-RC) at the origin [6, 22-26] (Figure 1.1). At this stage, origins are said to be "licensed" or poised for DNA replication, but Mcm2-7 is inactive in the pre-RC. The loading of Mcm2-7 can only occur during G1 phase when cyclin-dependent kinase (CDK) activity is low and anaphase promoting complex/cyclosome (APC/C) activity is high [27-30]. In budding yeast, CDK activity prevents Mcm2-7 loading by phosphorylating and inhibiting each pre-RC component, thereby limiting DNA replication to once per cell cycle [31-36]. The pre-RC is activated and converted to a pre-initiation complex (pre-IC) in S phase by the combined action of two protein kinases, CDK and the Dbf4-dependent kinase (DDK), and the recruitment of other factors [19, 37-43]. After Mcm2-7 is loaded, DDK is required for the recruitment of Cdc45 and Sld3 to early-firing origins before S-phase-specific CDK (S-CDK) activity. After S-CDK activation, GINS, Sld2, Dpb11 and DNA polymerase ε (Pol ε) are recruited to the origin [20].

While the Mcm2-7 helicase is the major target of DDK (discussed below), the key targets of CDK during initiation of replication in budding yeast are factors required specifically for initiation, but which are not incorporated into the replisome [44, 45]. CDK phosphorylates Sld2 and Sld3, which in turn, promotes their association with Dpb11 [46, 47]. All groups of eukaryotes possess a single ortholog of Dbp11 that is essential for the initiation of DNA replication [48]. These orthologs contain a series of BRCT repeats which act as phosphoprotein-binding elements [49, 50]. The N-terminal pair of BRCT repeats of Dpb11 binds Sld3, whereas the C-terminal pair binds Sld2 [51-53]. Studies suggest that Sld3 associates with some factors at origins (possibly Mcm2-7) and helps recruit the replication factor Cdc45, while Dbp11 bridges phosphorylated Sld3 to phosphorylated Sld2 and recruits DNA Pol ε and the tetrameric GINS complex to origins [38, 52, 54, 55]. These events lead to the stable association of a large helicase complex consisting of Cdc45, Mcm2-7 and GINS (CMG). Activation of Mcm2-7 throughout S phase ultimately

unwinds the origin and enables the priming of leading and lagging strands by DNA polymerase ε.

1.2 Mechanisms of Mcm2-7 activity

Replicative DNA polymerases require a single-stranded DNA (ssDNA) template, but several lack the ability to unwind double-stranded DNA (dsDNA) [56]. In this regard, ssDNA is generated by a DNA helicase, a molecular motor enzyme that uses NTP-dependent conformational changes to unwind duplex DNA. All helicases share at least three common biochemical properties: (i) nucleic acid binding; (ii) NTP/dNTP binding and hydrolysis; and (iii) NTP/dNTP hydrolysis-dependent unwinding of duplex nucleic acids in a 3' to 5' or 5' to 3' direction (reviewed in 39, 57). Mcm2-7 complexes are toroidal in shape and are broadly distributed along chromatin [58, 59]. Mcm2-7 is chromatin-bound in G1 phase, displaced from origins in S phase as it translocates ahead of the replication fork, and absent from chromatin in G2 phase [60]. A new round of Mcm2-7 origin loading occurs at the end of mitosis [61]. As mentioned above, Mcm2-7 loading into the pre-RC at origins of replication depends on the concerted effort of ORC, Cdc6 and Cdt1 [23, 24, 26].

1.2.1 Identification of MCM proteins

MCM proteins were first identified in *S. cerevisiae* as mutants defective in the maintenance of circular minichromosomes [62]. Mcm subunits are members of the AAA+ (ATPases associated with various cellular activities) superfamily [63]. Mcm2-7 complexes bind and hydrolyze ATP to unwind dsDNA, a feature common to all AAA+ proteins. In this case, the energy produced from ATP hydrolysis is transferred from the AAA+ helicase motor to the central channel of the Mcm2-7 complex to facilitate translocation and unwinding of duplex DNA ahead of the replication fork [64-66]. Deletion of any of the *MCM* genes is lethal in *S. cerevisiae* and *Schizosaccharomyces pombe*. The six Mcm proteins are paralogs, as they share considerable sequence similarity with one another, particularly within a 200-250 amino acid core region that encodes the ATPase active site, or AAA+ domain (reviewed in 58, 67, 68). Mcm2-7 predominantly exists as a heterohexamer, but when not functioning as the replicative DNA helicase, can exist as

trimers, dimers and monomers [69-71]. Studies in the fission yeast *Schizosaccharomyces pombe* revealed that purified Mcm2-7 complexes were toroidal in shape consistent with a hexamer comprising a 1:1 subunit stoichiometry [72].

Other *MCM* genes, including *MCM1* and *MCM10,* were identified in the screen mentioned above, but do not share significant amino acid similarity to Mcm2-7 [62]. Mcm1 is a transcription factor that regulates the expression of *CDC6* and some *MCM* genes [73] and has been implicated to play a role at yeast replication origins [74, 74, 75]. Mcm10 is essential for growth in budding yeast, assembles onto replication origins and travels with the replication fork [76, 77]. Additionally, two other *MCM* genes, *MCM8* and *MCM9*, have been identified in humans, *Xenopus*, mouse and rat, but appear absent in yeast and nematodes (reviewed in 78). Mcm9 exists only in vertebrates and is more closely related to Mcm8 than to other Mcm2-7 proteins [79-81]. Most recently, a novel Mcm-binding protein (Mcm-BP) that interacted with all Mcm2-7 subunits except Mcm2 was found in humans [82]. It is distantly related to the Mcm2-9 family and is present in multicellular organisms, some fungi and other unicellular eukaryotes. Mcm-BP regulates the unloading of Mcm2-7 after DNA replication [83].

1.2.2   Structural biology of MCM helicases

Mcm proteins are composed of three domains: an N-terminal domain, an AAA+ domain, and a C-terminal domain that is predicted to fold into a winged-helix domain (Fig 1.2A). While the majority of the archaeal Mcms conform to this convention, some eukaryotic Mcms contain additional N- or C-terminal extensions (reviewed in 84).

The N-terminal domain of Mcm proteins is poorly conserved from archaea to eukaryotes, and even between Mcm subunits of a given organism [85, 86]. Despite this low sequence similarity, structure-based sequence alignments indicated the conservation of hydrophobic residues within buried regions and charged residues within the central channel. The central channel of MCM is large enough to accommodate both ssDNA and dsDNA. Indeed, studies of MCMs in *Methanothermobacter thermautrophicus* (MtMCM) and *Sulfolobus solfataricus* (SsoMCM) revealed that these positively charged residues interact with DNA [87, 88]. Reconstitution studies in *S. Solfataricus* have shown that the

addition of the N-terminal half of SsoMCM *in trans* influences both processivity and substrate recognition [89]. Studies have also shown that archaeal MCMs can form dodecamers and hexamers. For instance, the crystal structure of MtMCM reveals a head-to-head double hexamer, formed from opposing N-terminal faces.

In contrast, SsoMCM crystallized as a single hexamer (Fig. 1.2B). Further studies show that SsoMCM binds forked substrates with the C-terminal facing the ssDNA/dsDNA junction [88]. However, there are data to suggest that the latter may form a double hexamer [89] and indeed the SsoMCM hexamer fits well into the electron density microscope map of the double-hexameric MtMCM [90]. Interestingly, eukaryotic Mcm2-7 is a single hexamer in solution, yet is loaded onto origins of replication as a head-to-head double hexamer, with the C-termini containing the AAA+ ATPase domains facing outward [91-93], in similar fashion to SsoMCM [88].

Moreover, the N-terminal domain plays a role in regulating Mcms via kinases [87, 94]. In fact, a proline to leucine mutation (P83L), also called the *bob1* mutation, within this region in budding yeast Mcm5, bypasses the requirement for DDK [94, 95]. The distal portion of the N-terminus contains a positively charged β-hairpin that protrudes into the central channel and an allosteric communication loop, which together modulate this region via contacts with hairpins in the AAA+ core [87, 96, 97]. In the E1 helicase of bovine papillomavirus (Fig. 1.2C), these hairpins look like a spiral staircase as they track the sugar-phosphate backbone of ssDNA through the central channel [98]. This feature is thought to be analogous in the central channel of archaeal [87] and eukaryotic MCM [99].

The AAA+ domain is responsible for the catalytic activity of MCM proteins. Members of the AAA+ superfamily of ATPases share several conserved residues that contribute to the binding and hydrolysis of ATP. These include the Walker A and B motifs and other elements unique to the family, such as sensor I, sensor II and an arginine finger motif, characterized by the residues serine, arginine and phenylalanine (Figures 1.2A, B; reviewed in 84). The ATPase site of Mcm proteins is located at the interface between adjacent subunits (Fig. 1.2D) whereby one subunit contributes the Walker A or phosphate binding loop (P-loop) and Walker B motifs, while the other subunit contributes

the arginine finger motif. The P-loop contains a Walker A lysine that coordinates and binds the γ phosphate of ATP. The Walker B motif coordinates Mg^{2+} and water around the docked ATP molecule. In the adjacent subunit, the catalytic arginine residue of the arginine finger protrudes into the interface to promote ATP hydrolysis [66, 69, 100]. Studies of SV40 large T antigen [101] and archaeal MCMs [90] suggest that in addition to the role in ATP binding and hydrolysis, these motifs make variable contributions to the inter-site communication required to pump DNA through the central channel and unwind DNA [100].

Most known hexameric helicases are formed from six identical subunits and thus are assumed to be functionally equal. The heterohexameric Mcm2-7 complex with its six different ATPase sites is unique in this regard.

A

N-term   AAA+   C-term

Zn   ACL   EXT   A   H2i   B   PS1   SI   R   SII   WH

B: ssoMCM

EXT
PS1
SRF motif
Walker A
Walker B
H2i

C: BPV E1

PS1
ssDNA
ADP

D

5   SRF   3   SRF   7
P-loop   P-loop   P-loop
2   SRF   SRF   4
P-loop   SRF   P-loop
6
P-loop
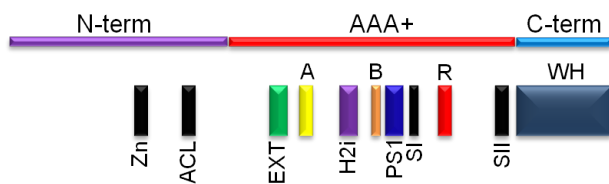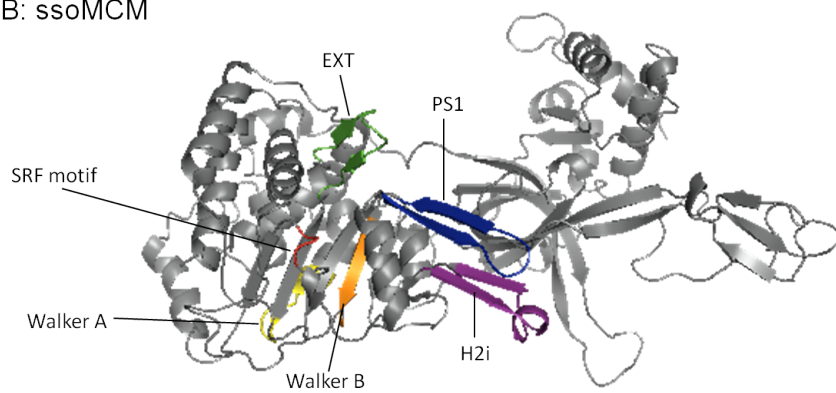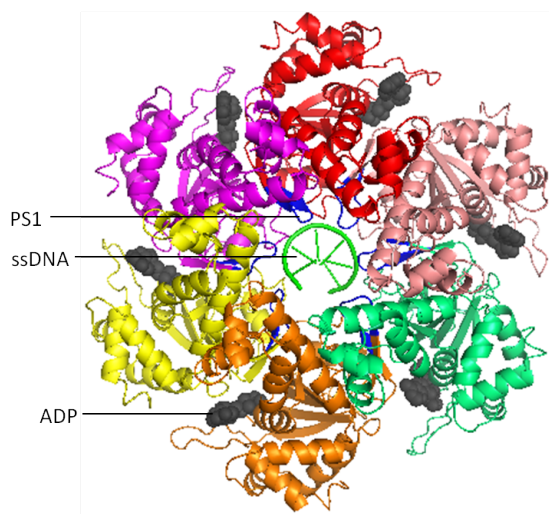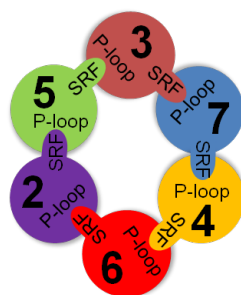
Figure 1.2: Architecture of MCM proteins and BPV E1 helicase

(A) The primary structure of MCM proteins consists of an N-terminal domain (purple), a AAA+ domain (red) and a C-terminal domain (blue). The N-terminal domain includes a number of functional sequence elements, such as the Zn binding motif (Zn) and the allosteric communication loop (ACL). The AAA+ domain contains the Walker A (A, yellow), Walker B (B, orange), sensor I (SI), sensor II (SII) and arginine finger (R, red) motifs. Unique insertions characteristic of the MCM clade include the external β-hairpin (EXT, green), helix 2 insert (H2i, purple) and the pre-sensor I β-hairpin (PS1). The C-terminal domain is predicted to fold into a winged-helix motif (WH). Figure adapted from Costa and Onesti [84]. **(B)** Near-full length structure of *Sulfolobus solfataricus* MCM (PDB code 3F9V). Motifs are colour-coded as in A. **(C)** Bovine papillomavirus E1 DNA helicase complex bound to ssDNA (PDB code 2GXA). Shown are the individual subunits of the hexamer (red, pink, cyan, orange, yellow, purple), ssDNA (green) in the central channel, Pre-sensor1 β-hairpin (PS1, blue), and ADP (grey) bound at subunit interfaces. **(D)** The subunit arrangement of the Mcm2-7 heterohexamer based on the view from the C-terminal face. Shown are the ATP binding site (P-loop) contributed by one subunit and the catalytic arginine residue (SRF) contributed by the adjacent subunit. Figure adapted from Davey *et al.* [69].

1.2.3   DNA binding and unwinding by helicases

Crystallographic studies and biochemical examination of viral helicases and archaeal MCMs have yielded a considerable amount of structural information regarding amino acid residues important for DNA binding and unwinding. Such structural information exists for the simian virus 40 large T antigen (SV40 LTag) [102], bovine papillomavirus (BPV) E1 helicase [98], *M. thermoautrophicus* MCM [87] and *S. solfataricus* MCM [90, 103]. As mentioned above, the N-terminal domain of MCMs is poorly conserved from archaea to eukaryotes, but conserved positively charged residues within this domain form β-hairpins

that protrude into the central channel and interact with DNA [87, 88]. Moreover, biochemical characterization of this domain in MtMCM and SsoMCM revealed that it binds both ssDNA and dsDNA, with a preference for ssDNA [87, 97, 103]. In addition, the crystal structure of a near-full length SsoMCM showed the presence of four β-hairpins located throughout the N- and C-terminal domains and are proposed to be involved in DNA binding and unwinding [90]. Three hairpins, NT, H2I and PS1 are located in the central channel and two hairpins, PS1 and EXT are located near the side channels. The PS1 hairpin is located at the junction between the central and side channels. This hairpin also aligns with the only β-hairpin in the central channel of SV40 LTag. As well, studies showed that the latter protrudes into the central channel and moves in response to the nucleotide binding state [102].

Mutation of conserved basic residues in β-hairpins of either the N- or C-terminal domains of full length SsoMCM resulted in reduced DNA binding. Mutation of both N- and C-terminal domains together negates binding of DNA by MCM [88]. Of note, mutations in the β-hairpins of these domains had variable effects on DNA unwinding activity. Reduction in the affinity for DNA from mutations in the N-terminal β-hairpins of SsoMCM resulted in a concomitant reduction in helicase activity, whereas mutations in the C-terminal domain that reduced the affinity for DNA showed no effect on helicase activity [88]. In MtMCM, deletion within the H2I hairpin abrogated DNA unwinding activity [104].

1.2.4   DNA binding and unwinding by Mcm2-7

The heterohexameric organization of eukaryotic Mcm2-7 is unique among helicases since it is formed from six distinct subunits, as opposed to the homohexamers of Archaea [105]. Biochemical analyses of eukaryotic Mcms have enabled the classification of Mcm2-7 subunits into two functional groups: helicase subunits and regulatory subunits. Subcomplexes containing derivations of Mcms 4, 6 and 7 exhibit *in vitro* DNA unwinding activity [70, 106, 107], whereas Mcms 2, 3 and 5 play a regulatory role and under certain conditions, inhibit *in vitro* helicase activity [70, 72, 108, 109].

As with other hexameric helicases, both *S. cerevisiae* Mcm467 and Mcm2-7 showed ATP-dependent ssDNA binding. However, these complexes demonstrated a preference for poly(dT) ssDNA, unlike homohexameric helicases [110]. Interestingly, Mcm2-7 showed a significantly higher affinity for circular ssDNA than Mcm467 [108]. This difference was found to be dependent on the order of addition of ATP. In this case, when Mcm2-7 and ATP were mixed together prior to the addition of DNA, Mcm2-7 bound circular ssDNA weakly. However, when Mcm2-7 and circular ssDNA were mixed before the addition of ATP, higher levels of DNA binding by Mcm2-7 were seen [108]. In addition, Mcm2-7 bound linear ssDNA very slowly compared to Mcm467. Both Mcm467 and Mcm2-7 form ring-shaped structures and exhibit *in vitro* helicase activity [106, 108]. These data implicate Mcms 2, 3 and 5 in regulating the loading or activation of Mcm2-7 *in vivo* [110]. Indeed, Mcm2-7 is thought to possess an ATP-dependent "gate" at the Mcm2/5 interface which allows the ring to open and permit entry of ssDNA into the central channel [69, 108]. Consistent with this, Bochman and Schwacha [108] observed *in vitro* helicase activity under reaction conditions that putatively closed the Mcm2-7 ring. The Schwacha lab also identified ATPase active sites (Walker B and arginine finger) in Mcm6/2 and Mcm5/3 that play a role in the putative Mcm2/5 gate within Mcm2-7 [111].

As aforementioned, replicative DNA helicases such as SV40 LTag, archaeal MCMs and eukaryotic Mcm2-7 subunits form hexameric toroidal structures with a large central channel through which DNA can pass [87, 90, 101, 112]. As such, several models on how Mcm2-7 unwinds DNA have been proposed: (i) steric exclusion, (ii) rotary pump, (iii) T-antigen, and (iv) ploughshare (Figure 1.3; reviewed in 113).

In the steric exclusion model, ssDNA passes through the central channel of Mcm2-7 while displacing the complementary strand on the outside of the ring [107, 114]. This is akin to the DNA helicase DnaB in *Escherichia coli* and has been proposed for Mcm467 [107]. Indeed, biochemical analyses have shown that archaeal and eukaryotic MCM proteins translocate along ssDNA with 3' to 5' polarity [107, 108, 115, 116]. Recently, studies in *Xenopus* egg extracts revealed that a large helicase complex consisting of Cdc45, Mcm2-7 and GINS (CMG) unwound DNA by translocating along ssDNA with 3' to 5' polarity, consistent with DNA unwinding by steric exclusion.

The rotary pumping model was proposed to explain the 'MCM paradox'. While Mcm2-7 co-localizes with sites of DNA synthesis in budding yeast, Mcm2-7 does not co-localize with replication foci in vertebrate systems (reviewed in 117). Under this model, Mcm2-7 complexes first load onto replication origins in G1 phase and move away from the origin by rotation along the helical axis of the duplex DNA. Next, during S phase, these dispersed Mcm2-7 complexes become attached to an immobile nuclear structure and the rotary action is repeated such that only the duplex DNA would be able to rotate and effectively unwind DNA at a distance from the replication fork [117].

SV40 LTag must form a double hexamer in order to unwind DNA. In the T-antigen model, dsDNA is pumped into each SV40 LTag hexamer and ssDNA is forced out from the hexamer interface. EM images show SV40 LTag bound to dsDNA from which two loops of ssDNA originate. Based on crystal structures of SV40 LTag, ATP-dependent movements of a β-hairpin protruding into the central channel pulls in duplex DNA and rotation of one section of the channel relative to the other causes DNA unwinding. Next, ssDNA is extruded from positively charged channels within subunit interfaces, which would also prevent re-annealing (reviewed in 113). Indeed, putative ssDNA channels at subunit interfaces have been shown in MtMCM [87] and SsoMCM [90].

The ploughshare model was predicated on the belief that a single Mcm2-7 hexamer would be unable to induce sufficient torsional strain to unwind DNA. In this regard, DNA unwinding is achieved by a protein located behind Mcm2-7 that acts as a wedge to separate the two strands of the duplex DNA as they exit from the central channel of the helicase [113].

A: Steric exclusion   B: Rotary pump

C: T-antigen   D: Ploughshare
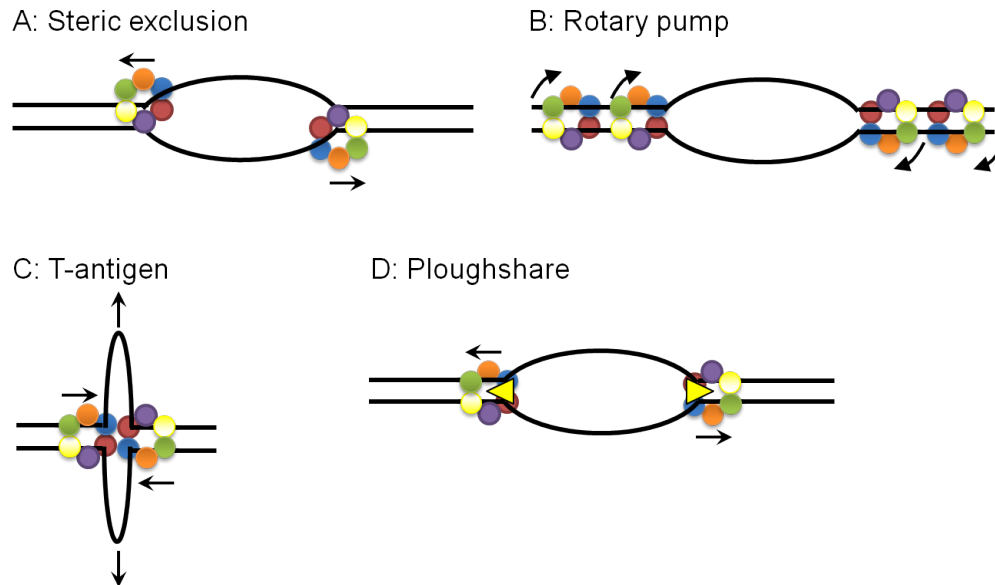
Figure 1.3: Models of DNA unwinding by Mcm2-7

(A) The steric exclusion model, whereby Mcm2-7 translocates along ssDNA while displacing the complementary strand on the outside of the hexamer. **(B)** The rotary pump model predicts that two groups of Mcm2-7 complexes encircling dsDNA rotate the DNA in opposite directions and unwind the duplex by torsional stress at a distance from the replication fork. **(C)** The T-antigen model stipulates that two physically associated Mcm2-7 molecules encircling dsDNA pump DNA towards the double hexamer interface. Single stranded DNA is then extruded through channels at subunit interfaces. **(D)** The ploughshare model suggests that while Mcm2-7 translocates along dsDNA, a protein at the trailing edge of the helicase acts as a wedge, or pin, to separate the DNA strands. Arrows indicate the direction or rotation of Mcm2-7. Figure adapted from Takahashi *et al.* [113].

The ploughshare model was predicated on the belief that a single Mcm2-7 hexamer would be unable to induce sufficient torsional strain to unwind DNA. In this regard, DNA unwinding is achieved by a protein located behind Mcm2-7 that acts as a wedge to separate the two strands of the duplex DNA as they exit from the central channel of the helicase [113].

1.3 Regulation of Mcm2-7 activity

1.3.1 Regulation by ATPase activity

To ensure once per cell cycle genome duplication, the activity of the Mcm2-7 replicative DNA helicase must be modulated on several fronts. As mentioned above, the eukaryotic Mcm2-7 complex contains six distinct subunits with six unique ATPase sites. Indeed, previous studies on Walker A and arginine finger mutations identified three ATPase active sites, Mcm3/7, Mcm7/4 and Mcm6/2, which serve a functional importance to ATPase activity within Mcm2-7 and cell viability [69, 118]. ATP hydrolysis and ssDNA binding are requisite events for DNA unwinding. The ATPase active sites Mcm3/7 and Mcm7/4 are thought to play an essential role in coupling ATPase activity to helicase activity since mutations within these sites inhibit hydrolysis of ATP by Mcm2-7. As well, mutations in the Walker A motif in either of Mcm7 or Mcm4 inhibit ssDNA binding by Mcm2-7 in an ATP-dependent manner [110, 118]. Interestingly, mutations in the Walker B motif of Mcm6 and in the arginine finger motif of Mcm4 showed no effect on yeast cell viability or growth rate, yet blocked hydrolysis of ATP at the Mcm4/6 site [118]. As aforementioned, Walker B and arginine finger motifs play more of a catalytic role, whereas the Walker A motif is predominantly involved in nucleotide binding [66, 69, 100]. In light of this, it has been proposed that the Mcm4/6 active site need only bind, not hydrolyze, ATP for Mcm2-7 function *in vivo* [118].

Moreover, data suggest a physical discontinuity between Mcm2 and Mcm5, an ATP-dependent "gate" which allows the Mcm2-7 hexamer to load onto ssDNA [69, 108]. Indeed, the rate of ssDNA association with Mcm2-7 was slow relative to a subcomplex consisting of Mcm467. However, incubation of Mcm2-7 with ATP prior to addition of ssDNA or mutations in the Mcm2/5 ATPase active site increased the rate of Mcm2-7

association with ssDNA [110]. Further investigation on mutations in Walker B and arginine finger motifs demonstrated that the ATPase active sites in Mcm6/2 and Mcm5/3 modulate the activity of the alleged Mcm2/5 gate [111].

In another study, ATP binding and hydrolysis by Mcm2 was implicated in modulating DNA binding by Mcm2-7 [109]. In this study, biochemical analyses employing a mutation in the P-loop of Mcm2 as well as the poorly hydrolysable analogue of ATP, ATPγS, revealed that ADP binding by Mcm2 is required to inhibit DNA binding and unwinding by Mcm467. Additionally, when the P-loop mutant of Mcm2 was reconstituted into Mcm2-7, enhanced ssDNA binding relative to wild type Mcm2-7 was observed. From these findings, the authors suggested that Mcm2 affects DNA unwinding by or activation of Mcm2-7. During translocation, the ability of Mcm2 to inhibit DNA binding by Mcm2-7 may play a role in release of the complex from DNA. On the other hand, ATP hydrolysis by Mcm2 may be switched off during the activation of Mcm2-7, thus relieving the inhibitory role played by Mcm2 [109].

1.3.2   Post-translational modifications of Mcm2-7

Mcm2-7 subunits are phosphorylated by several different kinases including Mec1, cyclin-dependent kinase (CDK), Dbf4-dependent kinase (DDK) and casein kinase 2 (CK2) [19, 20, 119-121]. An overview of the phosphoregulation of Mcm2-7 is illustrated in Figure 1.4. The relationship between Mcm2-7 and these kinases is underscored by the essential processes involved, such as DNA replication initiation, helicase activation and checkpoint pathways. Mec1 is characterized in Chapter 2, and the role of phosphorylation of Mcm2-7 by DDK is investigated in Chapter 4.

As discussed above, during S phase, Mcm2-7 is activated to unwind DNA in a series of events that requires CDK and DDK (Figure 1.1) [19]. The activity by these kinases promotes the binding of Cdc45 and GINS to Mcm2-7 [91, 93, 115, 122]. While the essential targets of CDK are Sld2 and Sld3 (discussed above), a role for CDK in modifying Mcm subunits has been proposed (Figure 1.4A) [121]. The N-terminal tail of budding yeast Mcm4 is phosphorylated *in vivo* during S phase by CDK [121], and in the absence of DDK, CDK phosphorylation of a distal portion the N-terminus of Mcm4 is essential [123].

A

G1 phase

3
5   7
2   6   4

G1-CDK?
Pho85?

S-CDK
and DDK

S phase

Mec1

DDK

DDK

P   P   P

Initiation   Initiation

B

Unperturbed cell cycle

Mec1   CDK, Pho85?

RNR   Mcm2-7

dNTP   activate
levels   initiation
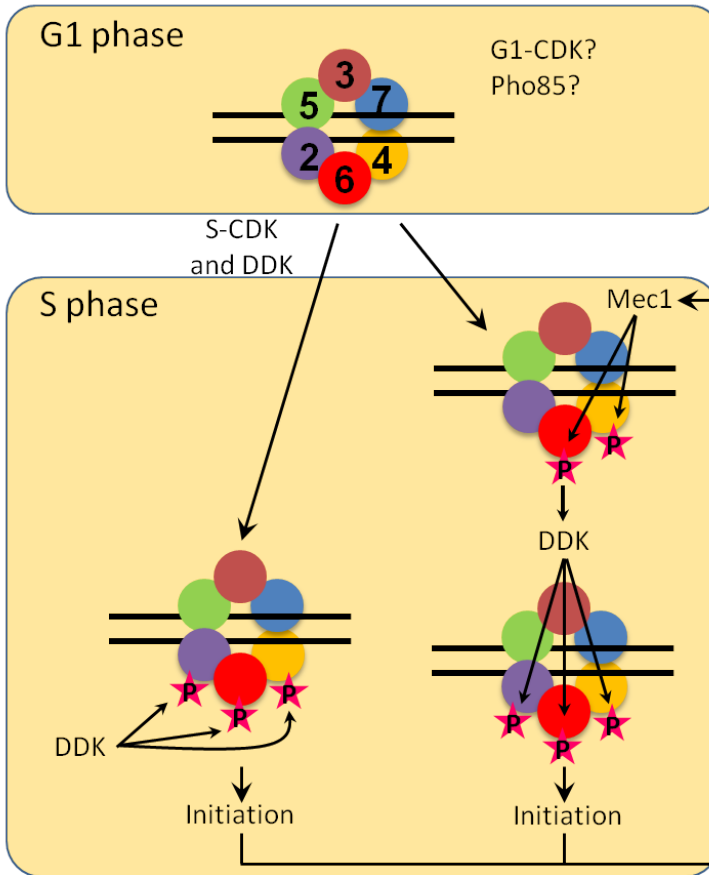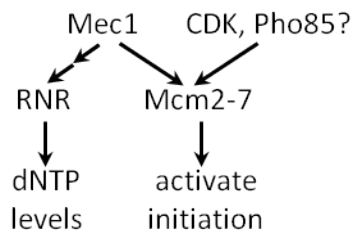
DNA damage/stalled forks

Mec1

Rad53   Mcm2-7

stabilizes forks/   activate
inhibits   initiation
initiation   during restart
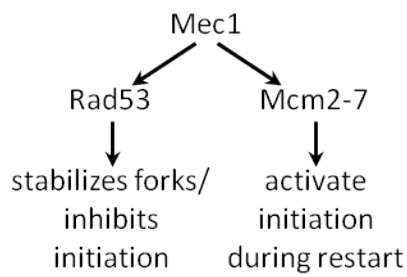
Figure 1.4: An overview of the phosphoregulation of Mcm2-7

(A) Prior to replication, Mcm4 and Mcm6 are thought to be phosphorylated by either G1-CDKs or Pho85. This phosphorylation may also occur during S phase in the previous cell cycle by S-CDKs and is not removed during G1. During the G1-S phase transition, DDK phosphorylates the N-termini of Mcm2, Mcm4 and Mcm6 to trigger helicase activation. Mec1 may also phosphorylate the N-termini of Mcm4 and Mcm6 followed by DDK phosphorylation of these regions to trigger replication initiation. **(B)** Mec1 regulates several events in both unperturbed and perturbed cell cycles. In a normal S phase, Mec1 increases RNR activity, which in turn increases dNTP synthesis. Mec1 also helps to target DDK to Mcm2-7. Under a perturbed cell cycle, such as during DNA damage or stalled replication forks, the Mec1 checkpoint pathway stabilizes stalled forks and inhibits late origin firing. Mec1 may also mediate the firing of additional origins upon replication restart after recovery from the checkpoint. (Figure adapted from 6).

Furthermore, mass spectrometry analysis of *in vitro* kinase reactions revealed that the N-terminus of human Mcm2 contains CDK consensus sites [120].

DDK consists of a catalytic subunit, Cdc7, and a regulatory subunit, Dbf4, and is required throughout S phase for the activation of early and late origins of replication [124, 125]. DDK phosphorylates every Mcm2-7 subunit except Mcm5 [126, 127]. A single point mutation (P83L) in the N-terminal region of Mcm5, also called the *bob1* mutation, can bypass the requirement for DDK in budding yeast [37, 128]. The analogous mutation in MtMCM suggested that the *bob1* mutation causes subtle allosteric changes in the Mcm2-7 complex [95], possibly mimicking what typically occurs when other Mcm subunits are phosphorylated by DDK [19].

The N-terminal tails of eukaryotic Mcm2, 4 and 6 are the major substrates for DDK, and also contain sites for other kinases (Figure 1.4A) [119, 120]. Whereas non-chromatin-bound Mcm2 is the primary target of DDK [120], phosphorylation of Mcm4 and Mcm6 is stimulated within the pre-RC [129]. In this regard, phosphorylation of Mcm2-7 by

DDK during late G1 or S phase allows origin recruitment of Sld3 and Cdc45 [20]. Additionally, while phosphorylation of Mcm2 is not required for viability in budding yeast, it has been implicated in the cell's response to DNA damage and replication stress [119, 130, 131].

The Stillman lab has extensively characterized the N-terminal tail of budding yeast Mcm4, aptly named the NSD or N-terminal Ser/Thr-rich domain (residues 2-174) [123, 132]. The NSD of Mcm4 is hyperphosphorylated by DDK, yet DDK substrate specificity is conferred by a DDK-docking domain (DDD) adjacent to the NSD. In addition, the hyperphosphorylated form of Mcm4 is highly enriched in the Cdc45-Mcm2-7 complex, the assembly of which is induced by DDK exclusively on chromatin in S phase [132]. Furthermore, the NSD was found to contain an inhibitory activity that is alleviated by DDK phosphorylation of this domain. Yeast cells lacking a portion of the NSD (residues 74-174) were viable in the absence DDK, but grew more slowly and the Cdc45-Mcm2-7 complex did not form in a timely fashion under this bypass state [123]. Studies in other eukaryotes reveal that the mechanism of Mcm2-7 phosphorylation by DDK orthologs may be similar to that in budding yeast. As such, work in human cells have shown the N-termini of Mcm2 and Mcm4 are phosphorylated by Cdc7, as well as during S phase in *Xenopus* [19]. In addition, the DDK ortholog in *S. pombe* phosphorylates Mcm2 and Mcm4 and is required for the hyperphosphorylation of Mcm6 [133].

Using *in vitro* assembled pre-RCs as a DDK substrate, the Bell lab [119] mapped phosphorylation sites on Mcm2-7 by mass spectrometry. Phosphorylation sites were found in the N-termini of Mcm2, Mcm4 and Mcm6 and the C-terminus of Mcm3. A cluster of phosphosites in the C-terminus of Mcm3 matched a CDK-mediated nuclear transport signal. Four sites within the N-terminus of Mcm2 corresponded to casein kinase 2 (CK2) consensus sites [119]. This study also identified two classes of DDK target sequences on Mcm4 and Mcm6: intrinsic (S/T-D/E) and phosphorylation-generated (PG, S/T-P/Q), or "priming" sites. Recognition of the latter by DDK required prior phosphorylation by another kinase. Both classes of target sites were found to be important for Mcm2-7 function as a budding yeast strain bearing mutations of intrinsic and PG sites in both Mcm4 and Mcm6 showed a severe proliferation defect. Mutations of

these sites alone or together in Mcm4 or Mcm6 showed little to no proliferation defect [119]. In addition, S/T-P priming sites within Mcm4 and Mcm6 were found to be phosphorylated independently of chromatin loading in G1, S and G2/M phases [119]. The kinase responsible for priming of these sites has not been elucidated.

Randell and colleagues [119] also found and analyzed S/T-Q priming sites on Mcm4 and Mcm6 targeted by Mec1 (Figure 1.4). This phosphorylation was spatially restricted to chromatin-bound Mcm2-7 and temporally constrained to S phase [119]. Mec1 is discussed in more detail below and in Chapter 2 where we characterize the C-terminal tail of this protein and show that it plays an essential role in the localization, stability and function of Mec1.

Mec1, the budding yeast ortholog of ataxia-telangiectasia and Rad3-related (ATR), is a member of the phosphoinositide-3-kinase-related kinase (PIKK) family. The Mec1 signaling cascade, or checkpoint, of *S. cerevisiae* serves an essential role in mediating cellular responses to DNA damage, in responding to stalled replication forks and in protecting against genomic instability (Figure 1.4B) [134]. The mode of action of the Mec1 checkpoint pathway is to prevent the firing of late origins upon replication fork stalling or DNA damage [135, 136]. In budding yeast, DNA damage typically causes Mec1-dependent phosphorylation and activation of the transducer protein kinases Rad53 and Chk1 [137], which in turn phosphorylate effector proteins regulating cell cycle progression and DNA repair. Moreover, cells harboring mutations in *MEC1* exhibit profound sensitivity to genotoxins and inhibitors of DNA replication, such as hydroxyurea (HU) and show defects in the DNA damage checkpoint at all stages of the cell cycle [138, 139]. Overexpression of dominant-negative forms of ATR has similar effects in human cells [140]. Mec1 also plays a role during normal S phase to regulate dNTP synthesis by increasing ribonucleotide reductase (RNR) activity via the removal of the RNR inhibitor, Sml1 [141-143]. Mec1 is also proposed to help target DDK to Mcm2-7 (Figure 1.4B) [119].

1.3.3   Interaction of Mcm2-7 with Cdt1

Cdt1 was originally found in fission yeast [144], and is essential for Mcm2-7 loading in fission yeast [145], budding yeast [146] and *Xenopus* [26], as well as for DNA replication in

Drosophila [147] and humans [148]. During G1 phase of the cell cycle, Mcm2-7 is imported into the nucleus and loaded onto origins of DNA replication in a Cdt1-dependent manner [91, 149]. It is noteworthy that Mcm2-7 is loaded onto origin DNA in an inactive form. *In vitro* studies show that Mcm2-7 is loaded as a head-to-head double hexamer, encircling dsDNA through its central channel [91-93]. While essential, the role Cdt1 plays in Mcm2-7 origin loading is transient. Upon origin recruitment, Cdt1 is rapidly expelled through ATP hydrolysis by Cdc6 and Orc1 [150, 151]. Cdt1 is discussed in more detail below and a role for Cdt1 as a negative regulator of Mcm2-7 activity is explored in Chapter 3.

In *Xenopus*, the C-terminal 377 residues of Cdt1 are required for Mcm2-7 origin loading, and the extreme Cdt1 C-terminus bound to the Mcm2467 subcomplex of Mcm2-7 [152]. Studies of mammalian Cdt1 demonstrated that the C-terminus plays a role in regulating DNA binding and helicase activity of Mcm proteins [153-155]. The C-terminus of Cdt1 was also found to bind Mcm2-7 in budding yeast and this interaction was required for efficient origin recruitment of both proteins [156]. Also, multiple Cdt1 molecules were required for origin loading of Mcm2-7 as a Cdt1 mutation that only allowed recruitment of one Cdt1 molecule to the origin prevented Mcm2-7 loading. In addition, while dispensable for origin loading of Mcm2-7 double hexamers, the essential N-terminus of Cdt1 was required to load Mcm2-7 complexes that were competent to interact with the helicase-activating proteins Cdc45 and GINS [156]. The role Cdc45 and GINS play in modulating Mcm2-7 activity will be discussed in more detail in the following section.

Recently, the Diffley lab demonstrated that while Cdt1 was dispensable for origin-association of Mcms 3, 5 and 7 in the presence of the poorly hydrolysable analog of ATP, ATPγS, Cdt1 was required for all six MCM subunits to bind ORC and Cdc6 at the origin in equimolar ratio. In this sense, Cdt1 plays a role in stabilizing Mcm2-7 on origins of DNA replication [157, 158]. In another recent study, Cdt1 was required to alleviate an autoinhibitory domain in the C-terminus of Mcm6 that blocked origin recruitment of Mcm2-7 by ORC and Cdc6. Upon formation of an Mcm2-7-Cdt1 complex, the C-terminus of Mcm6 both induced pre-RC assembly and allowed Orc1/Cdc6-dependent ATP hydrolysis [150].

1.3.4 Interaction of Mcm2-7 with Cdc45 and GINS

Loading of Mcm2-7 onto origins of replication requires the concerted effort of ORC, Cdc6 and Cdt1 [6]. The action of CDK and DDK switches Mcm2-7 from an inactive to an active helicase (reviewed in 19). While Mcm2-7 exhibited helicase activity *in vitro* (this study, [108]), *in vivo* data showed that both Cdc45 and GINS are required during the initiation and elongation steps of DNA replication [54, 159-163]. Studies in budding yeast showed that during initiation, GINS is required for Mcm2-7 to stably interact with essential regulatory factors such as Cdc45, the checkpoint mediator Mrc1, the Tof1-Csm3 complex which allows replication fork pausing at protein-DNA barriers, the histone chaperone FACT and Ctf4, which facilitates sister chromatid cohesion. GINS was also required for Mcm2-7 to specifically interact with, albeit weakly, topoisomerase I and Mcm10. These large complexes were named replisome progression complexes or RPCs [45]. Furthermore, Mcm2-7, Cdc45 and GINS were found as part of large and stable replisome complexes at paused replication forks [164]. In *Xenopus,* along with DNA polymerases and Mcm10, Mcm2-7, Cdc45 and GINS were found as components of the replisome. Also in that study, only Mcm2-7, Cdc45 and GINS were enriched at paused forks induced by aphidicolin which causes uncoupling of the helicase from DNA polymerases [43].

Studies with *Drosophila melanogaster* embryo extracts demonstrated that Mcm2-7 copurifies with Cdc45 and GINS through stringent fractionation steps [115]. Reconstitution experiments using *Drosophila* recombinant proteins revealed that the Mcm2-7 complex was activated when associated with Cdc45 and GINS, relative to Mcm2-7 alone. In addition, this large CMG (Cdc45/Mcm2-7/GINS) complex showed enhanced ATPase and helicase activity and better DNA substrate recognition [122].

Recent structural studies using single-particle electron microscopy of *D. melanogaster* proteins have provided further insight into how Cdc45 and GINS activate Mcm2-7 [165]. Mcm2-7 alone formed open ring hexamers with discontinuity between the Mcm2 and Mcm5 subunits. In the presence of Cdc45 and GINS, this opening was sealed off along with adopting a more planar helicase configuration. In the presence of a nonhydrolyzable ATP analog, ADP•BeF$_3$, the Mcm2/5 gate closed forming a large

central channel and expanded the contact area of GINS to include the AAA+ domains of Mcm3 and Mcm5. This, in turn, created two topologically distinct openings. The authors speculate that the more intimate contacts in the CMG complex [165] help explain the enhanced ATPase and DNA binding activities relative to Mcm2-7 alone [122].

Further significance of the CMG complex was recently substantiated through phylogenomic analysis showing that a complex consisting of a Cdc45 homolog (RecJ), Mcm2-7 and GINS exists in archaea. This CMG complex is an essential constituent of the DNA replication machinery in archaea that is most likely homologous and functionally analogous to the eukaryotic CMG complex [166].

1.4 Scope of thesis

The regulation of DNA replication is crucial to ensure the genome is duplicated once per cell division cycle in *S. cerevisiae* and other eukaryotes. Aberrations during this process can lead to diseases arising from genomic instability, such as cancer. The Mcm2-7 replicative DNA helicase plays a key role in this endeavor. Using budding yeast as a model organism, and through *in vitro* and *in vivo* techniques, this study examines the factors and the mechanisms involved in the modulation of Mcm2-7 activity to unwind DNA.

The work presented in Chapter 2 examines Mec1, the budding yeast homolog of ATR that plays a role in normal cell cycle progression and in the checkpoint response to DNA damage and replication fork stalling. Through *in vivo* and *in vitro* techniques, I show that the C-terminus of Mec1 is important for the localization, stability and function of the protein.

In Chapter 3, I explore the role of Cdt1 in modulating Mcm2-7 activity. Using recombinant proteins expressed in *E. coli*, I demonstrate that Cdt1 inhibits both ATPase and helicase activity of Mcm2-7.

Chapter 4 looks at the role of phosphorylation in the regulation of Mcm2-7 activity. Using *in vitro* techniques, I reveal that a phosphomimetic Mcm2-7 complex exhibits wildtype ATPase and helicase activities.

Chapter 5 summarizes what is known about Mcm2-7, including the processes and associated replication factors involved in the early stages of the initiation of DNA replication. As many of the protein factors and pathways involved in DNA replication show potential as biomarkers and/or pharmacological inhibition, I relate the importance of deciphering the mechanisms involved in the regulation of DNA replication to the development of anti-cancer therapeutics. Furthermore, I summarize my results and discuss the implications of my studies. I also propose a model in which Cdt1 negatively regulates the activity of Mcm2-7.

1.5 References

1.   Aguilera,A. & Gomez-Gonzalez,B. Genome instability: a mechanistic view of its causes and consequences. *Nat. Rev. Genet.* **9**, 204-217 (2008).

2.   Lee,D.G. & Bell,S.P. Architecture of the yeast origin recognition complex bound to origins of DNA replication. *Mol Cell Biol.* **17**, 7159-7168 (1997).

3.   Arias,E.E. & Walter,J.C. Strength in numbers: preventing rereplication via multiple mechanisms in eukaryotic cells. *Genes Dev.* **21**, 497-518 (2007).

4.   Riera,A., Fernandez-Cid,A., & Speck,C. The ORC/Cdc6/MCM2-7 complex, a new power player for regulated helicase loading. *Cell Cycle* **12**, (2013).

5.   Boos,D., Frigola,J., & Diffley,J.F. Activation of the replicative DNA helicase: breaking up is hard to do. *Curr. Opin. Cell Biol.* **24**, 423-430 (2012).

6.   Bell,S.P. & Dutta,A. DNA replication in eukaryotic cells. *Annu. Rev. Biochem* **71**, 333-374 (2002).

7.   Chen,K.C., Csikasz-Nagy,A., Gyorffy,B., Val,J., Novak,B. *et al.* Kinetic analysis of a molecular model of the budding yeast cell cycle. *Mol Biol. Cell* **11**, 369-391 (2000).

8.   Dutta,A. & Bell,S.P. Initiation of DNA replication in eukaryotic cells. *Annu. Rev. Cell Dev Biol.* **13**, 293-332 (1997).

9.   Robinson,N.P. & Bell,S.D. Origins of DNA replication in the three domains of life. *FEBS J* **272**, 3757-3766 (2005).

10.   Bolon,Y.T. & Bielinsky,A.K. The spatial arrangement of ORC binding modules determines the functionality of replication origins in budding yeast. *Nucleic Acids Res.*(2006).

11.   Aladjem,M.I. & Fanning,E. The replicon revisited: an old model learns new tricks in metazoan chromosomes. *EMBO Rep.* **5**, 686-691 (2004).

12.   Gilbert,D.M. Making sense of eukaryotic DNA replication origins. *Science* **294**, 96-100 (2001).

13.   Hsiao,C.L. & Carbon,J. High-frequency transformation of yeast by plasmids containing the cloned yeast ARG4 gene. *Proc. Natl. Acad. Sci U. S. A* **76**, 3829-3833 (1979).

14.   Fangman,W.L. & Brewer,B.J. Activation of replication origins within yeast chromosomes. *Annu. Rev. Cell Biol.* **7**, 375-402 (1991).

15. Rao,H. & Stillman,B. The origin recognition complex interacts with a bipartite DNA binding site within yeast replicators. *Proc. Natl. Acad. Sci. U. S. A* **92**, 2224-2228 (1995).

16. Rao,H., Marahrens,Y., & Stillman,B. Functional conservation of multiple elements in yeast chromosomal replicators. *Mol. Cell Biol.* **14**, 7643-7651 (1994).

17. Stinchcomb,D.T., Struhl,K., & Davis,R.W. Isolation and characterisation of a yeast chromosomal replicator. *Nature* **282**, 39-43 (1979).

18. Chan,C.S. & Tye,B.K. Autonomously replicating sequences in Saccharomyces cerevisiae. *Proc. Natl. Acad. Sci U. S. A* **77**, 6329-6333 (1980).

19. DePamphilis,M.L. Cell cycle dependent regulation of the origin recognition complex. *Cell Cycle* **4**, 70-79 (2005).

20. Labib,K. How do Cdc7 and cyclin-dependent kinases trigger the initiation of chromosome replication in eukaryotic cells? *Genes Dev.* **24**, 1208-1219 (2010).

21. Heller,R.C., Kang,S., Lam,W.M., Chen,S., Chan,C.S. *et al.* Eukaryotic origin-dependent DNA replication in vitro reveals sequential action of DDK and S-CDK kinases. *Cell* **146**, 80-91 (2011).

22. Bell,S.P. The origin recognition complex: from simple origins to complex functions. *Genes Dev* **16**, 659-672 (2002).

23. Tanaka,T., Knapp,D., & Nasmyth,K. Loading of an Mcm protein onto DNA replication origins is regulated by Cdc6p and CDKs. *Cell* **90**, 649-660 (1997).

24. Donovan,S., Harwood,J., Drury,L.S., & Diffley,J.F. Cdc6p-dependent loading of Mcm proteins onto pre-replicative chromatin in budding yeast. *Proc. Natl. Acad. Sci U. S. A* **94**, 5611-5616 (1997).

25. Bell,S.P. & Stillman,B. ATP-dependent recognition of eukaryotic origins of DNA replication by a multiprotein complex. *Nature* **357**, 128-134 (1992).

26. Maiorano,D., Moreau,J., & Mechali,M. XCDT1 is required for the assembly of pre-replicative complexes in Xenopus laevis. *Nature* **404**, 622-625 (2000).

27. Amon,A., Irniger,S., & Nasmyth,K. Closing the cell cycle circle in yeast: G2 cyclin proteolysis initiated at mitosis persists until the activation of G1 cyclins in the next cycle. *Cell* **77**, 1037-1050 (1994).

28. Honey,S. & Futcher,B. Roles of the CDK phosphorylation sites of yeast Cdc6 in chromatin binding and rereplication. *Mol Biol. Cell* **18**, 1324-1336 (2007).

29.   Zachariae,W. & Nasmyth,K. TPR proteins required for anaphase progression mediate ubiquitination of mitotic B-type cyclins in yeast. *Mol Biol. Cell* **7**, 791-801 (1996).

30.   Visintin,R., Prinz,S., & Amon,A. CDC20 and CDH1: a family of substrate-specific activators of APC-dependent proteolysis. *Science* **278**, 460-463 (1997).

31.   Piatti,S., Lengauer,C., & Nasmyth,K. Cdc6 is an unstable protein whose de novo synthesis in G1 is important for the onset of S phase and for preventing a 'reductional' anaphase in the budding yeast Saccharomyces cerevisiae. *EMBO J* **14**, 3788-3799 (1995).

32.   Weinreich,M., Liang,C., Chen,H.H., & Stillman,B. Binding of cyclin-dependent kinases to ORC and Cdc6p regulates the chromosome replication cycle. *Proc. Natl. Acad. Sci U. S. A* **98**, 11211-11217 (2001).

33.   Drury,L.S., Perkins,G., & Diffley,J.F. The cyclin-dependent kinase Cdc28p regulates distinct modes of Cdc6p proteolysis during the budding yeast cell cycle. *Curr. Biol.* **10**, 231-240 (2000).

34.   Labib,K., Diffley,J.F., & Kearsey,S.E. G1-phase and B-type cyclins exclude the DNA-replication factor Mcm4 from the nucleus. *Nat. Cell Biol.* **1**, 415-422 (1999).

35.   Nguyen,V.Q., Co,C., Irie,K., & Li,J.J. Clb/Cdc28 kinases promote nuclear export of the replication initiator proteins Mcm2-7. *Curr. Biol.* **10**, 195-205 (2000).

36.   Nguyen,V.Q., Co,C., & Li,J.J. Cyclin-dependent kinases prevent DNA re-replication through multiple mechanisms. *Nature* **411**, 1068-1073 (2001).

37.   Jackson,A.L., Pahl,P.M., Harrison,K., Rosamond,J., & Sclafani,R.A. Cell cycle regulation of the yeast Cdc7 protein kinase by association with the Dbf4 protein. *Mol Cell Biol.* **13**, 2899-2908 (1993).

38.   Araki,H. Regulatory mechanism of the initiation step of DNA replication by CDK in budding yeast. *Biochim. Biophys. Acta* **1804**, 520-523 (2010).

39.   Bochman,M.L. & Schwacha,A. The Mcm complex: unwinding the mechanism of a replicative helicase. *Microbiol. Mol. Biol. Rev.* **73**, 652-683 (2009).

40.   Remus,D. & Diffley,J.F. Eukaryotic DNA replication control: lock and load, then fire. *Curr. Opin. Cell Biol.* **21**, 771-777 (2009).

41.   Queralt,E. & Igual,J.C. Functional connection between the Clb5 cyclin, the protein kinase C pathway and the Swi4 transcription factor in Saccharomyces cerevisiae. Genetics 171, 1485-1498. 2005.

42. Liang,C. & Stillman,B. Persistent initiation of DNA replication and chromatin-bound MCM proteins during the cell cycle in cdc6 mutants. *Genes Dev* **11**, 3375-3386 (1997).

43. Pacek,M., Tutter,A.V., Kubota,Y., Takisawa,H., & Walter,J.C. Localization of MCM2-7, Cdc45, and GINS to the site of DNA unwinding during eukaryotic DNA replication. *Mol. Cell* **21**, 581-587 (2006).

44. Kanemaki,M. & Labib,K. Distinct roles for Sld3 and GINS during establishment and progression of eukaryotic DNA replication forks. *EMBO J* **25**, 1753-1763 (2006).

45. Gambus,A., Jones,R.C., Sanchez-Diaz,A., Kanemaki,M., van,D.F. *et al.* GINS maintains association of Cdc45 with MCM in replisome progression complexes at eukaryotic DNA replication forks. *Nat. Cell Biol.* **8**, 358-366 (2006).

46. Kamimura,Y., Masumoto,H., Sugino,A., & Araki,H. Sld2, which interacts with Dpb11 in Saccharomyces cerevisiae, is required for chromosomal DNA replication. *Mol Cell Biol.* **18**, 6102-6109 (1998).

47. Kamimura,Y., Tak,Y.S., Sugino,A., & Araki,H. Sld3, which interacts with Cdc45 (Sld4), functions for chromosomal DNA replication in Saccharomyces cerevisiae. *EMBO J* **20**, 2097-2107 (2001).

48. Garcia,V., Furuya,K., & Carr,A.M. Identification and functional analysis of TopBP1 and its homologs. *DNA Repair (Amst)* **4**, 1227-1239 (2005).

49. Manke,I.A., Lowery,D.M., Nguyen,A., & Yaffe,M.B. BRCT repeats as phosphopeptide-binding modules involved in protein targeting. *Science* **302**, 636-639 (2003).

50. Yu,X., Chini,C.C., He,M., Mer,G., & Chen,J. The BRCT domain is a phospho-protein binding domain. *Science* **302**, 639-642 (2003).

51. Masumoto,H., Muramatsu,S., Kamimura,Y., & Araki,H. S-Cdk-dependent phosphorylation of Sld2 essential for chromosomal DNA replication in budding yeast. *Nature* **415**, 651-655 (2002).

52. Tanaka,S., Umemori,T., Hirai,K., Muramatsu,S., Kamimura,Y. *et al.* CDK-dependent phosphorylation of Sld2 and Sld3 initiates DNA replication in budding yeast. *Nature* **445**, 328-332 (2007).

53. Tak,Y.S., Tanaka,Y., Endo,S., Kamimura,Y., & Araki,H. A CDK-catalysed regulatory phosphorylation for formation of the DNA replication complex Sld2-Dpb11. *EMBO J.* **25**, 1987-1996 (2006).

54. Takayama,Y., Kamimura,Y., Okawa,M., Muramatsu,S., Sugino,A. *et al.* GINS, a novel multiprotein complex required for chromosomal DNA replication in budding yeast. *Genes Dev* **17**, 1153-1165 (2003).

55. Zegerman,P. & Diffley,J.F. Phosphorylation of Sld2 and Sld3 by cyclin-dependent kinases promotes DNA replication in budding yeast. *Nature* **445**, 281-285 (2007).

56. Kawasaki,Y. & Sugino,A. Yeast replicative DNA polymerases and their role at the replication fork. *Mol. Cells* **12**, 277-285 (2001).

57. Tuteja,N. & Tuteja,R. Unraveling DNA helicases. Motif, structure, mechanism and function. *Eur. J. Biochem.* **271**, 1849-1863 (2004).

58. Forsburg,S.L. Eukaryotic MCM proteins: beyond replication initiation. *Microbiol. Mol Biol. Rev.* **68**, 109-131 (2004).

59. Kuipers,M.A., Stasevich,T.J., Sasaki,T., Wilson,K.A., Hazelwood,K.L. *et al.* Highly stable loading of Mcm proteins onto chromatin in living cells requires replication to unload. *J. Cell Biol.* **192**, 29-41 (2011).

60. Diffley,J.F. & Labib,K. The chromosome replication cycle. *J. Cell Sci.* **115**, 869-872 (2002).

61. Blow,J.J. & Dutta,A. Preventing re-replication of chromosomal DNA. *Nat. Rev. Mol. Cell Biol.* **6**, 476-486 (2005).

62. Maine,G.T., Sinha,P., & Tye,B.K. Mutants of S. cerevisiae defective in the maintenance of minichromosomes. *Genetics* **106**, 365-385 (1984).

63. Neuwald,A.F., Aravind,L., Spouge,J.L., & Koonin,E.V. AAA+: A class of chaperone-like ATPases associated with the assembly, operation, and disassembly of protein complexes. *Genome Res.* **9**, 27-43 (1999).

64. Labib,K., Tercero,J.A., & Diffley,J.F. Uninterrupted MCM2-7 function required for DNA replication fork progression. *Science* **288**, 1643-1647 (2000).

65. Sclafani,R.A., Fletcher,R.J., & Chen,X.S. Two heads are better than one: regulation of DNA replication by hexameric helicases. *Genes Dev.* **18**, 2039-2045 (2004).

66. Iyer,L.M., Leipe,D.D., Koonin,E.V., & Aravind,L. Evolutionary history and higher order classification of AAA+ ATPases. *J. Struct. Biol.* **146**, 11-31 (2004).

67. Sakakibara,N., Kelman,L.M., & Kelman,Z. Unwinding the structure and function of the archaeal MCM helicase. *Mol. Microbiol.* **72**, 286-296 (2009).

68.   Koonin,E.V. A common set of conserved motifs in a vast variety of putative nucleic acid-dependent ATPases including MCM proteins involved in the initiation of eukaryotic DNA replication. *Nucleic Acids Res.* **21**, 2541-2547 (1993).

69.   Davey,M.J., Indiani,C., & O'Donnell,M. Reconstitution of the Mcm2-7p heterohexamer, subunit arrangement, and ATP site architecture. *J. Biol. Chem.* **278**, 4491-4499 (2003).

70.   Ishimi,Y. A DNA helicase activity is associated with an MCM4, -6, and -7 protein complex. *J. Biol. Chem.* **272**, 24508-24513 (1997).

71.   Schwacha,A. & Bell,S.P. Interactions between two catalytically distinct MCM subgroups are essential for coordinated ATP hydrolysis and DNA replication. *Mol. Cell* **8**, 1093-1104 (2001).

72.   Lee,J.K. & Hurwitz,J. Isolation and characterization of various complexes of the minichromosome maintenance proteins of Schizosaccharomyces pombe. *J. Biol. Chem.* **275**, 18871-18878 (2000).

73.   Tye,B.K. MCM proteins in DNA replication. *Annu. Rev. Biochem* **68**, 649-686 (1999).

74.   Chang,V.K., Fitch,M.J., Donato,J.J., Christensen,T.W., Merchant,A.M. *et al.* Mcm1 binds replication origins. *J. Biol. Chem.* **278**, 6093-6100 (2003).

75.   Chang,V.K., Donato,J.J., Chan,C.S., & Tye,B.K. Mcm1 promotes replication initiation by binding specific elements at replication origins. *Mol. Cell Biol.* **24**, 6514-6524 (2004).

76.   Ricke,R.M. & Bielinsky,A.K. Mcm10 regulates the stability and chromatin association of DNA polymerase-alpha. *Mol Cell* **16**, 173-185 (2004).

77.   Cook,C.R., Kung,G., Peterson,F.C., Volkman,B.F., & Lei,M. A novel zinc finger is required for Mcm10 homocomplex assembly. *J. Biol. Chem.* **278**, 36051-36058 (2003).

78.   Maiorano,D., Lutzmann,M., & Mechali,M. MCM proteins and DNA replication. *Curr. Opin. Cell Biol.* **18**, 130-136 (2006).

79.   Lutzmann,M., Maiorano,D., & Mechali,M. Identification of full genes and proteins of MCM9, a novel, vertebrate-specific member of the MCM2-8 protein family. *Gene* **362**, 51-56 (2005).

80.   Gozuacik,D., Chami,M., Lagorce,D., Faivre,J., Murakami,Y. *et al.* Identification and functional characterization of a new member of the human Mcm protein family: hMcm8. *Nucleic Acids Res.* **31**, 570-579 (2003).

81.   Maiorano,D., Cuvier,O., Danis,E., & Mechali,M. MCM8 is an MCM2-7-related protein that functions as a DNA helicase during replication elongation and not initiation. *Cell* **120**, 315-328 (2005).

82.   Sakwe,A.M., Nguyen,T., Athanasopoulos,V., Shire,K., & Frappier,L. Identification and characterization of a novel component of the human minichromosome maintenance complex. *Mol. Cell Biol.* **27**, 3044-3055 (2007).

83.   Nishiyama,A., Frappier,L., & Mechali,M. MCM-BP regulates unloading of the MCM2-7 helicase in late S phase. *Genes Dev.* **25**, 165-175 (2011).

84.   Costa,A. & Onesti,S. Structural biology of MCM helicases. *Crit Rev. Biochem. Mol. Biol.* **44**, 326-342 (2009).

85.   Slaymaker,I.M. & Chen,X.S. MCM Structure and Mechanics: What We Have Learned from Archaeal MCM. *Subcell. Biochem.* **62**, 89-111 (2012).

86.   Costa,A., van Duinen G., Medagli,B., Chong,J., Sakakibara,N. *et al.* Cryo-electron microscopy reveals a novel DNA-binding site on the MCM helicase. *EMBO J.* **27**, 2250-2258 (2008).

87.   Fletcher,R.J., Bishop,B.E., Leon,R.P., Sclafani,R.A., Ogata,C.M. *et al.* The structure and function of MCM from archaeal M. Thermoautotrophicum. *Nat. Struct. Biol.* **10**, 160-167 (2003).

88.   McGeoch,A.T., Trakselis,M.A., Laskey,R.A., & Bell,S.D. Organization of the archaeal MCM complex on DNA and implications for the helicase mechanism. *Nat. Struct. Mol. Biol.* **12**, 756-762 (2005).

89.   Barry,E.R., McGeoch,A.T., Kelman,Z., & Bell,S.D. Archaeal MCM has separable processivity, substrate choice and helicase domains. *Nucleic Acids Res.* **35**, 988-998 (2007).

90.   Brewster,A.S., Wang,G., Yu,X., Greenleaf,W.B., Carazo,J.M. *et al.* Crystal structure of a near-full-length archaeal MCM: functional insights for an AAA+ hexameric helicase. *Proc. Natl. Acad. Sci. U. S. A* **105**, 20191-20196 (2008).

91.   Remus,D., Beuron,F., Tolun,G., Griffith,J.D., Morris,E.P. *et al.* Concerted loading of Mcm2-7 double hexamers around DNA during DNA replication origin licensing. *Cell* **139**, 719-730 (2009).

92.   Gambus,A., Khoudoli,G.A., Jones,R.C., & Blow,J.J. MCM2-7 form double hexamers at licensed origins in Xenopus egg extract. *J. Biol. Chem.* **286**, 11855-11864 (2011).

93.   Evrin,C., Clarke,P., Zech,J., Lurz,R., Sun,J. *et al.* A double-hexameric MCM2-7 complex is loaded onto origin DNA during licensing of eukaryotic DNA replication. *Proc. Natl. Acad. Sci. U. S. A* **106**, 20240-20245 (2009).

94. Hoang,M.L., Leon,R.P., Pessoa-Brandao,L., Hunt,S., Raghuraman,M.K. *et al.* Structural changes in Mcm5 protein bypass Cdc7-Dbf4 function and reduce replication origin efficiency in Saccharomyces cerevisiae. *Mol. Cell Biol.* **27**, 7594-7602 (2007).

95. Fletcher,R.J. & Chen,X.S. Biochemical activities of the BOB1 mutant in Methanobacterium thermoautotrophicum MCM. *Biochemistry* **45**, 462-467 (2006).

96. Barry,E.R., Lovett,J.E., Costa,A., Lea,S.M., & Bell,S.D. Intersubunit allosteric communication mediated by a conserved loop in the MCM helicase. *Proc. Natl. Acad. Sci. U. S. A* **106**, 1051-1056 (2009).

97. Sakakibara,N., Kasiviswanathan,R., Melamud,E., Han,M., Schwarz,F.P. *et al.* Coupling of DNA binding and helicase activity is mediated by a conserved loop in the MCM protein. *Nucleic Acids Res.* **36**, 1309-1320 (2008).

98. Enemark,E.J. & Joshua-Tor,L. Mechanism of DNA translocation in a replicative hexameric helicase. *Nature* **442**, 270-275 (2006).

99. Leon,R.P., Tecklenburg,M., & Sclafani,R.A. Functional conservation of beta-hairpin DNA binding domains in the Mcm protein of Methanobacterium thermoautotrophicum and the Mcm5 protein of Saccharomyces cerevisiae. *Genetics* **179**, 1757-1768 (2008).

100. Erzberger,J.P. & Berger,J.M. Evolutionary relationships and structural mechanisms of AAA+ proteins. *Annu. Rev. Biophys. Biomol. Struct.* **35**, 93-114 (2006).

101. Gai,D., Zhao,R., Li,D., Finkielstein,C.V., & Chen,X.S. Mechanisms of conformational change for a replicative hexameric helicase of SV40 large tumor antigen. *Cell* **119**, 47-60 (2004).

102. Li,D., Zhao,R., Lilyestrom,W., Gai,D., Zhang,R. *et al.* Structure of the replicative helicase of the oncoprotein SV40 large tumour antigen. *Nature* **423**, 512-518 (2003).

103. Liu,W., Pucci,B., Rossi,M., Pisani,F.M., & Ladenstein,R. Structural analysis of the Sulfolobus solfataricus MCM protein N-terminal domain. *Nucleic Acids Res.* **36**, 3235-3243 (2008).

104. Jenkinson,E.R. & Chong,J.P. Minichromosome maintenance helicase activity is controlled by N- and C-terminal motifs and requires the ATPase domain helix-2 insert. *Proc. Natl. Acad. Sci. U. S. A* **103**, 7613-7618 (2006).

105. Patel,S.S. & Picha,K.M. Structure and function of hexameric helicases. *Annu. Rev. Biochem.* **69**, 651-697 (2000).

106.   Kanter,D.M., Bruck,I., & Kaplan,D.L. Mcm subunits can assemble into two different active unwinding complexes. *J. Biol. Chem.* **283**, 31172-31182 (2008).

107.   Kaplan,D.L., Davey,M.J., & O'Donnell,M. Mcm4,6,7 uses a "pump in ring" mechanism to unwind DNA by steric exclusion and actively translocate along a duplex. *J Biol. Chem.* **278**, 49171-49182 (2003).

108.   Bochman,M.L. & Schwacha,A. The Mcm2-7 complex has in vitro helicase activity. *Mol. Cell* **31**, 287-293 (2008).

109.   Stead,B.E., Sorbara,C.D., Brandl,C.J., & Davey,M.J. ATP binding and hydrolysis by Mcm2 regulate DNA binding by Mcm complexes. *J. Mol. Biol.* **391**, 301-313 (2009).

110.   Bochman,M.L. & Schwacha,A. Differences in the single-stranded DNA binding activities of MCM2-7 and MCM467: MCM2 and MCM5 define a slow ATP-dependent step. *J. Biol. Chem.* **282**, 33795-33804 (2007).

111.   Bochman,M.L. & Schwacha,A. The Saccharomyces cerevisiae Mcm6/2 and Mcm5/3 ATPase active sites contribute to the function of the putative Mcm2-7 'gate'. *Nucleic Acids Res.* **38**, 6078-6088 (2010).

112.   Sato,M., Gotow,T., You,Z., Komamura-Kohno,Y., Uchiyama,Y. *et al.* Electron microscopic observation and single-stranded DNA binding activity of the Mcm4,6,7 complex. *J. Mol. Biol.* **300**, 421-431 (2000).

113.   Takahashi,T.S., Wigley,D.B., & Walter,J.C. Pumps, paradoxes and ploughshares: mechanism of the MCM2-7 DNA helicase. *Trends Biochem. Sci.* **30**, 437-444 (2005).

114.   Lee,J.K. & Hurwitz,J. Processive DNA helicase activity of the minichromosome maintenance proteins 4, 6, and 7 complex requires forked DNA structures. *Proc. Natl. Acad. Sci. U. S. A* **98**, 54-59 (2001).

115.   Moyer,S.E., Lewis,P.W., & Botchan,M.R. Isolation of the Cdc45/Mcm2-7/GINS (CMG) complex, a candidate for the eukaryotic DNA replication fork helicase. *Proc. Natl. Acad. Sci. U. S. A* **103**, 10236-10241 (2006).

116.   Kelman,Z., Lee,J.K., & Hurwitz,J. The single minichromosome maintenance protein of Methanobacterium thermoautotrophicum DeltaH contains DNA helicase activity. *Proc. Natl. Acad. Sci. U. S. A* **96**, 14783-14788 (1999).

117.   Laskey,R.A. & Madine,M.A. A rotary pumping model for helicase function of MCM proteins at a distance from replication forks. *EMBO Rep.* **4**, 26-30 (2003).

118.   Bochman,M.L., Bell,S.P., & Schwacha,A. Subunit organization of Mcm2-7 and the unequal role of active sites in ATP hydrolysis and viability. *Mol. Cell Biol.* **28**, 5865-5873 (2008).

119. Randell,J.C., Fan,A., Chan,C., Francis,L.I., Heller,R.C. *et al.* Mec1 is one of multiple kinases that prime the Mcm2-7 helicase for phosphorylation by Cdc7. *Mol. Cell* **40**, 353-363 (2010).

120. Montagnoli,A., Valsasina,B., Brotherton,D., Troiani,S., Rainoldi,S. *et al.* Identification of Mcm2 phosphorylation sites by S-phase-regulating kinases. *J. Biol. Chem.* **281**, 10281-10290 (2006).

121. Devault,A., Gueydon,E., & Schwob,E. Interplay between S-cyclin-dependent kinase and Dbf4-dependent kinase in controlling DNA replication through phosphorylation of yeast Mcm4 N-terminal domain. *Mol. Biol. Cell* **19**, 2267-2277 (2008).

122. Ilves,I., Petojevic,T., Pesavento,J.J., & Botchan,M.R. Activation of the MCM2-7 helicase by association with Cdc45 and GINS proteins. *Mol. Cell* **37**, 247-258 (2010).

123. Sheu,Y.J. & Stillman,B. The Dbf4-Cdc7 kinase promotes S phase by alleviating an inhibitory activity in Mcm4. *Nature* **463**, 113-117 (2010).

124. Bousset,K. & Diffley,J.F. The Cdc7 protein kinase is required for origin firing during S phase. *Genes Dev.* **12**, 480-490 (1998).

125. Donaldson,A.D., Fangman,W.L., & Brewer,B.J. Cdc7 is required throughout the yeast S phase to activate replication origins. *Genes Dev.* **12**, 491-501 (1998).

126. Lei,M., Kawasaki,Y., Young,M.R., Kihara,M., Sugino,A. *et al.* Mcm2 is a target of regulation by Cdc7-Dbf4 during the initiation of DNA synthesis. *Genes Dev* **11**, 3365-3374 (1997).

127. Weinreich,M. & Stillman,B. Cdc7p-Dbf4p kinase binds to chromatin during S phase and is regulated by both the APC and the RAD53 checkpoint pathway. *EMBO J* **18**, 5334-5346 (1999).

128. Hardy,C.F., Dryga,O., Seematter,S., Pahl,P.M., & Sclafani,R.A. mcm5/cdc46-bob1 bypasses the requirement for the S phase activator Cdc7p. *Proc. Natl. Acad. Sci. U. S. A* **94**, 3151-3155 (1997).

129. Francis,L.I., Randell,J.C., Takara,T.J., Uchima,L., & Bell,S.P. Incorporation into the prereplicative complex activates the Mcm2-7 helicase for Cdc7-Dbf4 phosphorylation. *Genes Dev.* **23**, 643-654 (2009).

130. Stead,B.E., Brandl,C.J., & Davey,M.J. Phosphorylation of Mcm2 modulates Mcm2-7 activity and affects the cell's response to DNA damage. *Nucleic Acids Res.* **39**, 6998-7008 (2011).

131. Stead,B.E., Brandl,C.J., Sandre,M.K., & Davey,M.J. Mcm2 phosphorylation and the response to replicative stress. *BMC. Genet.* **13**, 36 (2012).

132.   Sheu,Y.J. & Stillman,B. Cdc7-Dbf4 phosphorylates MCM proteins via a docking site-mediated mechanism to promote S phase progression. *Mol Cell* **24**, 101-113 (2006).

133.   Brown,G.W. & Kelly,T.J. Purification of Hsk1, a minichromosome maintenance protein kinase from fission yeast. *J. Biol. Chem.* **273**, 22083-22090 (1998).

134.   Myung,K., Chen,C., & Kolodner,R.D. Multiple pathways cooperate in the suppression of genome instability in Saccharomyces cerevisiae. *Nature* **411**, 1073-1076 (2001).

135.   Santocanale,C. & Diffley,J.F. A Mec1- and Rad53-dependent checkpoint controls late-firing origins of DNA replication. *Nature* **395**, 615-618 (1998).

136.   Shirahige,K., Hori,Y., Shiraishi,K., Yamashita,M., Takahashi,K. *et al.* Regulation of DNA-replication origins during cell-cycle progression. *Nature* **395**, 618-621 (1998).

137.   Sanchez,Y., Bachant,J., Wang,H., Hu,F., Liu,D. *et al.* Control of the DNA damage checkpoint by chk1 and rad53 protein kinases through distinct mechanisms. *Science* **286**, 1166-1171 (1999).

138.   Weinert,T.A., Kiser,G.L., & Hartwell,L.H. Mitotic checkpoint genes in budding yeast and the dependence of mitosis on DNA replication and repair. *Genes Dev.* **8**, 652-665 (1994).

139.   Sanchez,Y., Desany,B.A., Jones,W.J., Liu,Q., Wang,B. *et al.* Regulation of RAD53 by the ATM-like kinases MEC1 and TEL1 in yeast cell cycle checkpoint pathways. *Science* **271**, 357-360 (1996).

140.   Cliby,W.A., Roberts,C.J., Cimprich,K.A., Stringer,C.M., Lamb,J.R. *et al.* Overexpression of a kinase-inactive ATR protein causes sensitivity to DNA-damaging agents and defects in cell cycle checkpoints. *EMBO J.* **17**, 159-169 (1998).

141.   Zhao,X., Muller,E.G., & Rothstein,R. A suppressor of two essential checkpoint genes identifies a novel protein that negatively affects dNTP pools. *Mol. Cell* **2**, 329-340 (1998).

142.   Zegerman,P. & Diffley,J.F. DNA replication as a target of the DNA damage checkpoint. *DNA Repair (Amst)* **8**, 1077-1088 (2009).

143.   Chabes,A., Domkin,V., & Thelander,L. Yeast Sml1, a protein inhibitor of ribonucleotide reductase. *J. Biol. Chem.* **274**, 36679-36683 (1999).

144. Hofmann,J.F. & Beach,D. cdt1 is an essential target of the Cdc10/Sct1 transcription factor: requirement for DNA replication and inhibition of mitosis. *EMBO J.* **13**, 425-434 (1994).

145. Nishitani,H., Lygerou,Z., Nishimoto,T., & Nurse,P. The Cdt1 protein is required to license DNA for replication in fission yeast. *Nature* **404**, 625-628 (2000).

146. Devault,A., Vallen,E.A., Yuan,T., Green,S., Bensimon,A. *et al.* Identification of Tah11/Sid2 as the ortholog of the replication licensing factor Cdt1 in Saccharomyces cerevisiae. *Curr. Biol.* **12**, 689-694 (2002).

147. Whittaker,A.J., Royzman,I., & Orr-Weaver,T.L. Drosophila double parked: a conserved, essential replication protein that colocalizes with the origin recognition complex and links DNA replication with mitosis and the down-regulation of S phase transcripts. *Genes Dev.* **14**, 1765-1776 (2000).

148. Wohlschlegel,J.A., Dwyer,B.T., Dhar,S.K., Cvetic,C., Walter,J.C. *et al.* Inhibition of eukaryotic DNA replication by geminin binding to Cdt1. *Science* **290**, 2309-2312 (2000).

149. Tanaka,S. & Diffley,J.F. Interdependent nuclear accumulation of budding yeast Cdt1 and Mcm2-7 during G1 phase. *Nat. Cell Biol.* **4**, 198-207 (2002).

150. Fernandez-Cid,A., Riera,A., Tognetti,S., Herrera,M.C., Samel,S. *et al.* An ORC/Cdc6/MCM2-7 complex is formed in a multistep reaction to serve as a platform for MCM double-hexamer assembly. *Mol. Cell* **50**, 577-588 (2013).

151. Randell,J.C., Bowers,J.L., Rodriguez,H.K., & Bell,S.P. Sequential ATP hydrolysis by Cdc6 and ORC directs loading of the Mcm2-7 helicase. *Mol Cell* **21**, 29-39 (2006).

152. Ferenbach,A., Li,A., Brito-Martins,M., & Blow,J.J. Functional domains of the Xenopus replication licensing factor Cdt1. *Nucleic Acids Res.* **33**, 316-324 (2005).

153. Jee,J., Mizuno,T., Kamada,K., Tochio,H., Chiba,Y. *et al.* Structure and mutagenesis studies of the C-terminal region of licensing factor Cdt1 enable the identification of key residues for binding to replicative helicase Mcm proteins. *J. Biol. Chem.* **285**, 15931-15940 (2010).

154. Yanagi,K., Mizuno,T., You,Z., & Hanaoka,F. Mouse geminin inhibits not only Cdt1-MCM6 interactions but also a novel intrinsic Cdt1 DNA binding activity. *J. Biol. Chem.* **277**, 40871-40880 (2002).

155. You,Z. & Masai,H. Cdt1 forms a complex with the minichromosome maintenance protein (MCM) and activates its helicase activity. *J. Biol. Chem.* **283**, 24469-24477 (2008).

156. Takara,T.J. & Bell,S.P. Multiple Cdt1 molecules act at each origin to load replication-competent Mcm2-7 helicases. *EMBO J.* **30**, 4885-4896 (2011).

157. Frigola,J., Remus,D., Mehanna,A., & Diffley,J.F. ATPase-dependent quality control of DNA replication origin licensing. *Nature* **495**, 339-343 (2013).

158. Samson,R.Y. & Bell,S.D. MCM loading--an open-and-shut case? *Mol. Cell* **50**, 457-458 (2013).

159. Pacek,M. & Walter,J.C. A requirement for MCM7 and Cdc45 in chromosome unwinding during eukaryotic DNA replication. *EMBO J* **23**, 3667-3676 (2004).

160. Tercero,J.A., Labib,K., & Diffley,J.F. DNA synthesis at individual replication forks requires the essential initiation factor Cdc45p. *EMBO J.* **19**, 2082-2093 (2000).

161. Kanemaki,M., Sanchez-Diaz,A., Gambus,A., & Labib,K. Functional proteomic identification of DNA replication proteins by induced proteolysis in vivo. *Nature* **423**, 720-724 (2003).

162. Aparicio,O.M., Weinstein,D.M., & Bell,S.P. Components and dynamics of DNA replication complexes in S. cerevisiae: redistribution of MCM proteins and Cdc45p during S phase. *Cell* **91**, 59-69 (1997).

163. Aparicio,T., Ibarra,A., & Mendez,J. Cdc45-MCM-GINS, a new power player for DNA replication. *Cell Div.* **1**, 18 (2006).

164. Calzada,A., Hodgson,B., Kanemaki,M., Bueno,A., & Labib,K. Molecular anatomy and regulation of a stable replisome at a paused eukaryotic DNA replication fork. *Genes Dev* **19**, 1905-1919 (2005).

165. Costa,A., Ilves,I., Tamberg,N., Petojevic,T., Nogales,E. *et al.* The structural basis for MCM2-7 helicase activation by GINS and Cdc45. *Nat. Struct. Mol. Biol.* **18**, 471-477 (2011).

166. Makarova,K.S., Koonin,E.V., & Kelman,Z. The CMG (CDC45/RecJ, MCM, GINS) complex is a conserved component of the DNA replication system in all archaea and eukaryotes. *Biol. Direct.* **7**, 7 (2012).

Chapter 2

2   The C-terminal residues of *Saccharomyces cerevisiae* Mec1 are required for its localization, stability and function

Mec1, a member of the PIKK (phosphoinositide three-kinase-related kinase) family of proteins, is involved in the response to replicative stress and DNA damage, and in telomere maintenance. An essential 30-35 residue FATC domain is found at the C-terminus of all PIKK family members. To investigate the roles of the C-terminal residues of Mec1, we characterized alleles of *Saccharomyces cerevisiae mec1* that alter the FATC domain. A change of the terminal tryptophan to alanine resulted in temperature sensitive growth, sensitivity to hydroxyurea, and diminished kinase activity *in vitro*. Addition of a terminal glycine or deletion of one, two or three residues resulted in loss of cell viability and kinase function. Each of these Mec1 derivatives was less stable than wild-type Mec1, eluted abnormally from a size exclusion column, and showed reduced nuclear localization. We identified *rpn3-L140P*, which encodes a component of the 19S proteasomal regulatory particle of the 26S proteasome, as a suppressor of the temperature-sensitive growth caused by *mec1-W2368A*. The *rpn3-L140P* allele acted in a partially dominant fashion. It was neither able to suppress the inviability of the C-terminal truncations or additions, nor the hydroxyurea sensitivity of *mec1-W2368A*. The *rpn3-L140P* allele restored Mec1-W2368A to near wild-type protein levels at 37°C, an effect partially mimicked by the proteasome inhibitor MG-132. Our study supports a role for the C-terminus in Mec1 folding and stability, and suggests a role for the proteasome in regulating Mec1 levels.

2.1   Introduction

Members of the PIKK (phosphoinositide three-kinase-related kinase) family of proteins are important in the cellular response to various forms of stress (reviewed in 1). The PIKK proteins are large (for example, Tra1 and Mec1 are 3744 and 2368 residues, respectively), and are characterized by a C-terminally positioned domain that resembles the phosphatidylinositol-3-kinases (PI3K) [1-3].

Three members of the PIKK family have principal roles in DNA damage response (DDR) pathways. ATM (ataxia telangiectasia mutated, Tel1 in *S. cerevisiae*), ATR (ataxia telangiectasia and Rad3-related, Mec1 in *S. cerevisiae*), and the DNA-PKcs (DNA-dependent protein kinase catalytic subunit) transmit and amplify the damage signal through the phosphorylation of target proteins. Recruitment to sites of DNA damage is critical for their activation and function in checkpoint signaling and DNA repair (reviewed in 4). ATM/Tel1 acts principally in response to double strand breaks, whereas ATR/Mec1 responds to a number of DNA insults and particularly replicative stress caused by stalled replication forks (reviewed in 5). Both have roles in the maintenance of stable telomeres [6-8]. DNA-PKcs acts with Ku70 and Ku80 in nonhomologous end-joining of double strand breaks; a direct homolog has not been found in *S. cerevisiae*.

Mec1/ATR is an essential gene (reviewed in 9). It is recruited to stalled replication forks and sites of DNA damage through the direct interaction of its associated protein Lcd1/Ddc2 with RPA-coated single stranded DNA [10-14]. This recruitment is part of a series of events, which results in the phosphorylation of regulatory and effector molecules that activate a cell cycle checkpoint and/or apoptotic signals. Mec1 target molecules include histone H2A [15, 16], RPA [17], components of the Mcm2-7 DNA helicase complex [18, 19], the Ino80 subunit Ies4 [20], and the effector kinases Rad53 and Chk1 [21-23]. Fork stabilization is the essential function of Mec1 [24, 25] and occurs through multiple mechanisms including retaining DNA polymerase at the replication fork [26]. In addition, Mec1 is required to activate the expression of ribonucleotide reductase thus enhancing deoxyribonucleotide synthesis following DNA damage and perhaps during normal S phase (reviewed in 27). This function can be bypassed by increasing deoxyribonucleotide levels either by overexpressing Rnr3, one of the catalytic subunits of ribonucleotide reductase, or by deletion of the ribonucleotide reductase inhibitor Sml1 [24, 28]. Interestingly, Mec1 and ATR are required to prevent chromosome breaks even in the absence of genotoxic stress. Augmenting deoxyribonucleotide levels does not rescue the checkpoint defects or DNA damage sensitivity of cells lacking functional Mec1 [28].

Other PIKK family members include SMG-1 (suppressor with morphological effect on genitalia family member), TOR (target of rapamycin) and TRRAP (Transformation/transcription domain-associated protein). SMG-1 is found in metazoans. It has many similar roles related to genotoxic stress [29, 30] and telomere stability [31] as ATM and ATR, and is also the key signaling molecule required for the nonsense mediated decay pathway (reviewed in 32). TOR is found in two complexes, TORC1 and TORC2. TORC1 integrates nutrient and growth factor signals, inducing anabolic pathways including protein synthesis and inhibiting catabolic pathways (reviewed in 33). TORC2 is involved in spatial control of cell growth by regulating the actin cytoskeleton (reviewed in 34). The only member of the PIKK family that is not a Ser/Thr kinase is the transcriptional cofactor TRRAP [35, 36]. The *S. cerevisiae* homolog Tra1 is an essential component of the multisubunit, multifunctional SAGA and NuA4 histone acetyltransferase complexes [36, 37]. A key role for Tra1 is to recruit HAT complexes to promoters via its association with transcriptional activators [38-41].

As well as having the PI3K domain, the PIKK proteins share a number of other features. N-terminal to the PI3K domain is a FAT (FRAP-ATM-TRRAP) domain that consists largely of helical HEAT (Huntington, Elongation Factor 3, PR65/A, TOR) and TPR (tetratricopeptide) repeats; in fact, these repeats extend through to the proteins' N-termini making most of the protein helical [42-45]. C-terminal to the PI3K domain is a less highly conserved PRD (PIKK regulatory domain) [46]. At the C-terminus of the PIKK molecules is the 30-35 residue FATC domain [42]. The structure of the isolated FATC domain of *S. cerevisiae* Tor1 [47] is helical with a C-terminal loop held in place by a disulphide linkage. Though the cysteines are not conserved and the cellular FATC domain is not likely to always exist in an oxidized state, the helical structure is likely conserved [2, 48]. The crystal structure of mTOR (mammalian target of rapamycin) including the FAT through to the C-terminus reveals that the FATC domain is an integral part of the kinase, positioned adjacent to the activation loop [49]. The substrate binding groove also includes portions of the FATC domain. The importance of the FATC domain has been demonstrated with molecular studies. Deletion of the C-terminus of mTOR, or mutation of a conserved tryptophan five residues from the C-terminus, eliminate kinase activity [50]. Similar mutations within the FATC domains of DNA-PKcs and SMG-1 cause

a loss of kinase activity [51-53]. As suggested by Lempiäinen and Halazonetis [2] the FATC domain likely regulates the kinase domain through interactions with the activation loop similar to the helical domains of the PI3-kinases. The FATC domain is also critical for the function of Tra1. Addition of as little as a single glycine to the C-terminus of Tra1 results in loss of cellular viability [54]. A strain with a mutation of the terminal phenylalanine residue of Tra1 to alanine (*tra1-F3744A*) shows growth defects, including temperature sensitivity and slow growth on media containing ethanol, Calcofluor white or rapamycin. The F3744A mutation also results in mislocalization of the protein to the cytoplasm, particularly under conditions of stress [55]. We identified a partially dominant mutation within *tti2* as a suppressor of *tra1-F3744A* [55]. *TTI2* encodes a component of the TTT (Tel2, Tti1 and Tti2) complex that associates with chaperone proteins in the folding of PIKK proteins [56-60] . This suggested that the C-terminal residue of the molecule is required for folding, and was consistent with the *tti2* suppressor mutation decreasing the proteolytic degradation of Tra1-F3744A, and increasing its nuclear localization.

To determine if the C-terminus of the FATC domain is a general requirement for the folding and function of the PIKK proteins, we have examined alleles of *mec1* that disrupt this domain. Addition or deletion of residues results in loss of viability and kinase activity. Proteins containing these insertions or deletions, as well as a C-terminal change of tryptophan to alanine have reduced nuclear localization, and elute from a gel filtration column with an abnormally high molecular mass. They are also less stable after isolation than the wild-type protein. A second site mutation of *rpn3-L140P*, which encodes a component of the 19S proteasomal regulatory particle, restores the levels of the Mec1-W2368A protein and growth of the *mec1-W2368A* strain at 37°C, further supporting a role for the C-terminus in protein folding and stability.

2.2   Materials and Methods

2.2.1   Yeast strains and growth

Yeast strains are listed in Table 2.1 and are derivatives of the diploid strain BY4743 [61]. Strains containing one Flag^5-tagged (CY6172) or eGFP-tagged (CY6295) *MEC1* allele, marked with *URA3*, were made by one–step integration of the *Sph*I-*Eco*RI fragments of

Table 2.1

Table 2.1: Strains used in this study.

Strain	Genotype	Reference
BY4743	*MATa/α his3Δ1/his3Δ1 leu2Δ0/leu2Δ0 LYS2/lys2Δ0 met15Δ0/MET15 ura3Δ0/ura3Δ0*	Winzeler and Davis (1997)
BY4741	*MATa ura3Δ0 met15Δ0 his3Δ0 leu2Δ0*	Winzeler and Davis (1997)
BY4742	*MATα ura3Δ0 lys2Δ0 his3Δ0 leu2Δ0*	Winzeler and Davis (1997)
CY4350	*MATa ura3Δ0 his3Δ0 leu2Δ0 tra1-F3744A-HIS3*	Hoke et al. (2010)
CY4353	*MATa ura3Δ0 his3Δ0 leu2Δ0 TRA1-HIS3*	Hoke et al. (2010)
CY6076	*MATa ura3Δ0 his3Δ0 leu2Δ0 mec1-W2368A-HIS3*	Genereaux *et al.* (2012)
CY6077	*MATα ura3Δ0 his3Δ0 leu2Δ0 mec1-W2368A-HIS3*	This work
CY6106	*MATa ura3Δ0 his3Δ0 leu2Δ0 mec1-W2368A-URA3*	This work
CY6172	Isogenic to BY4743 except *MEC1/URA3-Flag[5]-MEC1*	This work
CY6175	*MATa ura3Δ0 his3Δ0 leu2Δ0 URA3-Flag[5]-mec1-W2368A-HIS3*	This work
CY6192	Isogenic to BY4743 except *MEC1/URA3-Flag[5]-mec1-W2368A-HIS3*	This work
CY6184	Isogenic to BY4743 except *MEC1/URA3-Flag[5]-mec1-Δ1-HIS3*	This work
CY6194	*MATa ura3Δ0 his3Δ0 leu2Δ0 URA3-Flag[5]-MEC1*	This work
CY6203	Isogenic to BY4743 except *MEC1/URA3-Flag[5]-mec1-2369G-HIS3*	This work
CY6233	Isogenic to BY4743 except *MEC1/URA3-Flag[5]-mec1-Δ3-HIS3*	This work
CY6250	Isogenic to BY4743 except *MEC1/URA3-Flag[5]-mec1-Δ2-HIS3*	This work
CY6265	*MATα ura3Δ0 his3Δ0 leu2Δ0 mec1-W2368A-URA3 rpn3-L140P*	This work
CY6291	Isogenic to BY4743 except *LEU2-MEC1/URA3-eGFP-MEC1-Δ1-HIS3*	This work
CY6292	Isogenic to BY4743 except *LEU2-MEC1/URA3-eGFP-MEC1-Δ3-HIS3*	This work
CY6293	Isogenic to BY4743 except *LEU2-MEC1/URA3-eGFP-mec1-2369G-HIS3*	This work
CY6294	Isogenic to BY4743 except *LEU2-MEC1/URA3-eGFP-MEC1-Δ2-HIS3*	This work
CY6295	Isogenic to BY4743 except *MEC1/URA3-eGFP-MEC1*	This work
CY6296	Isogenic to BY4743 except *MEC1/URA3-eGFP-mec1-W2368A-HIS3*	This work
CY6302	*MATa ura3Δ0 his3Δ0 leu2Δ0 URA3-eGFP-mec1-W2368A-HIS3*	This work
CY6303	*MATα ura3Δ0 his3Δ0 leu2Δ0 URA3-eGFP-mec1-W2368A-HIS3*	This work

CY6306	*MAT**α** ura3Δ0 his3Δ0 leu2Δ0 URA3-eGFP-MEC1*	This work
CY6307	*MAT**a** ura3Δ0 his3Δ0 leu2Δ0 URA3-eGFP-MEC1*	This work
CY6319	*MAT**a** ura3Δ0 his3Δ0 leu2Δ0 sml1Δ0::KanMX URA3-eGFP-MEC1*	This work
CY6321	*MAT**a** ura3Δ0 his3Δ0 leu2Δ0 sml1Δ0::KanMX URA3-Flag^5-MEC1*	This work
CY6330	*MAT**a** ura3Δ0 his3Δ0 leu2Δ0 sml1Δ0::KanMX URA3-eGFP-mec1-Δ1-HIS3*	This work
CY6342	*MAT**a** ura3Δ0 his3Δ0 leu2Δ0 sml1Δ0::KanMX URA3-eGFP-mec1-2369G-HIS3*	This work
CY6344	*MAT**a** ura3Δ0 his3Δ0 leu2Δ0 sml1Δ0::KanMX URA3-eGFP-mec1-Δ2-HIS3*	This work
CY6349	*MAT**a** ura3Δ0 his3Δ0 leu2Δ0 sml1Δ0::KanMX URA3-Flag^5-mec1-2369G-HIS3*	This work
CY6391	*MAT**α** ura3Δ0 his3Δ0 leu2Δ0 mec1-W2368A-HIS3 rpn3-L140P*	This work
CY6398	*MAT**a** ura3Δ0 his3Δ0 leu2Δ0 rpn3-L140P*	This work
CY6399	*MAT**α** ura3Δ0 his3Δ0 leu2Δ0 rpn3-L140P*	This work
CY6400	*MAT**a**/**α** ura3Δ0/ura3Δ0 his3Δ0/his3Δ0 leu2Δ0/leu2Δ0 URA3- Flag^5-mec1-W2368A/MEC1 rpn3-L140P/rpn3-L140P*	This work
CY6418	*MAT**a** ura3Δ0 his3Δ0 leu2Δ0 tra1-F3744A-HIS3 rpn3-L140P*	This work
CY6449	*MAT**a** ura3Δ0 his3Δ0 leu2Δ0 sml1Δ0::KanMX URA3-Flag^5-mec1-2369G-HIS3 rpn3-L140P*	This work

pCB2363 and pCB2395, respectively. Expression of these alleles is driven by the *TRA1* promoter. Integration of the *mec1-W2368A* allele has been previously described [55]. This strain, strains with C-terminal truncations of one, two or three residues (*mec1-Δ1, Δ2* and *Δ3*), and the strain with the addition of a glycine residue (*mec1-2369G*) were similarly integrated as *Sph*I-*Sac*I fragments of a *HIS3*-tagged allele. Haploid strains containing *mec1-W2368A* (CY6175) or wild-type *MEC1* (CY6194) were generated by sporulation of their respective diploid strains. Haploid strains containing *mec1* deletion and addition alleles were made by integrating the *mec1* allele into CY6319 or CY6321, *MATa sml1::KanMX* deletion strains derived from the consortium collection, and containing *eGFP-MEC1 or Flag^5-MEC1*, respectively. Diploid strains expressing eGFP-tagged Mec1, Mec1-W2388A, Mec1-Δ1, Mec1-Δ2 or Mec1-2369G, and RFP-tagged Nic96 were made by mating of CY6307, CY6302, CY6330, CY6344 and CY6342 with the RFP-tagged *NIC96* strain in the EY0987 background (*MATα his3Δ1 lys2Δ0 ura3Δ0*; [62]; kindly provided by Peter Arvidson). CY6265 containing *mec1-W2368A* and *rpn3-L140P* was isolated in the selection scheme described below. CY6398 (*rpn3-L140P*) was obtained after backcrossing with BY4741. The diploid strain CY6400 (*MEC1/Flag^5-mec1-W2368A rpn3-L140P/rpn3-L140P*) was obtained by mating of CY6391 and CY6399. CY6418 (*tra1-W3744A rpn3-L140P*) was obtained after crossing with CY4350 [55] and selecting for spore colonies that grew in the absence of histidine and carried the *rpn3-L140P* allele as determined by sequencing. CY6465 was derived from CY6076 by integrating *rpn3-L140P* contained in the *URA3*-containing yeast integrating plasmid YIPlac211 (CB2457) after digestion with *Bsa*B1.

Growth comparisons were performed on YP media containing 2% glucose (YPD) or selective plates after 3-5 days at 30°C unless stated otherwise. Standard concentrations used for the selections were 0.03% methyl methanesulfonate (Sigma-Aldrich), 6% ethanol and 200 mM hydroxyurea (Sigma-Aldrich). Growth on plates containing MG-132 (Calbiochem) were adapted from Liu *et al.* [63], conditions which permeablize cells. Strains were grown overnight in synthetic complete media lacking uracil and containing 0.1% proline as the nitrogen source, then four hours in the same media also containing 0.003% sodium dodecyl sulphate (SDS). Serial dilutions were spotted onto synthetic complete media containing 0.003% sodium dodecyl sulphate and 10, 25 or 50 μM MG-

132 and grown at 30°C.

2.2.2 DNA molecules

An integrative vector to generate Flag[5] (pCB6192) fusion of Mec1 was constructed from pCB2143 [55], by replacing *TRA1* flanking sequences with *MEC1* as *Sph*I-*Hin*dIII and *Not*I-*Eco*RI fragments using oligonucleotides 6288-1/6288-2 and 6288-3/6288-4 (Table 2.2). A 1.1 kilobase pair *Hin*dIII genomic fragment encoding *URA3* was inserted into this molecule to allow selection. The plasmid pCB6295 allowing integration of eGFP was created from pCB2143 by the replacement of the Flag cassette with a *Bam*HI-*Not*1 cassette encoding eGFP [54]. The *mec1* mutant alleles were constructed by PCR using the oligonucleotides indicated in Table 2 and inserted into pCB2317 (*mec1-W2368A*). Myc[9]-tagged *LCD1* and *RPN3* were expressed from the *DED1* promoter in YCplac111, a *LEU2* centromeric plasmid, by inserting a *Not*I-*Sst*I fragment amplified from genomic DNA using oligonucleotides 6486-1/6486-2 and 6518-1/6522-1, respectively, downstream of the *DED1* promoter-myc[9] cassette [54]. For integration in cells, *rpn3-L140P* including its native promoter was synthesized by PCR using oligonucleotides 6577-1 and 6510-2 and cloned as a *Hin*dIII-*Eco*R1 fragment into YIPlac211.

Table 2.2

Table 2.2: Oligonucleotides used in this study.

Number	Sequence	Description
6288-1	5'-ATAAGGCGGCCGCCATGGAATCACACGTCAAATATC-TTG-3'	5' coding region of *MEC1* to insert tags
6288-2	5'-ATATGTCGACCGCCTCATAAACCATATTCTGTG-3'	5' coding region of *MEC1* to insert tags
6288-3	5'-TTCGCATGCCTTTTCAAGGCTCCATAACTAT-3'	*MEC1* promoter region to insert tags
6288-4	5'-GGAAAGCTTGGAGCGTGCGTTCCATCTA-3'	*MEC1* promoter region to insert tags
6313-1	5'-AAGCTTGCATGCGTTGATGAATGTG-3'	3' coding region of *MEC1* for cloning of deletions
6313-2	5'-GCGTGATCAAAATGGAAGCCAACCAATATAC-3'	*mec1-Δ1*
6338-1	5'-GCGTGATCATGGAAGCCAACCAATATACATC-3'	*mec1-Δ2*
6338-2	5'-GCGTGATCAACCCCAAAATGGAAGCCAACCAATATA-CATC-3'	*mec1-2369G*
6349-3	5'-GCGTGATCAAAGCCAACCAATATACATCTTGC-3'	*mec1-Δ3*
6408-1	5'-CCCAGTCCGCCCTGAGCAAAG-3'	eGFP to confirm integration of tag
6408-2	5'-CCGTAAAATTCGACACATGCTTTG-3'	5' coding of *MEC1* to confirm integration of tags
6486-1	5'-ATAAGAATGCGGCCGCGATGAGACGAGAAACGGTG-GG-3'	5' coding of *LCD1*
6486-2	5'-CGGAATTCCAAACCGGTTCTGCTAAG	3' coding of *LCD1*
6518-1	5'-ATAAGAATGCGGCCGCAATGGCTAGCACTGCAGTA-AT-3'	5' coding of *RPN3*
6522-1	5'-CGGAATTCGCGCCCTTATAAGAATCCCAAATCG-3'	3' coding of *RPN3*
6577-1	5'-CCCAAGCTTCGGAGTACGACCAGACGCTGA-3'	Promoter of *RPN3*

2.2.3   Fluorescence Microscopy

Yeast cells expressing eGFP and/or RFP fusions were grown in synthetic complete media to stationary phase then diluted 1:20 into synthetic complete media and grown for six hours with shaking. Fluorescent images were obtained using a Zeiss Axioskop 2 microscope driven by ImageJ 1.41 software (National Institutes of Health) and a Scion CFW Monochrome CCD Firewire Camera (Scion Corporation, Frederick Maryland) using RFP and GFP filter sets.

2.2.4   Protein extracts and immunoprecipitation

Yeast strains were grown in YP media containing 2% glucose to an A_{600}~3.0. Extracts were prepared cryogenically as previously described [64] . For immunoprecipitations, all steps were performed at 4°C. 4.0 mg of extract from the Mec1 derivative strains or 2 mg of the wild-type extract was suspended in IP buffer (50 mM HEPES pH 7.5, 100 mM KCl, 0.1 mM EDTA, 0.2% Tween20, 1.0 mM dithiothreitol) containing protease inhibitors (1.0 mM phenylmethylsulfonyl fluoride, 1.0 mM benzamidine, 50 μg/ml trypsin inhibitor, 5 μg/ml pepstatin and 5 μg/ml leupeptin; Sigma-Aldrich). Immunoprecipitations were performed with 100 μl of a 50% slurry of anti-Flag M2 magnetic beads (Sigma-Aldrich) and rotated for 2.5 hours. Beads were washed five-times with 1.0 ml of IP buffer. Protein was eluted in 1x-SDS loading buffer (without reducing agent) at 65° for 6 minutes, and then transferred to a fresh tube. Dithiothreitol was added to 20 mM and the sample heated at 65° for 2 minutes.

2.2.5   Protein kinase assays

Proteins captured by immunoprecipitation described above were processed as in Mallory and Petes [65] with modifications. Washed anti-Flag M2 beads (30 μl) containing the immunoprecipitated proteins were resuspended at a ratio of 1:1 in kinase buffer (10 mM Hepes-NaOH, pH 7.4; 50 mM NaCl; 10 mM MnCl2; 1 mM DTT). Kinase reactions contained the washed beads in which buffer was removed and 11.5 μl of kinase buffer, 1.5 μl of 200 μM ATP, 10 μCi of γ-32P-labeled ATP (4500 Ci/mmol; 1 Ci = 37 GBq) and 1 μl of rat 4E-BP1 (1μg/μl; Santa Cruz Biotechnology, Inc.). The reactions were performed at 30°C for 30 min. Protein was eluted in 1x SDS loading buffer, boiled for

two minutes and then separated on a 15% Tris-Tricine PAGE gel. The gel was stained with Coomassie brilliant blue, destained and incubated 30 min in 20% polyethylene glycol 400: 50% methanol. The gel was dried, exposed to a storage phosphor screen and analyzed on a Storm 860 Phosphorimager (GE Healthcare Life Sciences). Densitometry analysis of the gel image was done using ImageQuant 5.2 (Molecular Dynamics).

2.2.6 Gel filtration chromatography

4.5 mg of yeast extract prepared in 50 mM sodium phosphate pH 7.0, 150 mM NaCl was loaded at a flow rate of 0.3 ml/min. onto a 24 ml FPLC Superose 6HR10/30 column (Amersham Pharmacia Biotech.). Protein from 20 µl aliquots of 250 µl fractions was resolved by SDS-PAGE and proteins detected by western blotting. Densitometric scanning of films was performed using AlphaImager 3400 software (Alpha Innotech, San Leandro, CA).

2.2.7 Western blotting

Western blotting was performed using PVDF membranes and anti-Flag (M2; Sigma-Aldrich) or anti-Myc antibodies as described by Mutiu *et al.* [66] and Hoke *et al.* [54].

2.2.8 Selection of suppressor strains

CY6106 (*mec1-W2368A-URA3*) was grown to stationary phase in YPD. In two separate experiments, 10 µl of culture, approximately 2 million cells, was plated onto each of five YPD plates and UV irradiated at a wavelength of 302 nm for 10 s. Survival was approximately 10%. Colonies growing at 37°C were colony purified under nonselective conditions and reanalyzed for growth at 37°C. The suppressor strains were crossed with the *HIS3*-tagged *mec1-W2368A* strain, CY6077, to determine linkage of the suppressor with *mec1-W2368A*. In the two selections, nine strains had an unlinked suppressor mutation that segregated in a 2:2 fashion. Spore colonies of each were backcrossed with BY4741 or BY4742 six times and a nonmutated *mec1-W2368A* strain three times at each stage, selecting for temperature resistant spore colonies. The final isolates were sent for genomic sequencing as described below. The *rpn3* mutation was verified after isolation of genomic DNA, PCR with oligonucleotides 6510-1 and 6510-2 (Table 2) and

sequencing of the PCR product using oligonucleotide 6510-1 as primer.

2.2.9   Genomic sequence analysis

Genomic DNAs were prepared from CY6076, CY6077 and four sister spore colonies from the final backcross of each of suppressor strains as described previously [55]. The DNAs from CY6076 and CY6077 were pooled, as were those from each of the identical suppressor strains, and 5 µg of DNA from each pooled sample was sent to the Biodiversity Research Centre (University of British Columbia; Vancouver, Canada) for DNA library construction and next-generation sequencing using 100 base pair paired-end reads with the Illumina HiSeq 2000 platform. The *Saccharomyces cerevisiae* genome sequence was downloaded from the *Saccharomyces* Genome Database (SGD; http://www.yeastgenome.org) on March 24, 2011. Custom bash and Perl scripts were written for the sequencing analysis. The program Bowtie [67], allowing up to three mismatches per read, was used to map the reads to each chromosome of the yeast genome and output mapped reads in SAM format (Sequence Alignment/Map; [68]). The VCF (variant call format) from SAMtools [68] was used to obtain a raw list of polymorphisms from the mapped reads. Those reads with a Phred quality score below 20 were eliminated to obtain a filtered list of polymorphisms. A custom Perl script was written to identify those polymorphisms that were unique to the suppressor strain.

2.3   Results

The penultimate and terminal amino acid residues of the PIKK molecules are hydrophobic in family members (Figure 2.1A). Changing the terminal phenylalanine of Tra1 to alanine (*tra1*-F3744A) results in stress-related phenotypes and partial mislocalization of the protein to the cytoplasm [55]. This mutation was suppressible by a F328S change in the chaperone component Tti2. A similar mutation in the terminal tryptophan of Mec1 (Mec1-W2368A) results in temperature sensitive growth, but is not suppressible by *tti2-F328S* [55]. Here we characterize Mec1 derivatives, altered at their C-terminus to determine if the FATC domain has a general role in stability of PIKK family members. For these studies we constructed strains that express a genomically encoded allele with either five tandem copies of the Flag epitope (Flag^5) or eGFP tag positioned at

A

C-terminal sequence

```
DNLSKMYIGWLPFW  Mec1
RNLARTDVNFMPWF  Tra1
ERLCQHYIGWCPFW  Tor1
ENLCQHYIGWCPFW  Tor2
SNLSVIYMGWSPFY  Tel1
 NL   Y GW PF   Cons
```
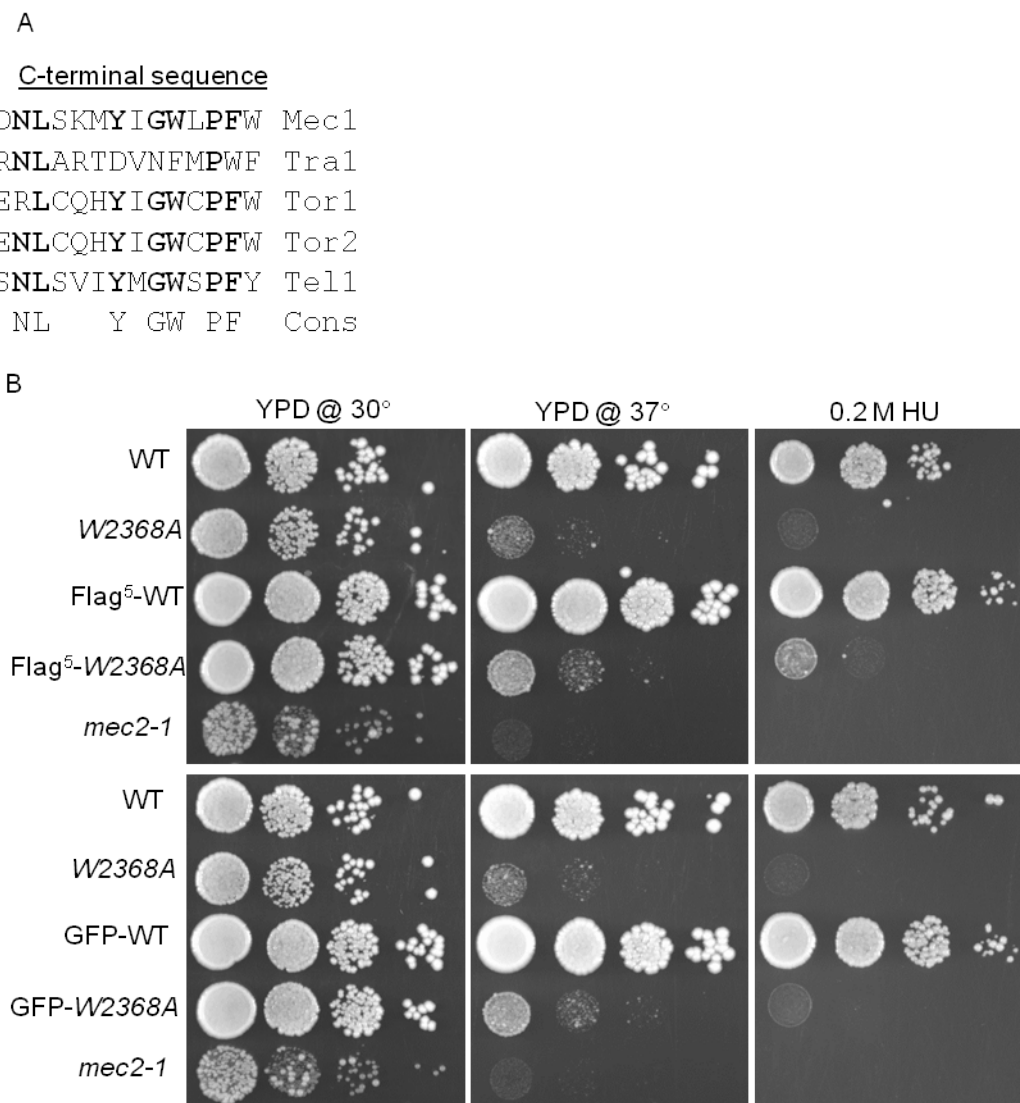

Figure 2.1: Phenotype of Flag[5] and GFP-tagged MEC1 strains

(A) Conservation of hydrophobic residues at the C-terminus of PIKK family members. The C-terminal residues of the five PIKK family members found in *S. cerevisiae* are shown with the consensus below. **(B)** Yeast strains BY4741 (*MEC1;* WT), CY6076 (*mec1-W2368A*), CY6194 (*Flag⁵-MEC1*), CY6175 (*Flag⁵-mec1-W2368A*), a *mec2-1* strain [235] (included to verify the hydroxyurea plates), CY6307 (*GFP-MEC1*), and CY6302 (*GFP-mec1-W2368A*) were grown to stationary phase diluted $1/10^2$ and ten-fold serial dilutions spotted onto selection plates as follows: YPD at 30°C, YPD at 37°C, and YPD at 30°C containing 0.2 M hydroxyurea (HU).

the N-terminus. As shown in Figure 2.1B, neither the Flag[5] nor eGFP-tag alters growth of a strain with the otherwise wild-type allele in YPD media at 30°C, 37°C or in the presence of 0.2 M hydroxyurea, a competitive inhibitor of ribonucleotide reductase (compare WT with Flag[5]-WT and GFP-WT). Growth of a strain with the *mec1-W2368A* allele was also examined. The *mec1-W2368A* strain was sensitive to hydroxyurea and as shown previously [55], was temperature sensitive. Neither Flag[5] nor eGFP-tags decreased the growth of the *mec1-W2368A* strain under these conditions.

Four additional *mec1* alleles were constructed and integrated into a diploid strain. *mec1-Δ1, mec1-Δ2 , mec1-Δ3* contain deletions of 1, 2 or 3 residues at the C-terminus of Mec1 (Figure 2.2A). Three deletions were constructed to decrease the likelihood that the C-terminal carboxyl might be artificially repositioned in a hydrophobic pocket in all of the derivatives. Mec1-2369G contains an additional glycine residue at the C-terminus. A comparable addition to Tra1 results in inviability [54]. After sporulation there was a 2:2 segregation of viable and inviable spore colonies for each, indicating that insertion or deletions to the C-terminus of Mec1 compromise viability. To determine if the C-terminal mutations affect expression of Mec1, diploid strains containing a single copy of Flag[5]-tagged wild-type or mutant Mec1, and an untagged wild-type allele, were analyzed by western blotting. As shown in Figure 2.2B, all of the *mec1* alleles were expressed when cells were grown at 30°C. Flag[5]-Mec1-W2368A and Flag[5]-Mec1-2369G were found at near wild-type levels. The deletion proteins were somewhat reduced, with the reduction paralleling the extent of the deletion. We also examined if the different *mec1* alleles interacted with Lcd1/Ddc2 (ATRIP in mammalian cells), an association required for the checkpoint functions of Mec1 [70-72]. Immunoprecipitations were performed with anti-Flag antibody and extracts prepared from strains containing myc[9]-tagged Lcd1/Ddc2 and a Flag[5]-tagged Mec1 derivative. As shown in Figure 2.2C, the ratio of myc[9]-tagged Lcd1/Ddc2 to Flag[5]-Mec1 was similar for each of the derivatives, indicating that Lcd1/Ddc2 interacted with Mec1-W2368A, Mec1-Δ1, and Mec1-G2369 as efficiently as the wild type protein.

A

MEC1 allele	C-terminal sequence
WT	YIGWLPFW
W2368A (w/a)	YIGWLPFA
Δ1	YIGWLPF
Δ2	YIGWLP
Δ3	YIGWL
2369G (Gly)	YIGWLPFWG

B
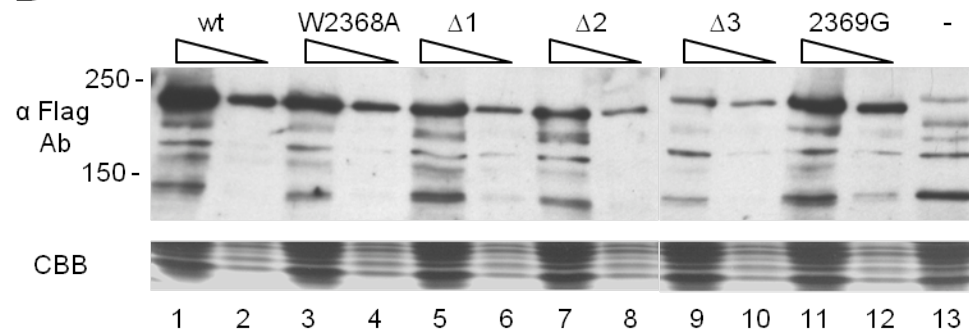
C
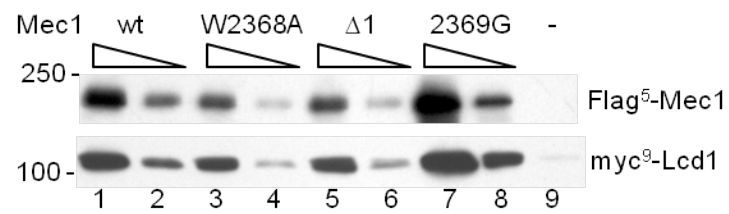
Figure 2.2: Expression of Mec1 derivatives with C-terminal mutations

(A) Amino acid sequences of the Mec1 derivatives. **(B)** Yeast strains CY6172 (*Flag[5]-MEC1;* lanes 1 and 2), CY6192 (*Flag[5]-mec1-W2368A;* lanes 3 and 4), CY6184 (*Flag[5]-mec1-Δ1;* lanes 5 and 6), CY6250 (*Flag[5]-mec1-Δ2*; lanes 7 and 8), CY6233 (*Flag[5]-mec1-Δ3*; lanes 9 and 10), CY6203 (*Flag[5]-mec1-2369G*; lanes 11 and 12), and BY4743 (lane 13) were grown in YPD media to mid-log phase and extracts prepared by grinding in liquid nitrogen. Extracts were solubilized in the presence of protease inhibitors (1.0 mM phenylmethylsulfonyl fluoride, 5μg/ml pepstatin, 1.0 mM benzamidine, 50 μg/ml trypsin inhibitor and 5 μg/ml leupeptin). 50 μg and 10 μg of protein was separated by SDS-PAGE; 50 μg for BY4743. The top portion of the gel was western blotted with anti-Flag (M2) antibody; the bottom portion was stained with Coomassie Brilliant Blue. **(C)** Interaction with Lcd1/Ddc2. Three mg of protein extract from yeast strains CY6172 (*Flag[5]-MEC1;* lanes 1 and 2), CY6192 (*Flag[5]-mec1-W2368A;* lanes 3 and 4), CY6184 (*Flag[5]-mec1-Δ1;* lanes 5 and 6), CY6203 (*Flag[5]-mec1-2369G*; lanes 7 and 8), and BY4743 (lane 9) containing YCplac111-myc[9]-Lcd1 were immunoprecipitated with anti-Flag antibody. Twenty (odd numbered lanes) and 5 μl of the immunoprecipitates were separated by SDS-PAGE and western blotted with anti-Flag antibody (top panel) or anti-myc antibody (lower panel).

2.3.1 The terminal residues of Mec1 are required for full kinase activity

As the phenotypes of the Mec1 derivatives were not due to their lack of expression or reduced interaction with Lcd1, we performed *in vitro* kinase assays to determine if this activity was impaired. We assayed the activity of Flag[5]-tagged Mec1, Mec1-Δ1, Mec1-Δ2, Mec1-Δ3, Mec1-2369G and Mec1-W2368A after isolating the proteins by immunoprecipitation on Flag-antibody resin from diploid yeast strains. The immunoprecipitates of the Flag[5]-tagged proteins used in the kinase assays are shown in Figure 2.3A. Kinase assays were performed with rat 4E-BP1 (PHAS-1) as the substrate

[239, 240]. The results for an assay performed at 30° are shown in Figure 2.3B. Immunoprecipitates from a strain wild-type for *MEC1*, but without tagged protein (BY4743; lane1), and from CY6172 (Flag[5]-tagged Mec1; lane 10) in the absence 4E-BP1, were performed to control for nonspecific phosphorylation and to identify 4E-BP1, respectively. Phosphorylation of 4E-BP1 was 7.5-fold greater than background with the wild-type protein (Figure 2.3B, compare lanes 1 and 2). Interestingly, phosphorylation by Flag[5]-Mec1-W2368A was less than 10% of that found for the wild-type protein (Figure 2.3B, compare lanes 2 and 9). Although 4E-BP1 is not necessarily indicative of all native Mec1 substrates, this result suggests that only low levels of kinase activity are essential for viability in rich media. Phosphorylation of 4E-BP1 was not above background levels for Mec1-2369G (lane 8), likely explaining the inviability of the strain containing this derivative. Similarly, the kinase activity of the Mec1 deletion derivatives (lanes 5-7) was not above background, though exact comparison with the wild type protein was difficult because of their somewhat reduced abundance in the immunoprecipitates.
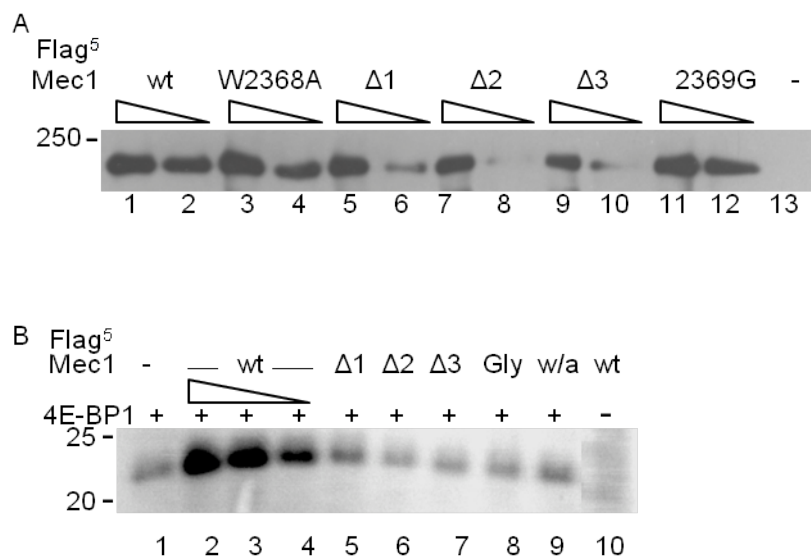
Figure 2.3: The terminal residues of Mec1 are required for its kinase activity

(A) Protein extracts were prepared from yeast strains CY6172 (*Flag⁵-MEC1;* lanes 1 and 2), CY6192 (*Flag⁵-mec1-W2368A;* lanes 3 and 4), CY6184 (*Flag⁵-mec1-Δ1;* lanes 5 and 6), CY6250 (*Flag⁵-mec1-Δ2*; lanes 7 and 8), CY6233 (*Flag⁵-mec1-Δ3*; lanes 9 and 10), CY6203 (*Flag⁵-mec1-2369G*; lanes 11 and 12), and BY4743 (lane 13), in the presence of protease inhibitors. Two milligrams of protein from CY6192 and 4 mg from the other strains was immunoprecipitated. One-third of the beads was suspended in 100 μl of 1x-SDS loading buffer, boiled and 10 or 5 μl separated by SDS-PAGE (5% gel) and western blotted with anti-Flag antibody. The BY4743 sample contained 10 μl of bead suspension. **(B)** Phosphorylation assays. Two-thirds of the immunoprecipitate in part A was suspended in 60 μl of kinase buffer. Aliquots (8, 4 and 2 μl for wt, 8 μl of the other samples) were used in kinase assays at 30°C with 4E-BP1 as substrate (with the exception of lane 10 which contained buffered glycerol). Lane 1, BY4743; lanes 2-4 and 10, CY6172 (*Flag⁵-MEC1*); lane 5, CY6184 (*Flag⁵-mec1-Δ1*); lane 6, CY6250 (*Flag⁵-mec1-Δ2*); lane 7, CY6233 (*Flag⁵-mec1-Δ3*); lane 8, CY6203 (*Flag⁵-mec1-2369G*); lane 9, CY6192 (*Flag⁵-mec1-W2368A*). Reactions were stopped with 3x-SDS loading buffer and protein separated on a 15% Tris-Tricine gel. The gel was fixed, and processed as described in Materials and Methods. Lane 10 was analyzed on the same gel but moved proximal to the other samples.

2.3.2   The terminal tryptophan is required for stability and localization of the protein

Based on the properties of Tra1 derivatives with C-terminal mutations [55], we predicted that the lack of kinase activity found for the Mec1 derivatives might result from improper folding of the molecules. The Mec1-W2368A, 2369G and Δ1 derivatives were found within cells at levels approaching the wild-type when extracts were prepared with protease inhibitors and analyzed directly after isolation (Figure 2.2B). Predicting that the C-terminus was required for stability of the protein, we addressed whether the Mec1 derivatives would be susceptible to proteolysis in the absence of protease inhibitors. Protein was isolated from diploid strains containing Flag[5] derivatives of Mec1, Mec1-2369G, Mec1-W2368A and Mec1-Δ1. The extract was then incubated at 30°C for 10 minutes or two hours, and aliquots analyzed by western blotting (Figure 2.4). The wild-type protein was very stable in extracts with no obvious degradation in two hours. In contrast, each of the Mec1 derivatives showed some sign of degradation at the 10-minute time point.

As another measure of whether the Mec1 derivatives were present in their functional forms, we performed size exclusion chromatography on extracts prepared from strains containing Flag[5]-tagged versions. As shown in Figure 2.5, wild-type Mec1 elutes from a Superose 6 column with an estimated mass of less than ~670 kDa. A portion of each of the mutant versions eluted from the column in a fraction with a significantly greater estimated mass, with none of the profiles paralleling the wild type. Mec1-2369G had a distinct profile in that it was dispersed almost equally across the high molecular mass fractions. The presence of the higher mass forms suggests the possibility of improper folding of the Mec1 derivatives, or perhaps prolonged association with chaperone complexes that are required for the formation of functional PIKK proteins [75, 76].

We also examined the localization of N-terminally eGFP-tagged versions of the proteins. Diploid strains expressing wild-type Mec1 and a single copy of eGFP-tagged Mec1 or a derivative were grown at 30°C. RFP-tagged Nic96 was used to mark the nuclear periphery. As shown in Figure 2.6, eGFP-tagged wild-type Mec1 is found
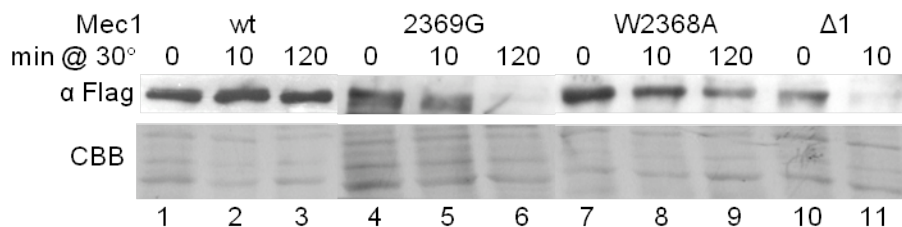
Figure 2.4: The terminal residues of Mec1 are required for its stability in extracts

Yeast strains CY6172 (*Flag⁵-MEC1;* lanes 1-3), CY6203 (*Flag⁵-mec1-2369G*; lanes 4-6) CY6192 (*Flag⁵-mec1-W2368A;* lanes 7-9) and CY6184 (*Flag⁵-mec1-Δ1;* lanes 10 and 11) were grown in YPD media to mid-log phase and extracts prepared by grinding with glass beads in the absence of protease inhibitors. Extracts were then incubated at 30°C for the indicated time period, 50 μg of protein from each extract was separated by SDS-PAGE and western blotted with anti-Flag antibody. The lower panel (CBB) is the lower portion of the gel after staining with Coomassie Brilliant Blue.
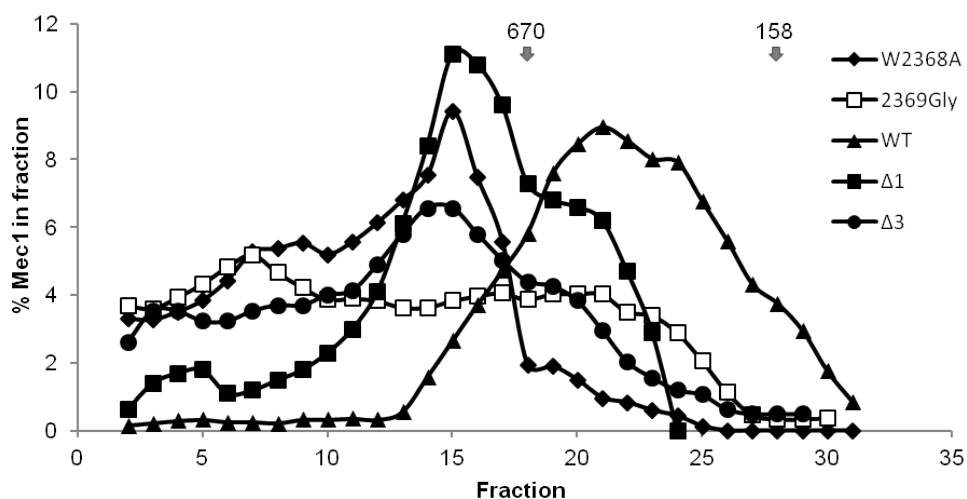
Figure 2.5: Resolution of Mec1 derivatives by size exclusion chromatography

Protein extracts were prepared from yeast strains CY6172 (*Flag[5]-MEC1*), CY6192 (*Flag[5]-mec1-W2368A*), CY6184 (*Flag[5]-mec1-Δ1*), CY6233 (*Flag[5]-mec1-Δ3*), and CY6203 (*Flag[5]-mec1-2369G*). 4.5 mg of protein from each strain was separated independently on a 24 ml FPLC Superose 6HR10/30 column (Amersham Pharmacia Biotech.). Protein from 20 μl aliquots of 250 μl fractions was resolved by SDS-PAGE and proteins detected by western blotting. The amount of protein in each fraction was determined by densitometry and calculated as a ratio of the total protein. The plot shows the average of a three-fraction window. The arrows indicate the migration of 670 and 158 kDa molecular mass standards.

principally in the nucleus. The distribution of each of Mec1-W2368A, Mec1-2369G, Mec1-Δ1 and Mec1-Δ2 is more disperse with both nuclear and cytoplasmic localization apparent. The experiment was also performed for cells grown at 37°C, but the signal was significantly reduced for the Mec1 derivatives.
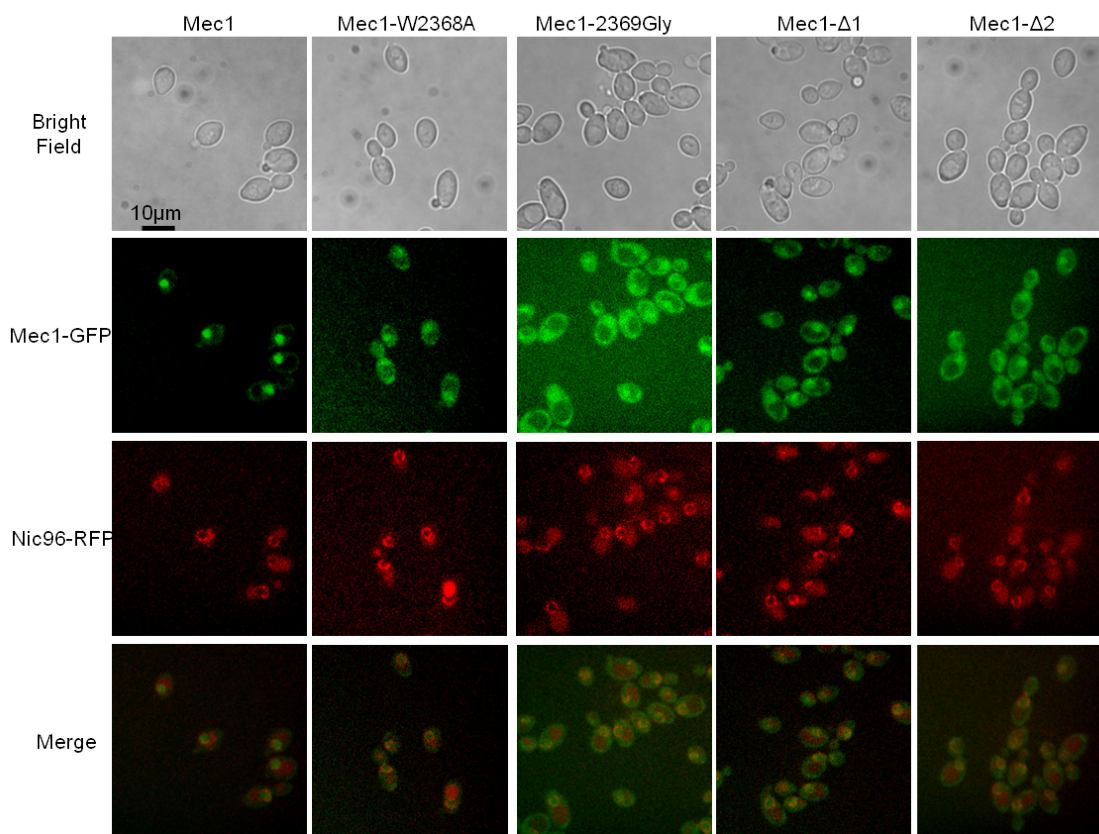
Figure 2.6: Localization of eGFP-Mec1

Diploid yeast strains containing an eGFP-tagged Mec1 derivative (CY6307, Mec1; CY6302, Mec1-W2368A; CY6330, Mec1-Δ1; CY6344, Mec1-Δ2 and CY6342, Mec1-2369G) were mated to a strain containing RFP-tagged Nic96 [62]. Diploid strains were grown at 30°C in synthetic complete (SC) media to stationary phase, diluted 1:20 in SC, grown a further six hours and visualized by fluorescence microscopy. A representative field of cells is shown.

2.3.3 *rpn3-L140P* suppresses the temperature sensitive growth of *mec1-W2368A*

Together the above results suggested that the C-terminal residues of Mec1 were required for the folding/stability of the molecule. If this was the case we predicted that it should be possible to identify second site suppressor mutations that restored the levels of the protein and allowed growth of the *mec1-W2368A* strain at 37°C. We plated approximately twenty million cells at a density of one million cells per plate, subjected them to a low dose of ultraviolet radiation, and selected colonies that grew at 37°C. Nine colonies were identified that carried a single extragenic suppressor mutation. These were backcrossed an additional nine times to eliminate variations unlinked to the suppressor mutation, and then their genomic sequence determined. Unique mutations were identified in four of the strains. These were: *rpn3* (L140P; a T to C transition at base pair 419; Figure 2.7A), *rfx1* (S213N), *rfx1* (S462L), and *sml1* (L62ochre). Loss of function of Sml1 and Rfx1 are known to suppress nonfunctional alleles of *mec1* [24, 69, 77]. In this regard, loss of the RNR inhibitor Sml1 or loss of the negative regulator of RNR transcription Rfx1 augment RNR activity resulting in increased dNTP levels which overcome the loss of Mec1. Consistent with these being causative mutations we found that our *sml1* and *rfx1* strains would also suppress *mec1-Δ1*. In contrast, the *rpn3-L140P* allele would not suppress *mec1-Δ1*, *mec1-Δ2* or *mec1-2369G*.

As Rpn3 encodes a component of the 19S proteasomal regulatory particle [78], thus potentially linking it to the stability of Mec1, we chose to examine *rpn3-L140P* in greater detail. The strain containing this mutation grew at 37°C, at a level comparable to a wild-type strain, and the mutation responsible did so in a partially dominant fashion (Figure 2.7B). The suppressor mutation did not facilitate growth on plates containing 0.2 M hydroxyurea, but rather resulted in a further reduction of growth (Figure 2.7C). Two approaches were used to demonstrate that suppression of *mec1-W2368A* was the result of *rpn3-L140P*. First, we compared the partially dominant effect of *rpn3-L140P/RPN3* as shown in Figure 2.7B, with the ability of *rpn3-L140P* inserted into CY6076 (*mec1-*

A

Rpn3	ATTAATTGCTTCATGCATCTACTAGTCCAGTTGTTTTTA IleAsnCysPheMetHisLeuLeuValGlnLeuPheLeu 140
Rpn3-L140P	ATTAATTGCTTCATGCATCCACTAGTCCAGTTGTTTTTA IleAsnCysPheMetHisProLeuValGlnLeuPheLeu 140

B

C

D
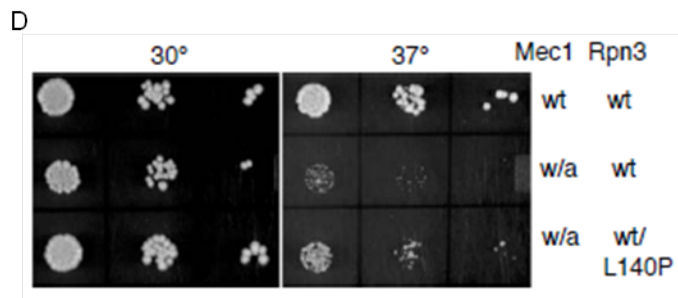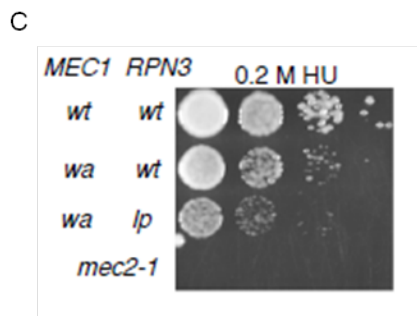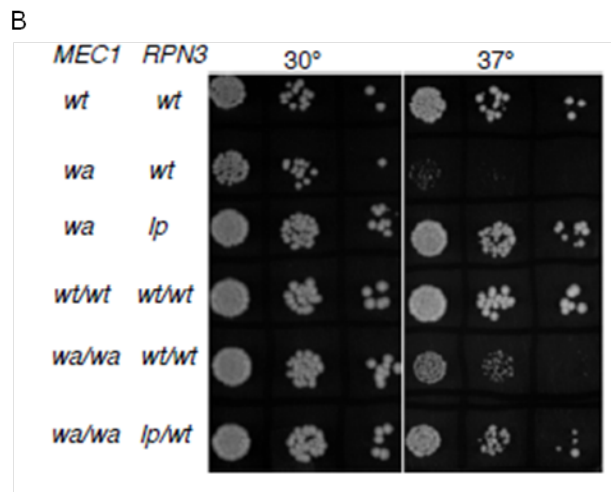
Figure 2.7: Suppression of the temperature sensitive growth resulting from
mec1-W2368A* by *rpn3-L140P

(A) Sequence of *RPN3* and the *rpn3-L140P* allele. **(B)** Yeast strains BY4742 (*MEC1 RPN3*), CY6077 (*mec1-W2368A RPN3*), CY6265 (*mec1-W2368A rpn3-L140P*), BY4743 (*MEC1/MEC1 RPN3/RPN3*), CY6368 (*mec1-W2368A/mec1-W2368A*) and CY6385 (*mec1-W2368A/mec1-W2368A RPN3/rpn3-L140P*) were grown to stationary phase diluted 1/10^2 and ten-fold serial dilutions spotted onto YPD plates at 30°C and 37°C. **(C)** Serial dilutions of BY4742, CY6077 and CY6265 were spotted onto a YPD plate containing 0.2 M hydroxyurea. A *mec2-1* strain was included to verify the quality of the hydroxyurea. **(D)** Serial dilutions of BY4741, CY6076 (*mec1-W2368A RPN3*) and CY6465 (*mec1-W2368A RPN3/rpn3-L140P-URA3*) were spotted onto YPD plates at 30°C and 37°C.

W2368A) on an integrating plasmid (Figure 2.7D). As was found for the heterozygous diploid, addition of the *rpn3-L140P*-containing plasmid partially, but not completely, reversed the slow growth at 37°C due to *mec1-W2368A*. Second, we analyzed independent spore colonies from a cross of CY6265 (*rpn3-L140P mec1-W2368A*) and CY6076 (*RPN3 mec1-W2368A*). The *RPN3* allele from each spore colony was isolated by PCR and sequenced. For 14 alleles (7 fast growing strains and 7 slow growing strains), the fast growth predicted the presence of the *rpn3-L140P* allele.

Rpn3 is an essential 524 amino acid residue protein that contains PAM (PCI/PINT associated module) and winged helix domains located C-terminally distal to residue 140. As shown in Figure 2.8A and B, L140 is in a hydrophobic region conserved in fungal species and more broadly in eukaryotes. The L140P mutation does not alter the level of Rpn3 found in the cell (Figure 2.8C). To determine the effect of Rpn3-L140P in isolation, yeast strain CY6398 (*MEC1 rpn3-L140P*) was engineered by backcrossing CY6265 with BY4741. As shown in Figure 2.8D, the *rpn3-L140P* allele had no detectable effect on growth of cells in rich media at 30°C. A very slight reduction in growth was observed for cells grown at 37°C and in media containing the arginine analog canavanine.

As mentioned above, *rpn3-L140P* does not suppress *mec1-Δ1*, *mec1-Δ2* or *mec1-2369G*. To address whether *rpn3-L140P* would suppress a mutation similar to *mec1-W2368A* in a related PIKK protein we introduced *rpn3-L140P* into a strain containing a Phe to Ala change of the terminal phenylalanine of Tra1 (*tra1-F3744A*). As shown in Figure 2.8E, *rpn3-L140P* did not suppress the slow growth at 37°C or in ethanol-containing media caused by *tra1-F3744A*, and in fact resulted in synthetic slow growth in this context.

The terminal tryptophan to alanine mutation in Mec1 reduced the stability of the protein (Figure 2.4). To investigate the effect of *rpn3-L140P* on Mec1-W2368A, the diploid strain CY6400 with the genotype *Flag⁵-mec1-W2368A/MEC1 rpn3-L140P/rpn3-L140P* was engineered. The level of Flag⁵-Mec1 in this strain was compared to that found in a wild-type *RPN3/RPN3* background (Figure 2.9A). For extracts prepared from cells

A

A. nidulans	248	SSKEVLPEIDIYLSILVQIYLYDRKEIQKG
S. cerevisiae	126	KTIEVTAEINCFMHLLVQLFLWDSKELEQL
C. glabrata	216	KSLAVSAEINAFIHLLTQLYLLDNQKIIEL
K. lactis	119	TSLDVSSEVNSFVHYIVQSLLLDSNRIDEL
Z. rouxii	121	TTIEVAAEVNSFVHLLVVLYLLDSGKYEEL
L. thermotolerans	116	NSVDVSGEVNSFLHLLVQLYLLDSNQVDHL
A. gossypii	116	GKIDLSAELNSFMHLLVQLYLLDSGQVEAL
L. elongisporus	103	QQANTIPEIELYIYLLTQTYLLDTSKLQEI
P. guilliermondii	94	TKSAVKPEVDLYIHLLVQVYLLDNNRLEEL
S. stipitis	105	STNAETPEAELYVHLLVQVYLLDTNQLA--
consensus		ssievtaEin flhllvqlyLlDsqkieel

B

S. pom	115	NGNGNTIFPEVDMYLQLLLSMTLYYNEKYEVGAE
D. mel	115	VATKAPI-AEVDAYFYLLLLVKLIDASDLKRAGI
X. lae	117	KAAAAPLLPEVETYLQLLLVIHLMNSKRYTEAQK
M. mus	149	KAASAPLLPEVEAYLQLLMVIFLMNSKRYKEAQK
H. sap	153	KAASTPLLPEVEAYLQLLVVIFMMNSKRYKEAQK
S. cer	124	EKKTIEVTAEINCFMHLLVQLFLWDSKELEQLVE

C

D

E

Figure 2.8: Leucine 140 is found in a conserved hydrophobic region

(A) Multiple sequence alignment of Rpn3 from a variety of fungal species. Leucine 140 (*S. cerevisiae*) is indicated by an asterisk. The alignment was performed with MUSCLE [79]. In order, the proteins are: *Aspergillus nidulans*, XP_660371.1; *Saccharomyces cerevisiae,* NP_010938.1; *Candida glabrata*, XP_447606.1; *Kluyveromyces lactis*, XP_453544.1; *Zygosaccharomyces rouxii*, XP_002496514.1; *Lachancea* t*hermotolerans*, XP_002554976.1; *Ashbya gossypii*, NP_983112.1; *Lodderomyces elongisporus*, XP_001526739.1; *Pichia guilliermondii*, XP_001487379.1; *Scheffersomyces stipitis,* XP_001383755.2. **(B)** Multiple sequence alignment of Rpn3 from a variety of eucaryotes. The proteins are *Schizosaccharomyces pombe*, NP_595282.2; *Drosophila melanogaster*, NP_477300; *Xenopus laevis*, NP_001085955.1; *Mus musculus*, NP_033465.1; *Homo sapiens*, NP_002800.2. **(C)** Expression of Rpn3-L140P. Extracts were prepared from BY4741 expressing myc^9-Rpn3 (lanes 1-3) or myc^9-Rpn3-L140P from a centromeric plasmid. 50, 25 and 10 μg of protein was separated by SDS-PAGE and western blotted with anti-Myc antibody (upper panel). The lower section of the gel was stained with Coomassie Brilliant Blue (lower panel). **(D)** Phenotype of *rpn3-L140P* in isolation. Yeast strains BY4741 (*RPN3*) and CY6398 (*rpn3-L140P*) were grown to stationary phase and serial dilutions spotted onto YPD plates at 30°C and 37°C, and onto a minimal plate containing 1.0 mg/l canavanine. **(E)** *rpn3-L140P* does not suppress *tra1-F3744A*. Yeast strains CY4353 (*TRA1 RPN3*), CY4350 (*tra1-F3744A RPN3*) and CY6418 (*tra1-F3744A rpn3-L140P*) were grown to stationary phase and serial dilutions spotted onto YPD plates at 30°C and 37°C, or a YPD plate containing 6% ethanol at 30°C.

grown at 30°C and in the absence of protease inhibitors, the level of Mec1-W2368A was somewhat reduced relative to the wild-type (Figure 2.9A, compare lanes 1 and 2). *rpn3-L140P* resulted in an increase in Mec1-W2368A (Figure 2.9A, compare lanes 2 and 3). For extracts prepared from cells grown at 37°C, the level of Mec1-W2368A was further reduced relative to the wild-type (Figure 2.9A, compare lanes 5 and 6), with *rpn3-L140P* resulting in a dramatic increase (Figure 2.9A, compare lanes 6 and 7). We conclude that *rpn3-L140P* acts to stabilize Mec1-W2368A, thus facilitating growth at elevated temperature. As shown in Figure 2.9B, *rpn3-L140P* acts more broadly, increasing the level of Mec1-2369G when cells are grown at 37°C.

The suppression of *mec1-W2368A* by *rpn3-L140P* introduces the possibility that Mec1 turnover is mediated by its degradation by the proteasome. To begin to address this issue, we analyzed Flag[5]-tagged Mec1 and Mec1-W2368A in cells treated with the proteasome inhibitor MG-132. Cells were treated under conditions described by Liu *et al.*[229] to increase their permeability to MG-132. As shown in Figure 2.9C, when grown in media containing proline as the nitrogen source and 0.003% SDS, yeast are sensitive to MG-132 in low micromolar concentrations. For the analysis of Mec1 and Mec1-W2368A, extracts were prepared from cells grown at 37°C in the presence or absence of 75 μM MG-132 for 2 hours. Wild-type Mec1 was not altered by the MG-132 treatment (Figure 2.9D, compare lanes 1 and 2). In contrast, Mec1-W2368A levels increased approximately two-fold upon treatment (Figure 2.9D, compare lanes 4 and 5) suggesting that the proteasome contributes at least in part to the protein's turnover. For neither the wild-type nor Mec1-W2368A proteins was there evidence of higher molecular mass forms that would be indicative of ubiquitylation of the protein.

A

30° 37°

Flag⁵-Mec1	wt	w/a	w/a	-	wt	w/a	w/a	-
Rpn3	wt	wt	L140P	wt	wt	wt	L140P	wt

α Flag
Ab

CBB

1   2   3   4   5   6   7   8

B

Rpn3   wt   LP

α Flag
Ab   Mec1-
                                2369G

CBB

1   2   3   4

C

[MG-132]

-

10 µM

25 µM

50 µM

D

Flag⁵-Mec1	wt	wt	-	w/a	w/a	w/a	w/a
MG-132	-	+	-	-	+	-	+

α Flag
Ab

CBB

1   2   3   4   5   6   7
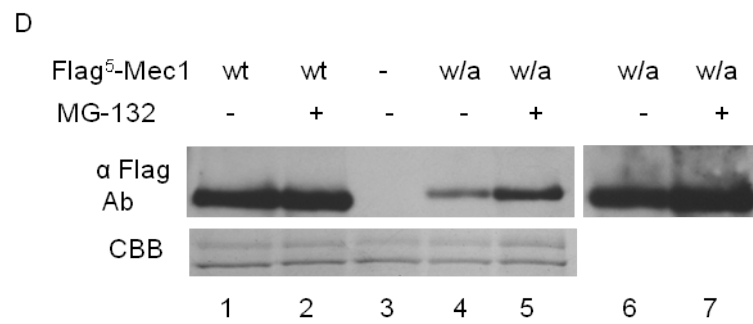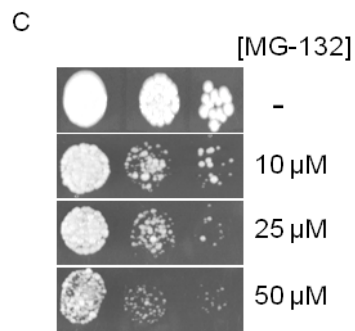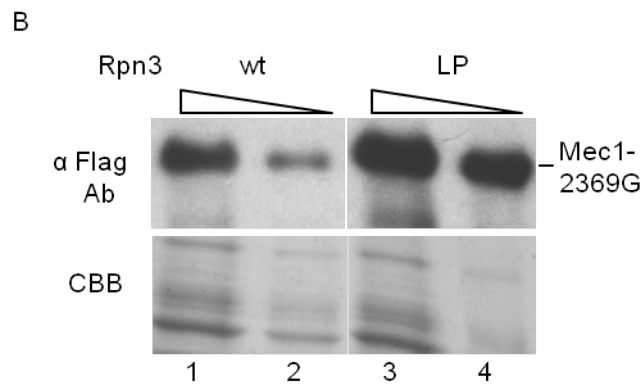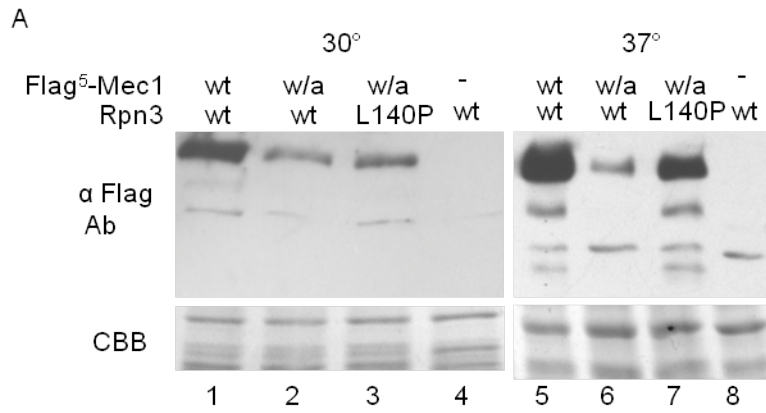
Figure 2.9: *rpn3-L140P* increases the level of C-terminally altered Mec1 derivatives

(A) Mec1-W2368A. Protein extracts were prepared by bead lysis in buffer lacking protease inhibitors from diploid yeast strains CY6172 (*MEC1/Flag^5-MEC1 RPN3/RPN3*), CY6192 (*MEC1/Flag^5-mec1-W2368A RPN3/RPN3*), CY6400 (*MEC1/Flag^5-mec1-W2368A rpn3-L140P/rpn3-L140P*) and BY4743 (*MEC1/MEC1 RPN3/RPN3*) grown at 30°C or 37°C. 50 μg of protein was separated by SDS-PAGE and the upper portion of the gel western blotted with anti-Flag antibody. The lower part of the gel was stained with Coomassie Brilliant Blue (CBB). **(B)** Mec1-2369G. Yeast strains CY6349 (*mec1-2369G RPN3 sml1Δ0::KanMX*; lanes 1 and 2) and CY6449 (*mec1-2369G rpn3-L140P sml1Δ0::KanMX;* lanes 3 and 4) were grown in YPD media for eight hours at 37°C. 40 (odd lanes) and 20 μg (even lanes) of protein extract was separated by SDS-PAGE and western blotted with anti Flag antibody or stained with Coomassie Brilliant Blue. **(C)** BY4742 was grown in media containing proline as the nitrogen source and 0.003% SDS for three hours then serial dilutions plated onto identical synthetic complete media with the indicated amount of MG-132. **(D)** CY6172 (*MEC1/Flag^5-MEC1*; lanes 1and 2), BY4743 (lane 3), and CY6192 (*MEC1/Flag^5-mec1-W2368A*; lanes 4-7) were grown in media containing proline as the nitrogen source and 0.003% SDS for three hours at 37°C. MG-132 was added to a final concentration of 75 μM (+) or the equivalent volume of dimethylsulfoxide (-) and the cells grown for an additional 2 hours. Extracts were prepared by glass bead lysis and 30 μg separated by SDS-PAGE. The upper portion of the gel was western blotted with anti-Flag antibody. The lower portion was stained with Coomassie Brilliant Blue. Lanes 6 and 7 are an overexposure of lanes 4 and 5.

2.4 Discussion

The FATC domain is found at the C-terminus of all the PIKK proteins. In each, the two most C-terminal residues are large and hydrophobic. We have shown that the terminal tryptophan residue of Mec1 is required for the function of the protein. Deletion of this residue results in a loss of viability; conversion to alanine results in temperature sensitive growth and reduced growth in hydroxyurea, a condition where deoxyribonucleotides are depleted. Moreover, the position of the terminal tryptophan is essential. Addition of a single glycine residue also results in loss of viability. As these results parallel those found for Tra1 [55], we conclude that the terminal residues are likely a key feature of all the PIKK proteins, a conclusion consistent with the positioning of the FATC domain in the structure of mTOR [49].

We propose that at least one role for the terminal residue is to assist in the folding of the protein. The C-terminally deleted Mec1 proteins were less abundant in crude protein lysates, and all of the derivatives analyzed were unstable in cell extracts prepared in the absence of protease inhibitors. This suggests that the temperature sensitive phenotype of the *mec1-W2368A* strain may result from decreased stability of the protein at elevated temperature, a conclusion supported by the increased levels found in the *rpn3-L140P* strain or in the presence of MG-132. Also suggesting the possibility of misfolding, we found that whereas wild-type Mec1 was found almost exclusively in the nucleus, the partially active and inactive forms of the protein showed partial cytoplasmic localization. In addition, each of the mutant forms of Mec1 chromatographed aberrantly on a size exclusion column. Structural models [2, 48, 49] position the FATC domain in a hydrophobic pocket that in porcine PI3K-γ interacts with helical domains [80]. Loss of hydrophobic interactions may decrease the stability of the PI3K domain, while addition of a glycine residue may not permit packing into the pocket. In both cases, the FATC domain and the core PI3K domain would be susceptible to proteolysis.

Our results with Mec1 closely parallel what we have observed with Tra1 [54]. In the case of Tra1, converting the terminal phenylalanine to alanine results in mislocalization, decreased protein levels and a number of stress related phenotypes. Consistent with a role for the FATC domain in folding, alleles of *tti2*, whose product with Tel2 and Tti1 is

proposed to act as a chaperone [57-60], suppress *tra1-F3744A* in a partially dominant fashion [55]. It was interesting that both Tra1-F3744A and Mec1-W2368A are mislocalized. Whether the other properties of the Mec1 and Tra1 derivatives result from or cause the mislocalization will require additional experimentation; however, our working model is that the molecules need to be specifically localized in the cytoplasm in complex with chaperones until they achieve a conformation that will support nuclear import, and if diverted from this pathway are at risk of being degraded.

Mutation of the terminal residue of Mec1 to alanine diminished kinase activity to a level approximately 10-fold less than the wild-type protein. The decrease in kinase activity of Mec1-W2368A and the other Mec1 derivatives can be explained by a role for the terminal residues in folding, and their possible participation in substrate recognition as found for mTOR [49]. As *mec1-W2368A* will support viability, minimal kinase activity must be sufficient for growth under optimal conditions. In media containing hydroxyurea, where replication fork collapse will increase, this same level of activity was insufficient. It is also this requirement for maximal levels of Mec1 activity during replicative stress that likely explains why *rpn3-L140P* would not suppress slow growth of the *mec1-W2368A* strain in hydroxyurea. We note that interpretation of this experiment is somewhat complicated because of the role of Rpn3 in aspects of cell cycle control [81].

Lcd1/Ddc2 interacts with the N-terminal HEAT domain sequences of Mec1 [71], thus providing a rationale for why it interacted with each of the altered Mec1 proteins with approximately the same efficiency. As some of these derivatives are partially excluded from the nucleus, this result suggests that the Mec1-Lcd1/Ddc2 interaction takes place in the cytoplasm.

We have shown that a mutation resulting in a change of leucine 140 to proline in Rpn3 suppresses the temperature sensitive growth of a *mec1-W2368A* strain. Rpn3 is a component of the 19S regulatory particle of the 26S proteasome [82-85]. The regulatory particle can be subdivided into a base and lid. The base, composed of ten components, interacts directly with the 20S proteolytic core particle, and contains ATPases (Rpt1-6) required for the unfolding of substrate proteins [86-88]. In addition to Rpn3, the lid contains

Rpn5–Rpn9, Rpn11, Rpn12, and Sem1. The 26S proteasome is the key enzymatic machinery required to degrade ubiquitylated proteins, either misfolded or short-lived, in the cell (reviewed in 89). Though the exact role of Rpn3 is unknown, the lid is involved in recognizing ubiquitylated target proteins [90-92] and removing the ubiquitin chains prior to the protein's degradation by the 20S proteolytic core particle [93]. Also of note, independent functions for the 19S regulatory particle have been observed in nucleotide excision repair [94, 95] and transcription [96-99].

We have considered possible models for how *rpn3-L140P* may suppress *mec1-W2368A*. It is unlikely that Rpn3-L140P acts indirectly by altering the DNA damage response as is seen with loss of function of Sml1 or Rfx1, because of the observed allele specificity and the increased levels of Mec1-W2368A in the *rpn3-L140P* background. Models for how *rpn3-L140P* suppresses the temperature sensitivity of *mec1-W238A* need to reflect the role of the terminal sequences in the folding, localization and/or stability of the protein. We present two models that are not mutually exclusive. Key in these is that *rpn3-L140P* increases the level of Mec1-W2368A, and does so more for Mec1-W2368A than wild-type Mec1, and also more at 37°C than 30°C. First, the proteasomal regulatory particle has chaperone activities that normally participate in the delivery of the protein target to the 20S core particle [100]. Independently, this activity could aid in the folding of Mec1-W2368A at elevated temperature and be enhanced by Rpn3-L140P. This model would account for the partial dominance of the *rpn3-L140P* allele, and be analogous to the suppression of *tra1-F3744A* by alleles encoding the chaperone component Tti2. Interestingly, the same *tti2* alleles do not suppress *mec1-W2368A* [55], and loss of interactions with the TTT-component Tel2 only modestly affects Mec1 function [101], leaving the possibility that another chaperone may replace or augment their activity. In the second model, the proteasome is involved in the turnover of improperly folded or mislocalized Mec1-W2368A. Subtle changes in targeting or activity of the proteasome caused by the L140P substitution in Rpn3 could decrease the rate of turnover affording additional time for Mec1-W2368A to fold into a stable conformation or be correctly localized. The *rpn3* allele would have partial dominance by altering the activity of half of the proteasome particles. We favor this model because inhibiting the proteolytic activity of the proteasome with MG-132 also increased the level of Mec1-W2368A. In addition,

the L140P mutation is in a highly conserved region of the protein, suggesting a functional role. While the phenotypes attributable to *rpn3-L140P* were not severe under most conditions, it does result in synthetic slow growth in combination with *tra1-F3744A* and reduced growth in combination with *mec1-W2368A* in media containing hydroxyurea. We did not observe an obvious loss of mobility of Mec1-W2368A in any of our western blots that would be indicative of Mec1 polyubiquitylation, the general signal for targeting to the proteasome. The model is actually simplified in the absence of Mec1-W2368A ubiquitylation since it is less likely that polyubiquitylated Mec1-W2368A could be restored to an active form. The question would remain, however, of how Mec1-W2368A might be targeted to the proteasome. Examples exist of proteasomal targeting that do not require direct ubiquitylation, but rather being mediated by a second molecule, which in some cases is ubiquitylated [102-106]. Due to the nature of the role of Rpn3 in the proteasome, we cannot exclude a third model whereby *rpn3-L140P* acts indirectly by altering the level or activity of an intermediary protein.

The *rpn3-L140P* mutation suppressed some (growth at 37°C) but not all (growth in hydroxyurea) phenotypes resulting from *mec1-W2368A*. We believe that this can be attributed to the threshold of Mec1 activity required for growth in hydroxyurea being greater than for growth at 37°C. In turn, this suggests that Rpn3-L140P is not sufficient to increase the activity of Mec1-W2368A above this threshold. We have considered whether Rpn3-L140P is able to increase the kinase activity of Mec1-W2368A by analyzing the activity of Flag^5-tagged Mec1-W2368A isolated by immunoprecipitation from wild-type *RPN3* and *rpn3-L140P* strains. The experiment was performed with cells grown at 30°C, where the control *mec1-W2368A RPN3* strain is able to grow. After normalizing to the amount of Mec1-W2368A present, an increase in activity was not observed for the protein from the *rpn3-L140P* strain (Figure 2.10). This result is consistent with *rpn3-L140P* suppressing *mec1-2368A* by increasing the level and localization of Mec1-W2368A protein rather than by increasing its per molecule activity.

As indicated above, the 19S regulatory particle has a role in transcriptional regulation. Rpn3-L140P could thus increase the level of active Mec1-W2368A by activating its transcription; however, several points argue against this. Of particular note,
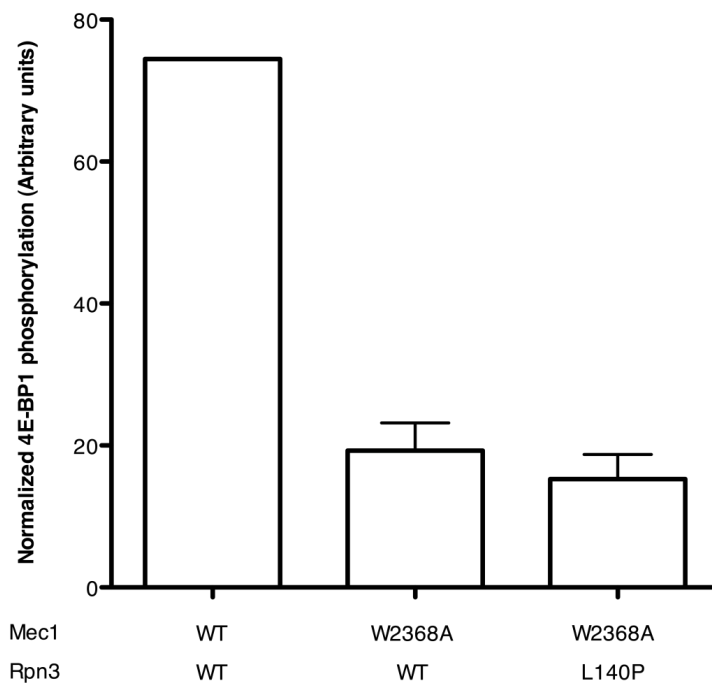
Figure 2.10: *rpn3-L140P* does not increase Mec1-W2368A kinase activity

Protein extracts were prepared by bead lysis in buffer containing protease inhibitors from strains CY6194 (*Flag⁵-MEC1 RPN3*), CY6175 (*Flag⁵-mec1-W2368A RPN3*) and CY6391 (*Flag⁵-mec1-W2368A rpn3-L140P*) grown at 30°C. Two milligrams of protein was immunoprecipitated with anti-Flag M2 magnetic beads. Two-thirds of the immunoprecipitate was suspended in 60 μl of kinase buffer. Aliquots of four microliters were used in kinase assays performed at 30°C with 4E-BP1 as substrate. Shown is the amount of 4E-BP1 phosphorylation normalized to Mec1 protein levels. Error bars represent the mean ± SD of three replicates.

the suppression by *rpn3-L140P* was observed when Mec1-W2368A was expressed from both its native promoter, the case for the original selections, and when expressed from the *TRA1* promoter, the case for the Flag-tagged derivatives. Furthermore, a role in transcription would be expected to be manifest by increased protein levels of approximately the same magnitude at both 30°C and 37°C. Increased expression was greater for cells grown at 37°C where Mec1-W2368A would have greater tendency to misfold. The finding that MG-132 mimics *rpn-L140P* also supports a role for the mutation in altering protein turnover rather than transcription. Finally, unlike the ATPase encoding genes *RPT6* (*SUG1*) and *RPT4* (*SUG2*), alleles of *RPN3* were not identified in screens for altered transcriptional regulation [107-109].

In summary, we have shown that the C-terminus of Mec1 is important for the stability of the protein, a feature likely common to the PIKK family. The reduced kinase activity of Mec1-W2368A suggests the C-terminal residues participate in the protein's activity, with viability of the *mec1-W2368A* strain indicating that minimal kinase activity is required for growth in rich media. Furthermore, suppression of the temperature sensitivity of *mec1-W2368A* by an allele encoding the proteasome component Rpn3 implicates the proteasome in regulating Mec1 levels, and Rpn3 as having a key role in this function.

2.5 References

1. Abraham,R.T. PI 3-kinase related kinases: 'big' players in stress-induced signaling pathways. *DNA Repair (Amst)* **3**, 883-887 (2004).

2. Lempiäinen,H. & Halazonetis,T.D. Emerging common themes in regulation of PIKKs and PI3Ks. *EMBO J.* **28**, 3067-3073 (2009).

3. Lovejoy,C.A. & Cortez,D. Common mechanisms of PIKK regulation. *DNA Repair (Amst)* **8**, 1004-1008 (2009).

4. Falck,J., Coates,J., & Jackson,S.P. Conserved modes of recruitment of ATM, ATR and DNA-PKcs to sites of DNA damage. *Nature* **434**, 605-611 (2005).

5. Labib,K. & De,P.G. Surviving chromosome replication: the many roles of the S-phase checkpoint pathway. *Philos. Trans. R. Soc. Lond B Biol. Sci.* **366**, 3554-3561 (2011).

6. Tomita,K. & Cooper,J.P. Fission yeast Ccq1 is telomerase recruiter and local checkpoint controller. *Genes Dev.* **22**, 3461-3474 (2008).

7. Moser,B.A., Chang,Y.T., Kosti,J., & Nakamura,T.M. Tel1ATM and Rad3ATR kinases promote Ccq1-Est1 interaction to maintain telomeres in fission yeast. *Nat. Struct. Mol. Biol.* **18**, 1408-1413 (2011).

8. Yamazaki,H., Tarumoto,Y., & Ishikawa,F. Tel1(ATM) and Rad3(ATR) phosphorylate the telomere protein Ccq1 to recruit telomerase and elongate telomeres in fission yeast. *Genes Dev.* **26**, 241-246 (2012).

9. Cimprich,K.A. & Cortez,D. ATR: an essential regulator of genome integrity. *Nat. Rev. Mol. Cell Biol.* **9**, 616-627 (2008).

10. Rouse,J. & Jackson,S.P. Lcd1p recruits Mec1p to DNA lesions in vitro and in vivo. *Mol. Cell* **9**, 857-869 (2002).

11. Zou,L. & Elledge,S.J. Sensing DNA damage through ATRIP recognition of RPA-ssDNA complexes. *Science* **300**, 1542-1548 (2003).

12. Ball,H.L., Myers,J.S., & Cortez,D. ATRIP binding to replication protein A-single-stranded DNA promotes ATR-ATRIP localization but is dispensable for Chk1 phosphorylation. *Mol. Biol. Cell* **16**, 2372-2381 (2005).

13. Katou,Y., Kanoh,Y., Bando,M., Noguchi,H., Tanaka,H. *et al.* S-phase checkpoint proteins Tof1 and Mrc1 form a stable replication-pausing complex. *Nature* **424**, 1078-1083 (2003).

14. Osborn,A.J. & Elledge,S.J. Mrc1 is a replication fork component whose phosphorylation in response to DNA replication stress activates Rad53. *Genes Dev.* **17**, 1755-1767 (2003).

15. Downs,J.A., Lowndes,N.F., & Jackson,S.P. A role for Saccharomyces cerevisiae histone H2A in DNA repair. *Nature* **408**, 1001-1004 (2000).

16. Cobb,J.A., Schleker,T., Rojas,V., Bjergbaek,L., Tercero,J.A. *et al.* Replisome instability, fork collapse, and gross chromosomal rearrangements arise synergistically from Mec1 kinase and RecQ helicase mutations. *Genes Dev.* **19**, 3055-3069 (2005).

17. Brush,G.S., Morrow,D.M., Hieter,P., & Kelly,T.J. The ATM homologue MEC1 is required for phosphorylation of replication protein A in yeast. *Proc. Natl. Acad. Sci. U. S. A* **93**, 15075-15080 (1996).

18. Cortez,D., Glick,G., & Elledge,S.J. Minichromosome maintenance proteins are direct targets of the ATM and ATR checkpoint kinases. *Proc. Natl. Acad. Sci. U. S. A* **101**, 10078-10083 (2004).

19. Yoo,H.Y., Shevchenko,A., Shevchenko,A., & Dunphy,W.G. Mcm2 is a direct substrate of ATM and ATR during DNA damage and DNA replication checkpoint responses. *J. Biol. Chem.* **279**, 53353-53364 (2004).

20. Morrison,A.J., Kim,J.A., Person,M.D., Highland,J., Xiao,J. *et al.* Mec1/Tel1 phosphorylation of the INO80 chromatin remodeling complex influences DNA damage checkpoint responses. *Cell* **130**, 499-511 (2007).

21. Pellicioli,A., Lucca,C., Liberi,G., Marini,F., Lopes,M. *et al.* Activation of Rad53 kinase in response to DNA damage and its effect in modulating phosphorylation of the lagging strand DNA polymerase. *EMBO J.* **18**, 6561-6572 (1999).

22. Sweeney,F.D., Yang,F., Chi,A., Shabanowitz,J., Hunt,D.F. *et al.* Saccharomyces cerevisiae Rad9 acts as a Mec1 adaptor to allow Rad53 activation. *Curr. Biol.* **15**, 1364-1375 (2005).

23. Ma,J.L., Lee,S.J., Duong,J.K., & Stern,D.F. Activation of the checkpoint kinase Rad53 by the phosphatidyl inositol kinase-like kinase Mec1. *J. Biol. Chem.* **281**, 3954-3963 (2006).

24. Desany,B.A., Alcasabas,A.A., Bachant,J.B., & Elledge,S.J. Recovery from DNA replicational stress is the essential function of the S-phase checkpoint pathway. *Genes Dev.* **12**, 2956-2970 (1998).

25. Friedel,A.M., Pike,B.L., & Gasser,S.M. ATR/Mec1: coordinating fork stability and repair. *Curr. Opin. Cell Biol.* **21**, 237-244 (2009).

26. Cobb,J.A., Bjergbaek,L., Shimada,K., Frei,C., & Gasser,S.M. DNA polymerase stabilization at stalled replication forks requires Mec1 and the RecQ helicase Sgs1. *EMBO J.* **22**, 4325-4336 (2003).

27. Zegerman,P. & Diffley,J.F. DNA replication as a target of the DNA damage checkpoint. *DNA Repair (Amst)* **8**, 1077-1088 (2009).

28. Zhao,X., Muller,E.G., & Rothstein,R. A suppressor of two essential checkpoint genes identifies a novel protein that negatively affects dNTP pools. *Mol. Cell* **2**, 329-340 (1998).

29. Brumbaugh,K.M., Otterness,D.M., Geisen,C., Oliveira,V., Brognard,J. *et al.* The mRNA surveillance protein hSMG-1 functions in genotoxic stress response pathways in mammalian cells. *Mol. Cell* **14**, 585-598 (2004).

30. Gehen,S.C., Staversky,R.J., Bambara,R.A., Keng,P.C., & O'Reilly,M.A. hSMG-1 and ATM sequentially and independently regulate the G1 checkpoint during oxidative stress. *Oncogene* **27**, 4065-4074 (2008).

31. Azzalin,C.M., Reichenbach,P., Khoriauli,L., Giulotto,E., & Lingner,J. Telomeric repeat containing RNA and RNA surveillance factors at mammalian chromosome ends. *Science* **318**, 798-801 (2007).

32. Chang,Y.F., Imam,J.S., & Wilkinson,M.F. The nonsense-mediated decay RNA surveillance pathway. *Annu. Rev. Biochem.* **76**, 51-74 (2007).

33. Loewith,R. & Hall,M.N. Target of rapamycin (TOR) in nutrient signaling and growth control. *Genetics* **189**, 1177-1201 (2011).

34. Cybulski,N. & Hall,M.N. TOR complex 2: a signaling pathway of its own. *Trends Biochem. Sci.* **34**, 620-627 (2009).

35. McMahon,S.B., Van Buskirk,H.A., Dugan,K.A., Copeland,T.D., & Cole,M.D. The novel ATM-related protein TRRAP is an essential cofactor for the c-Myc and E2F oncoproteins. *Cell* **94**, 363-374 (1998).

36. Saleh,A., Schieltz,D., Ting,N., McMahon,S.B., Litchfield,D.W. *et al.* Tra1p is a component of the yeast Ada.Spt transcriptional regulatory complexes. *J. Biol. Chem.* **273**, 26559-26565 (1998).

37. Grant,P.A., Schieltz,D., Pray-Grant,M.G., Yates,J.R., III, & Workman,J.L. The ATM-related cofactor Tra1 is a component of the purified SAGA complex. *Mol. Cell* **2**, 863-867 (1998).

38. Brown,C.E., Howe,L., Sousa,K., Alley,S.C., Carrozza,M.J. *et al.* Recruitment of HAT complexes by direct activator interactions with the ATM-related Tra1 subunit. *Science* **292**, 2333-2337 (2001).

39.   Bhaumik,S.R., Raha,T., Aiello,D.P., & Green,M.R. In vivo target of a transcriptional activator revealed by fluorescence resonance energy transfer. *Genes Dev.* **18**, 333-343 (2004).

40.   Fishburn,J., Mohibullah,N., & Hahn,S. Function of a eukaryotic transcription activator during the transcription cycle. *Mol. Cell* **18**, 369-378 (2005).

41.   Reeves,W.M. & Hahn,S. Targets of the Gal4 transcription activator in functional transcription complexes. *Mol. Cell Biol.* **25**, 9092-9102 (2005).

42.   Bosotti,R., Isacchi,A., & Sonnhammer,E.L. FAT: a novel domain in PIK-related kinases. *Trends Biochem. Sci.* **25**, 225-227 (2000).

43.   Knutson,B.A. & Hahn,S. Domains of Tra1 important for activator recruitment and transcription coactivator functions of SAGA and NuA4 complexes. *Mol. Cell Biol.* **31**, 818-831 (2011).

44.   Sibanda,B.L., Chirgadze,D.Y., & Blundell,T.L. Crystal structure of DNA-PKcs reveals a large open-ring cradle comprised of HEAT repeats. *Nature* **463**, 118-121 (2010).

45.   Perry,J. & Kleckner,N. The ATRs, ATMs, and TORs are giant HEAT repeat proteins. *Cell* **112**, 151-155 (2003).

46.   Mordes,D.A., Glick,G.G., Zhao,R., & Cortez,D. TopBP1 activates ATR through ATRIP and a PIKK regulatory domain. *Genes Dev.* **22**, 1478-1489 (2008).

47.   Dames,S.A., Mulet,J.M., Rathgeb-Szabo,K., Hall,M.N., & Grzesiek,S. The solution structure of the FATC domain of the protein kinase target of rapamycin suggests a role for redox-dependent structural and cellular stability. *J. Biol. Chem.* **280**, 20558-20564 (2005).

48.   Sturgill,T.W. & Hall,M.N. Activating mutations in TOR are in similar structures as oncogenic mutations in PI3KCalpha. *ACS Chem. Biol.* **4**, 999-1015 (2009).

49.   Yang,H., Rudge,D.G., Koos,J.D., Vaidialingam,B., Yang,H.J. *et al.* mTOR kinase structure, mechanism and regulation. *Nature* **497**, 217-223 (2013).

50.   Takahashi,T., Hara,K., Inoue,H., Kawa,Y., Tokunaga,C. *et al.* Carboxyl-terminal region conserved among phosphoinositide-kinase-related kinases is indispensable for mTOR function in vivo and in vitro. *Genes Cells* **5**, 765-775 (2000).

51.   Morita,T., Yamashita,A., Kashima,I., Ogata,K., Ishiura,S. *et al.* Distant N- and C-terminal domains are required for intrinsic kinase activity of SMG-1, a critical component of nonsense-mediated mRNA decay. *J. Biol. Chem.* **282**, 7799-7808 (2007).

52. Beamish,H.J., Jessberger,R., Riballo,E., Priestley,A., Blunt,T. *et al.* The C-terminal conserved domain of DNA-PKcs, missing in the SCID mouse, is required for kinase activity. *Nucleic Acids Res.* **28**, 1506-1513 (2000).

53. Priestley,A., Beamish,H.J., Gell,D., Amatucci,A.G., Muhlmann-Diaz,M.C. *et al.* Molecular and biochemical characterisation of DNA-dependent protein kinase-defective rodent mutant irs-20. *Nucleic Acids Res.* **26**, 1965-1973 (1998).

54. Hoke,S.M., Irina,M.A., Genereaux,J., Kvas,S., Buck,M. *et al.* Mutational analysis of the C-terminal FATC domain of Saccharomyces cerevisiae Tra1. *Curr. Genet.* **56**, 447-465 (2010).

55. Genereaux,J., Kvas,S., Dobransky,D., Karagiannis,J., Gloor,G.B. *et al.* Genetic evidence links the ASTRA protein chaperone component Tti2 to the SAGA transcription factor Tra1. *Genetics* **191**, 765-780 (2012).

56. Takai,H., Wang,R.C., Takai,K.K., Yang,H., & de Lange,T. Tel2 regulates the stability of PI3K-related protein kinases. *Cell* **131**, 1248-1259 (2007).

57. Takai,H., Xie,Y., de Lange,T., & Pavletich,N.P. Tel2 structure and function in the Hsp90-dependent maturation of mTOR and ATR complexes. *Genes Dev.* **24**, 2019-2030 (2010).

58. Horejsi,Z., Takai,H., Adelman,C.A., Collis,S.J., Flynn,H. *et al.* CK2 phospho-dependent binding of R2TP complex to TEL2 is essential for mTOR and SMG1 stability. *Mol. Cell* **39**, 839-850 (2010).

59. Hurov,K.E., Cotta-Ramusino,C., & Elledge,S.J. A genetic screen identifies the Triple T complex required for DNA damage signaling and ATM and ATR stability. *Genes Dev.* **24**, 1939-1950 (2010).

60. Kaizuka,T., Hara,T., Oshiro,N., Kikkawa,U., Yonezawa,K. *et al.* Tti1 and Tel2 are critical factors in mammalian target of rapamycin complex assembly. *J. Biol. Chem.* **285**, 20109-20116 (2010).

61. Winzeler,E.A. & Davis,R.W. Functional analysis of the yeast genome. *Curr. Opin. Genet. Dev.* **7**, 771-776 (1997).

62. Huh,W.K., Falvo,J.V., Gerke,L.C., Carroll,A.S., Howson,R.W. *et al.* Global analysis of protein localization in budding yeast. *Nature* **425**, 686-691 (2003).

63. Liu,C., Apodaca,J., Davis,L.E., & Rao,H. Proteasome inhibition in wild-type yeast Saccharomyces cerevisiae cells. *Biotechniques* **42**, 158, 160, 162 (2007).

64. Saleh,A., Lang,V., Cook,R., & Brandl,C.J. Identification of native complexes containing the yeast coactivator/repressor proteins NGG1/ADA3 and ADA2. *J. Biol. Chem.* **272**, 5571-5578 (1997).

65.   Mallory,J.C. & Petes,T.D. Protein kinase activity of Tel1p and Mec1p, two Saccharomyces cerevisiae proteins related to the human ATM protein kinase. *Proc. Natl. Acad. Sci. U. S. A* **97**, 13749-13754 (2000).

66.   Mutiu,A.I., Hoke,S.M., Genereaux,J., Hannam,C., MacKenzie,K. *et al.* Structure/function analysis of the phosphatidylinositol-3-kinase domain of yeast tra1. *Genetics* **177**, 151-166 (2007).

67.   Langmead,B., Trapnell,C., Pop,M., & Salzberg,S.L. Ultrafast and memory-efficient alignment of short DNA sequences to the human genome. *Genome Biol.* **10**, R25 (2009).

68.   Li,H., Handsaker,B., Wysoker,A., Fennell,T., Ruan,J. *et al.* The Sequence Alignment/Map format and SAMtools. *Bioinformatics.* **25**, 2078-2079 (2009).

69.   Weinert,T.A., Kiser,G.L., & Hartwell,L.H. Mitotic checkpoint genes in budding yeast and the dependence of mitosis on DNA replication and repair. *Genes Dev.* **8**, 652-665 (1994).

70.   Rouse,J. & Jackson,S.P. LCD1: an essential gene involved in checkpoint control and regulation of the MEC1 signalling pathway in Saccharomyces cerevisiae. *EMBO J.* **19**, 5801-5812 (2000).

71.   Wakayama,T., Kondo,T., Ando,S., Matsumoto,K., & Sugimoto,K. Pie1, a protein interacting with Mec1, controls cell growth and checkpoint responses in Saccharomyces cerevisiae. *Mol. Cell Biol.* **21**, 755-764 (2001).

72.   Paciotti,V., Clerici,M., Lucchini,G., & Longhese,M.P. The checkpoint protein Ddc2, functionally related to S. pombe Rad26, interacts with Mec1 and is regulated by Mec1-dependent phosphorylation in budding yeast. *Genes Dev.* **14**, 2046-2059 (2000).

73.   Lin,T.A., Kong,X., Haystead,T.A., Pause,A., Belsham,G. *et al.* PHAS-I as a link between mitogen-activated protein kinase and translation initiation. *Science* **266**, 653-656 (1994).

74.   von Manteuffel,S.R., Gingras,A.C., Ming,X.F., Sonenberg,N., & Thomas,G. 4E-BP1 phosphorylation is mediated by the FRAP-p70s6k pathway and is independent of mitogen-activated protein kinase. *Proc. Natl. Acad. Sci. U. S. A* **93**, 4076-4080 (1996).

75.   Boulon,S., Bertrand,E., & Pradet-Balade,B. HSP90 and the R2TP co-chaperone complex: building multi-protein machineries essential for cell growth and gene expression. *RNA. Biol.* **9**, 148-154 (2012).

76.   Makhnevych,T. & Houry,W.A. The role of Hsp90 in protein complex assembly. *Biochim. Biophys. Acta* **1823**, 674-682 (2012).

77.   Huang,M., Zhou,Z., & Elledge,S.J. The DNA replication and damage checkpoint pathways induce transcription by inhibition of the Crt1 repressor. *Cell* **94**, 595-605 (1998).

78.   Kominami,K., Okura,N., Kawamura,M., DeMartino,G.N., Slaughter,C.A. *et al.* Yeast counterparts of subunits S5a and p58 (S3) of the human 26S proteasome are encoded by two multicopy suppressors of nin1-1. *Mol. Biol. Cell* **8**, 171-187 (1997).

79.   Edgar,R.C. MUSCLE: multiple sequence alignment with high accuracy and high throughput. *Nucleic Acids Res.* **32**, 1792-1797 (2004).

80.   Walker,E.H., Perisic,O., Ried,C., Stephens,L., & Williams,R.L. Structural insights into phosphoinositide 3-kinase catalysis and signalling. *Nature* **402**, 313-320 (1999).

81.   Bailly,E. & Reed,S.I. Functional characterization of rpn3 uncovers a distinct 19S proteasomal subunit requirement for ubiquitin-dependent proteolysis of cell cycle regulatory proteins in budding yeast. *Mol. Cell Biol.* **19**, 6872-6890 (1999).

82.   Beck,F., Unverdorben,P., Bohn,S., Schweitzer,A., Pfeifer,G. *et al.* Near-atomic resolution structural model of the yeast 26S proteasome. *Proc. Natl. Acad. Sci. U. S. A* **109**, 14870-14875 (2012).

83.   Lander,G.C., Estrin,E., Matyskiela,M.E., Bashore,C., Nogales,E. *et al.* Complete subunit architecture of the proteasome regulatory particle. *Nature* **482**, 186-191 (2012).

84.   Lasker,K., Forster,F., Bohn,S., Walzthoeni,T., Villa,E. *et al.* Molecular architecture of the 26S proteasome holocomplex determined by an integrative approach. *Proc. Natl. Acad. Sci. U. S. A* **109**, 1380-1387 (2012).

85.   Kish-Trier,E. & Hill,C.P. Structural Biology of the Proteasome. *Annu. Rev. Biophys.*(2013).

86.   Tomko,R.J., Jr., Funakoshi,M., Schneider,K., Wang,J., & Hochstrasser,M. Heterohexameric ring arrangement of the eukaryotic proteasomal ATPases: implications for proteasome structure and assembly. *Mol. Cell* **38**, 393-403 (2010).

87.   Smith,D.M., Chang,S.C., Park,S., Finley,D., Cheng,Y. *et al.* Docking of the proteasomal ATPases' carboxyl termini in the 20S proteasome's alpha ring opens the gate for substrate entry. *Mol. Cell* **27**, 731-744 (2007).

88.   Rabl,J., Smith,D.M., Yu,Y., Chang,S.C., Goldberg,A.L. *et al.* Mechanism of gate opening in the 20S proteasome by the proteasomal ATPases. *Mol. Cell* **30**, 360-368 (2008).

89. Finley,D. Recognition and processing of ubiquitin-protein conjugates by the proteasome. *Annu. Rev. Biochem.* **78**, 477-513 (2009).

90. van Nocker,S., Sadis,S., Rubin,D.M., Glickman,M., Fu,H. *et al.* The multiubiquitin-chain-binding protein Mcb1 is a component of the 26S proteasome in Saccharomyces cerevisiae and plays a nonessential, substrate-specific role in protein turnover. *Mol. Cell Biol.* **16**, 6020-6028 (1996).

91. Husnjak,K., Elsasser,S., Zhang,N., Chen,X., Randles,L. *et al.* Proteasome subunit Rpn13 is a novel ubiquitin receptor. *Nature* **453**, 481-488 (2008).

92. Schreiner,P., Chen,X., Husnjak,K., Randles,L., Zhang,N. *et al.* Ubiquitin docking at the proteasome through a novel pleckstrin-homology domain interaction. *Nature* **453**, 548-552 (2008).

93. Verma,R., Aravind,L., Oania,R., McDonald,W.H., Yates,J.R., III *et al.* Role of Rpn11 metalloprotease in deubiquitination and degradation by the 26S proteasome. *Science* **298**, 611-615 (2002).

94. Russell,S.J., Reed,S.H., Huang,W., Friedberg,E.C., & Johnston,S.A. The 19S regulatory complex of the proteasome functions independently of proteolysis in nucleotide excision repair. *Mol. Cell* **3**, 687-695 (1999).

95. Gillette,T.G., Huang,W., Russell,S.J., Reed,S.H., Johnston,S.A. *et al.* The 19S complex of the proteasome regulates nucleotide excision repair in yeast. *Genes Dev.* **15**, 1528-1539 (2001).

96. Ferdous,A., Gonzalez,F., Sun,L., Kodadek,T., & Johnston,S.A. The 19S regulatory particle of the proteasome is required for efficient transcription elongation by RNA polymerase II. *Mol. Cell* **7**, 981-991 (2001).

97. Gonzalez,F., Delahodde,A., Kodadek,T., & Johnston,S.A. Recruitment of a 19S proteasome subcomplex to an activated promoter. *Science* **296**, 548-550 (2002).

98. Lee,D., Ezhkova,E., Li,B., Pattenden,S.G., Tansey,W.P. *et al.* The proteasome regulatory particle alters the SAGA coactivator to enhance its interactions with transcriptional activators. *Cell* **123**, 423-436 (2005).

99. Uprety,B., Lahudkar,S., Malik,S., & Bhaumik,S.R. The 19S proteasome subcomplex promotes the targeting of NuA4 HAT to the promoters of ribosomal protein genes to facilitate the recruitment of TFIID for transcriptional initiation in vivo. *Nucleic Acids Res.* **40**, 1969-1983 (2012).

100. Braun,B.C., Glickman,M., Kraft,R., Dahlmann,B., Kloetzel,P.M. *et al.* The base of the proteasome regulatory particle exhibits chaperone-like activity. *Nat. Cell Biol.* **1**, 221-226 (1999).

101.   Anderson,C.M. & Blackburn,E.H. Mec1 function in the DNA damage response does not require its interaction with Tel2. *Cell Cycle* **7**, 3695-3698 (2008).

102.   Bercovich,Z., Rosenberg-Hasson,Y., Ciechanover,A., & Kahana,C. Degradation of ornithine decarboxylase in reticulocyte lysate is ATP-dependent but ubiquitin-independent. *J. Biol. Chem.* **264**, 15949-15952 (1989).

103.   Sdek,P., Ying,H., Chang,D.L., Qiu,W., Zheng,H. *et al.* MDM2 promotes proteasome-dependent ubiquitin-independent degradation of retinoblastoma protein. *Mol. Cell* **20**, 699-708 (2005).

104.   Sheaff,R.J., Singer,J.D., Swanger,J., Smitherman,M., Roberts,J.M. *et al.* Proteasomal turnover of p21Cip1 does not require p21Cip1 ubiquitination. *Mol. Cell* **5**, 403-410 (2000).

105.   Perrotti,D., Iervolino,A., Cesi,V., Cirinna,M., Lombardini,S. *et al.* BCR-ABL prevents c-jun-mediated and proteasome-dependent FUS (TLS) proteolysis through a protein kinase CbetaII-dependent pathway. *Mol. Cell Biol.* **20**, 6159-6169 (2000).

106.   Isono,O., Ohshima,T., Saeki,Y., Matsumoto,J., Hijikata,M. *et al.* Human T-cell leukemia virus type 1 HBZ protein bypasses the targeting function of ubiquitination. *J. Biol. Chem.* **283**, 34273-34282 (2008).

107.   Swaffield,J.C., Bromberg,J.F., & Johnston,S.A. Alterations in a yeast protein resembling HIV Tat-binding protein relieve requirement for an acidic activation domain in GAL4. *Nature* **357**, 698-700 (1992).

108.   Russell,S.J., Sathyanarayana,U.G., & Johnston,S.A. Isolation and characterization of SUG2. A novel ATPase family component of the yeast 26 S proteasome. *J. Biol. Chem.* **271**, 32810-32817 (1996).

109.   Xu,Q., Singer,R.A., & Johnston,G.C. Sug1 modulates yeast transcription activation by Cdc68. *Mol. Cell Biol.* **15**, 6025-6035 (1995).

Chapter 3

3 Modulation of Mcm2-7 activity by Cdt1

3.1 Introduction

The regulation of DNA replication is crucial for genome maintenance. Replication occurs once and only once per cell division cycle and is confined to S-phase through several mechanisms that prevent re-replication and mistimed initiation. In budding yeast, Mcm2-7 requires Cdt1 for nuclear import and loading into the pre-RC during the M-G1 transition [1]. Interestingly, Mcm2-7 exists as a single hexamer in solution, but is loaded by ORC, Cdc6 and Cdt1 as a head-to-head double hexamer around double-stranded DNA (dsDNA) [2-5]. Cdt1 interacts with Mcm2-7 through a conserved motif in the C-terminus of Mcm6, while the C-terminus of Cdt1 contains a binding site for Mcm6 [6, 7]. Point mutations in either interaction motif abrogate nuclear import of a Mcm2-7-Cdt1 complex [8]. Fernandez-Cid and colleagues [6] reported that Cdt1 alleviates an autoinhibitory activity in Mcm6 to promote stable interaction of Mcm2-7 with ORC/Cdc6 and Mcm2-7 origin loading. Recently, the Diffley lab found that a point mutation in the C-terminus of Mcm3 blocks Mcm2-7-Cdt1 binding to an ORC/Cdc6 complex. Moreover, Mcm3 was shown to promote ATP hydrolysis by ORC/Cdc6, which in turn, induced Mcm2-7 release from origins in the absence of Cdt1 [9]. However, an N-terminal Cdt1 deletion mutant that still contains the Mcm2-7 interaction domain can be recruited to replication origins, but fails to facilitate Mcm2-7 loading [10, 11].

In this study, we sought to further investigate the role Cdt1 plays in interacting with and regulating Mcm2-7. Here, we assembled Mcm2-7•Cdt1 complexes and compared its activity to that of Mcm2-7 alone. We show that Mcm2-7•Cdt1 has lower ATPase and helicase activity than Mcm2-7. We further show that Cdt1 is required for origin loading of Mcm2-7. Moreover, Mcm2-7 dissociates into a Mcm357 subcomplex in the absence of ATP and that this subcomplex can bind origins in the absence of Cdt1. We propose that Cdt1 acts to negatively regulate Mcm2-7 helicase activity. We also provide data to support a role for Cdt1 in stabilizing the Mcm2-7 hexamer. Together, the effects

of Cdt1 on Mcm2-7 suggest mechanisms by which Cdt1 may carry out its essential role in the initiation of DNA replication.

3.2   Materials and Methods

3.2.1   Cloning of Mcm genes

Each of the MCM genes was amplified from *Saccharomyces cerevisiae* genomic DNA and cloned into pET plasmids as described in Davey *et al*. [12]. A PKA recognition motif was fused to *MCM3* as described in Stead *et al*. [13].

3.2.2   Purification of Mcms

Mcm subunits were purified as previously described [12], with the following modifications. Mcm2 and Mcm3pk were purified as described in Stead *et al*. [13]. Cell lysis was performed using an Avestin Emulsiflex C3 homogenizer.

3.2.3   Cdt1 purification

Cdt1 was purified from *E. coli* cells expressing Cdt1 (12 L) grown to an OD_{600} 0.5-0.6. The cells were lysed in Tris/Sucrose (50 mM Tris-HCl, pH 7.5; 10% (w/v) sucrose) containing 500 mM NaCl and 2 mM DTT. Insoluble material was removed by centrifugation at 27,000 x g for 40 min at 4°C. Ammonium sulfate was added to the soluble fraction to a final concentration of 0.3 mg/ml. The precipitate was pelleted by centrifugation then resuspended in Buffer A (20 mM Tris-HCl pH 7.5; 10% (v/v) glycerol; 2 mM DTT). The protein was dialyzed against Buffer A to a conductivity equivalent to 100 mM NaCl and then applied to a 30 ml Fast Flow Q Sepharose column equilibrated in Buffer A containing 50 mM NaCl. The column was washed with 150 ml of the same buffer and then bound proteins were eluted with a 300 ml, 50 mM to 500 mM NaCl gradient in Buffer A. Fractions containing Cdt1, as determined by Coomassie blue-stained SDS-PAGE, were pooled and dialyzed against Buffer H (20mM Tris-HCl, pH 7.5; 0.1mM EDTA; 10% Glycerol; 2mM DTT) containing 100 mM NaCl. The protein was then applied to a 10 ml Heparin agarose column equilibrated in the same buffer. After washing the column with 100 ml Buffer H containing 100 mM NaCl, the bound proteins were eluted with a 100 ml, 100-500 mM NaCl gradient in Buffer H. Peak

fractions containing Cdt1 were confirmed by Coomassie blue-stained SDS-PAGE and Western blotting, pooled and stored at -80ºC.

3.2.4   ORC purification

An *E. coli* strain that co-expresses all six of the ORC subunits each under the control of the T7 RNA polymerase promoter (M.J. Davey, J. Finkelstein and M. O'Donnell, unpublished) was grown to an OD_{600} of 0.5, chilled to 15°C and then induced by addition of 1 mM IPTG. After 18-20 h shaking at 15°C, the cells (12 L) were harvested by centrifugation and resuspended (10 % w/v) in 20 mM HEPES pH 7.5, 150 mM KCl, 10% sucrose, 1 mM PMSF, 1 mM DTT, and 1.5 mM $MgCl_2$. The lysate was centrifuged at 27,000 xg for one hour and the supernatant was applied to a 40 ml SP Sepharose column equilibrated in 20 mM HEPES pH 7.5, 150 mM KCl and 10% (v/v) glycerol and eluted with a 400 ml linear gradient of 150 mM to 700 mM KCl in the above buffer. The peak fractions, as determined by SDS-PAGE, were pooled (approximately 40 mg in 110 ml) and loaded onto a 1 ml Hi-Trap (GE Healthcare) Ni-affinity column equilibrated in 20 mM HEPES pH 7.5, 400 mM KCl, 5 mM imidazole and 10% (v/v) glycerol. The column was then washed with 20 ml of 20 mM HEPES pH 7.5, 400 mM KCl, 60 mM imidazole, 10% (v/v) glycerol, followed by elution with 20 ml of 20 mM HEPES pH 7.5, 400 mM KCl, 1 M imidazole and 10% (v/v) glycerol. The peak fractions, as determined by SDS-PAGE, were pooled and loaded onto a P-100 (polyacrylamide gel filtration beads) column equilibrated in 25 mM Tris pH 8.0, 400 mM KCl, 5mM MgOAc, 10% (v/v) glycerol, 0.02% NP-40, and 1 mM DTT. The resulting elution was analyzed by SDS-PAGE and stained with Coomassie Brilliant Blue R-250.

3.2.5   Reconstitution of Mcm2-7 complexes

Mcm2-7 complexes were reconstituted as described in Davey *et al.* [12] with the following exceptions. Two nmol of each protein was mixed and concentrated using an Amicon Ultra 10 kDa cutoff device (Millipore) at 4°C to a final volume of 0.2 ml and a conductivity equivalent to 350 mM NaCl. The mixture was then incubated at 15°C for 30 minutes, followed by centrifugation at 16,000 x g for 10 minutes at 4°C. The protein was then applied to a 24 ml Superose 6 10/300 GL size exclusion chromatography column

(GE Healthcare Life Sciences) equilibrated in Buffer H containing 100 mM NaCl. Fractions of 250 µl were collected and analyzed by 8% SDS-PAGE stained with Coomassie Brilliant Blue and confirmation of equal stoichiometry determined by densitometry using ImageQuant 5.2 software (Molecular Dynamics). Peak fractions were also examined for ATPase and DNA unwinding activity as described below.

3.2.6   DNA binding

DNA binding assays were performed with radiolabelled Mcm2-7^{3PK} as described in Stead *et al*. [13]. Two hundred fmol protein sample was incubated with the amount of DNA substrate indicated (50-200 fmol; M13mp19 ssDNA and Y70-Cdt1 dsDNA (yeast LEU2 CEN/ARS), both plasmids approximately 8 kb in size) in the presence or absence of 5 mM ATP in Tris-HCl pH 7.5, 0.1 mM EDTA, and 10 mM magnesium acetate for 10 minutes at 37°C. The sample was then analyzed on a 5ml, 4 % cross-linked agarose gel filtration column equilibrated in 20 mM Tris-HCl pH7.5, 10 mM magnesium acetate, 0.1 mM EDTA, 100 mM NaCl, 10% (v/v) glycerol, 50 µg/ml bovine serum albumin and 2 mM DTT. The amount of ^{32}P-Mcm2-7^{3PK} in each fraction was determined by scintillation counting. Analysis of the data (area under the curve for recovery and ANOVA for comparison of mean DNA binding) were conducted in GraphPad Prism (La Jolla, CA)

3.2.7   ATP hydrolysis

ATP hydrolysis by the pre-RC components in isolation or in combination with DNA substrate and with each other was assayed through the use of thin-layer chromatography (TLC). Each 12 µl reaction contained 20 mM Tris-HCl pH 7.5, 10mM magnesium acetate, 2 mM DTT, 1 mM [γ-^{32}P]-ATP (20 Ci/mmol; Perkin Elmer Life Sciences). For the experiments where Cdt1 was added to Mcm2-7, the proteins were incubated on ice for 60 min before the addition of ATP. After addition of ATP, the samples were incubated at 30°C for the indicated times. The reactions were quenched with an equal volume of ATPase stop buffer (40mM EDTA, 1% SDS). A portion (1 µl) was spotted onto polyethyleneimine cellulose TLC sheets (EM Science) and the sheets were developed in 0.6 M potassium phosphate monobasic (pH 3.4) for 15 min. The dried sheets were exposed to a PhosphorStorage screen before scanning on a Storm 860

scanner (GE Healthcare Life Sciences). Densitometry analysis using ImageQuant 5.2 (Molecular Dynamics) was used to determine the volume of the spots corresponding to P_i and ATP. The amount of P_i produced (in pmol) was determined by: [(volume P_i)/(volume P_i+volume ATP)] x 500 µM.

3.2.8   DNA unwinding

DNA unwinding assays were performed using a DNA substrate containing 30 base pairs of duplex with 60 nucleotides of single stranded DNA on one strand and a 5' biotin on the other as previously described [14]. Primer 2T, 5'-d(ATGTCCTAGCAAGCCAGAAT-TCGGCAGCGTC-(T)60)-3' was labelled with ^{32}P at the 5' end and annealed to 1B, 5'-biotin-d(GACGCTGCCGAATTCTGGCTTGCTAGGACAT)-3' by boiling 2 minutes in 10 mM Tris-HCl, pH 8.5, 30 mM sodium citrate and 300 mM NaCl, and then cooled slowly to room temperature. Each 6 µl reaction contained 20 mM Tris-acetate, pH 7.5, 10 mM magnesium acetate, 100 µM EDTA, 5 mM DTT, 5 mM ATP, 67 nM streptavidin, 5% PEG 3350, 100 mM sodium glutamate, 5 mM creatine phosphate, 20 µg/ml creatine kinase, 1 nM DNA substrate (concentration of labelled strand) and the indicated concentrations of Mcm2-7. If necessary, proteins were diluted in 20 mM Tris-acetate, pH 7.5, 100 µM EDTA, 2 mM DTT, 10% (v/v) glycerol and 40 µg/ml BSA. Reactions were incubated at 37°C for 10 minutes and then quenched by adding 0.7 µl of unlabelled 2T (1 µM) and 1.5 µl of Proteinase K (10 mg/ml) and incubated at 37°C for an additional 2 minutes. Samples were then treated with 2 µl of 5% SDS, 100 mM EDTA, 25% (v/v) glycerol, 0.1% bromophenol blue and 0.1% xylene cyanol FF. DNA products were resolved on 8% native polyacrylamide gels using 1x TBE (100 mM Tris, 90 mM borate, 1 mM EDTA) at 150 V for 40 minutes at room temperature. The gels were dried, exposed to PhosphorStorage screens and scanned on a Storm 860 scanner (GE Healthcare). The volume of bands corresponding to ssDNA and dsDNA as well as a background volume were determined by densitometry using ImageQuant 5.2 (Molecular Dynamics). The percentage of ssDNA product in an unreacted sample (no protein) was ≤ 5%. To normalize for the variability in these values, the percentage of unwinding was calculated by: % unwinding = (% ssDNA$_S$-% ssDNA$_{Np}$)/(1-% ssDNA$_{Np}$), where % ssDNA$_S$

represents the percentage of ssDNA in the sample lane and % ssDNA$_{Np}$ represents the percentage of ssDNA in the no protein lane.

3.2.9 Linear DNA templates for loading assay

ARS1 was PCR amplified from pMD187 using ARS1 Up, 5' biotin-d(GTTGTAAAAC-GACGGCCAGTGC)-3' and ARS1 down, 5'-d(AAGCGCCACGCTTCCCGAAG)-3'. Amplified ARS1 PCR products were purified by ethanol precipitation and resuspended in ddH$_2$O. Forty pmol ARS1 was coupled to 2 mg Dynabeads Kilobase Binder (Invitrogen, 601.01) as per manufacturer's instructions.
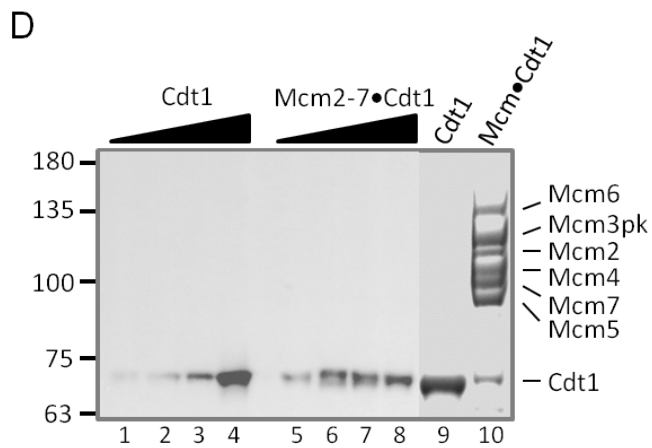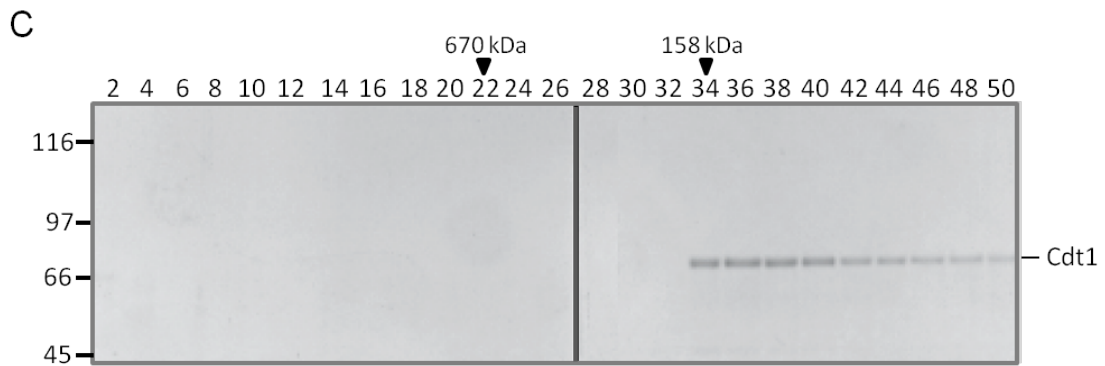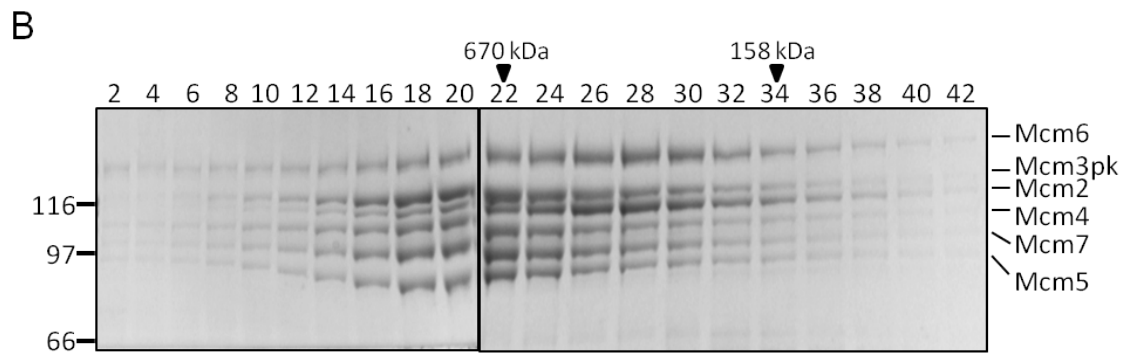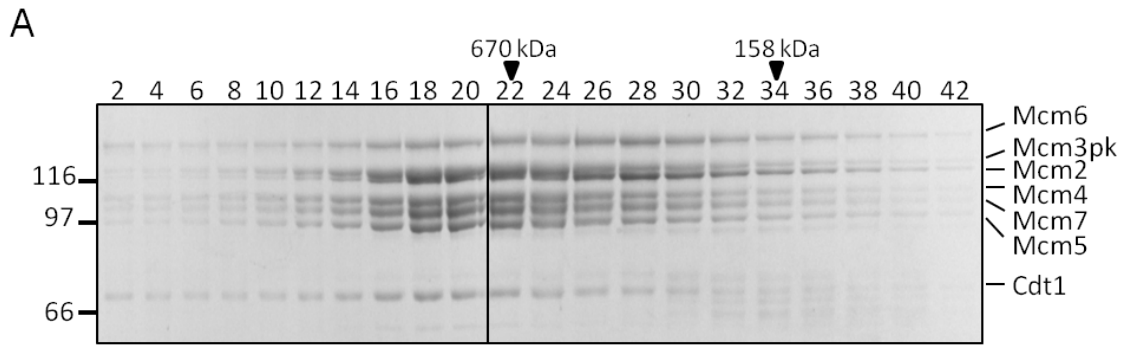
3.2.10 *In vitro* pre-RC loading assay

Loading reactions were based on Frigola *et al* [9] and each 40 µl reaction contained 100 nM ORC, 200 nM Cdc6, 400 nM Mcm2-7 or Mcm2-7•Cdt1 in 25 mM HEPES-KOH pH 7.6, 0.1 M potassium glutamate, 0.02% NP-40, 10 mM magnesium acetate, 5% (v/v) glycerol, 1 mM DTT and 5 mM ATP. DNA beads were included at 2.5 pmol of DNA molecules. Reactions were mixed on ice and incubated at 30°C for 30 minutes. Beads were washed once with 0.4 ml low-salt wash buffer (25 mM HEPES-KOH, pH 7.6; 0.3 M potassium glutamate; 0.02% NP-40; 5 mM magnesium acetate; 1 mM EDTA; 10% (v/v) glycerol; 1 mM DTT) and once with 0.4 ml high-salt wash buffer (as low-salt buffer, but 0.5 M NaCl instead of 0.3 M potassium glutamate).

3.3 Results

3.3.1 Interaction of Cdt1 with Mcm2-7

It has been known for some time that Cdt1 interacts with Mcm2-7 [15-18]. For example, Cdt1 and Mcm2-7 were co-purified from *S. cerevisiae* whole cell extracts and only Mcm2-7 complexed with Cdt1 was reconstituted into pre-replicative complexes *in vitro*; pre-RCs could not be reconstituted if Mcm2-7 and Cdt1 were added separately [5, 19]. These observations led to the proposal that an accessory factor may be required for Mcm2-7 and Cdt1 to interact [2, 5].

A

670 kDa   158 kDa

2 4 6 8 10 12 14 16 18 20 22 24 26 28 30 32 34 36 38 40 42

Mcm6
Mcm3pk
116
Mcm2
Mcm4
97
Mcm7
Mcm5
Cdt1
66

B

670 kDa   158 kDa

2 4 6 8 10 12 14 16 18 20 22 24 26 28 30 32 34 36 38 40 42

Mcm6
Mcm3pk
Mcm2
116
Mcm4
97
Mcm7
Mcm5
66

C

670 kDa   158 kDa

2 4 6 8 10 12 14 16 18 20 22 24 26 28 30 32 34 36 38 40 42 44 46 48 50

116

97

Cdt1
66

45

D

Cdt1   Mcm2-7•Cdt1   Cdt1   Mcm•Cdt1

180

135   Mcm6
                                                         Mcm3pk
                                                         Mcm2
100   Mcm4
                                                         Mcm7
                                                         Mcm5

75   Cdt1

63

1 2 3 4   5 6 7 8   9   10

Figure 3.1: Reconstitution of Mcm2-7•Cdt1 complexes

Mcm subunits and Cdt1 were expressed and purified separately from *E. coli* as described in Materials and Methods. **(A)** Reconstitution of Mcm2-7•Cdt1 from individual components. Shown is a Coomassie brilliant blue-stained SDS-PAGE (8%) of the indicated fractions from size exclusion chromatography. Controls with Mcm2-7 alone **(B)** and Cdt1 alone **(C)** are also shown. **(D)** Western blot analysis of Cdt1. 0.5, 1, 2 or 3 pmol recombinant Cdt1 (lanes 1-4) or Mcm2-7•Cdt1 complexes (lanes 5-8) were separated on a 6% SDS-PAGE gel and western blotted with rabbit polyclonal anti-Cdt1 antibody. Cdt1 (9 pmol) and Mcm2-7•Cdt1 (0.9 pmol) were run on the same gel and stained with Coomassie brilliant blue (lanes 9 and 10). The migration size of markers is shown on the left and of the proteins on the right. For size exclusion chromatography, the elution volume of molecular weight size standards run separately under the same conditions is shown above each of panels A-C.

To test this idea, we examined whether Cdt1 could interact and form a complex with Mcm2-7 without the addition of other factors. This was performed by mixing Cdt1 with each of the individual Mcm subunits and purifying complexes via size exclusion chromatography (Figure 3.1A) as described in Materials and Methods. For comparison, the elutions of Mcm2-7 alone (Figure 3.1B) and Cdt1 alone (Figure 3.1C) were also examined. In the presence of Mcm2-7, Cdt1 co-eluted with the Mcm2-7 complex, with the peak of elution corresponding to a size of ~670 kDa (Figure 3.1A). Notably, Mcm2-7•Cdt1 eluted much earlier than Cdt1 analyzed alone (Figure 3.1C). The identification of the Cdt1 band was confirmed by Western blotting using a polyclonal anti-Cdt1 antibody (Figure 3.1D). Densitometry analysis of Coomassie-stained SDS-PAGE gels demonstrated that Cdt1 was in a 1:1 ratio with each of the Mcm2-7 proteins. The change in apparent size of Cdt1, when in the presence of Mcm2-7 far exceeded the size seen when Cdt1 was alone and is indicative of a physical interaction between Mcm2-7 and Cdt1 (compare Figures 3.1A and C). The elution profile of Mcm2-7 (Figure 3.1B) and

Mcm2-7•Cdt1 (Figures 3.1A, B) are very similar. Not surprisingly, the addition of 68 kDa in the form of Cdt1 does not change the elution profile of the ~600 kDa Mcm2-7 complex. Together, these results indicate that a complex of Cdt1 and Mcm2-7 had formed. The interaction of Cdt1 and Mcm2-7 did not require addition of any other components or any post-translational modification of the proteins.

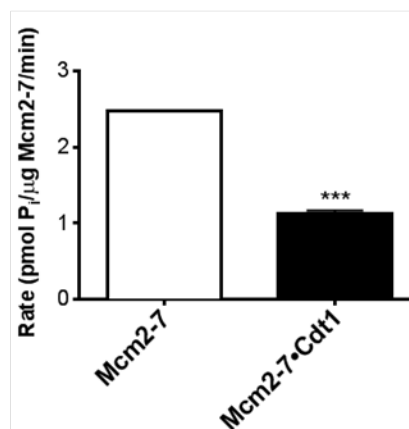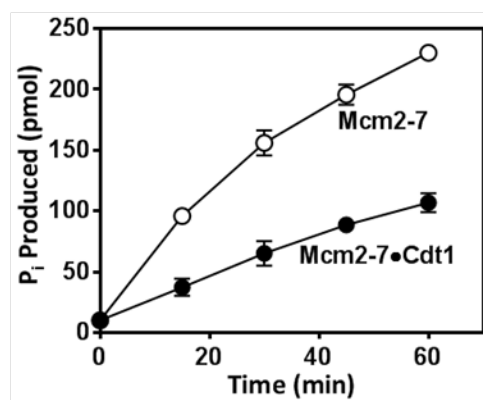## 3.3.2   Cdt1 inhibits ATP hydrolysis by Mcm2-7

We next asked whether the Mcm2-7•Cdt1 complex behaved differently from Mcm2-7. We first compared the ATPase activities of the two complexes. Cdt1 itself does not hydrolyze ATP, however Mcm2-7 does [12]. To this end, Mcm2-7 and Mcm2-7•Cdt1 were mixed with radiolabelled ATP and the products from hydrolysis separated by thin layer chromatography (TLC) as described in Materials and Methods. Despite equal amounts of protein, in both a protein titration (Figure 3.2A) and a time course experiment (Figure 3.2B), less ATPase activity was observed with Mcm2-7•Cdt1 than with Mcm2-7 alone. The rate of ATP hydrolysis by Mcm2-7•Cdt1 was approximately two-fold lower than that of Mcm2-7 alone (Figure 3.2B, right panel).

A lack of complete inhibition in ATPase activity by Mcm2-7•Cdt1 raised the possibility that this reconstitution contained a mixture of Mcm2-7 complexes with and without Cdt1. After all, the 68 kDa Cdt1 protein did not change the elution profile of Mcm2-7 (compare Figures 3.1A and B). As such, we asked whether or not ATPase activity would be inhibited to a greater extent if Cdt1 was added separately. As shown in Figure 3.2C, the rate of ATPase activity of Mcm2-7 and Mcm2-7•Cdt1 was reduced to a similar extent for substoichiometric and equimolar amounts of Cdt1. While the addition of two-fold excess Cdt1 reduced the rate of ATP hydrolysis by Mcm2-7 even further, a maximum reduction in Mcm2-7•Cdt1 ATPase activity was achieved at a 1:1 ratio. The amount of ATP hydrolyzed by Cdt1 alone was comparable to a sample lacking any protein (Figure 3.2D). These preliminary data suggest that majority, if not all, of the Cdt1 was complexed with Mcm2-7 in the Mcm2-7•Cdt1 reconstitution.
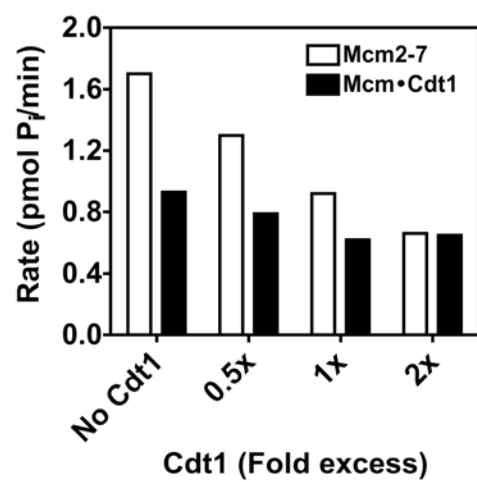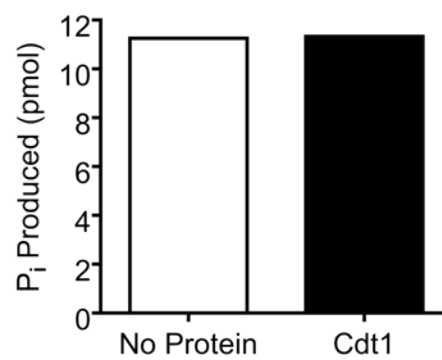
A
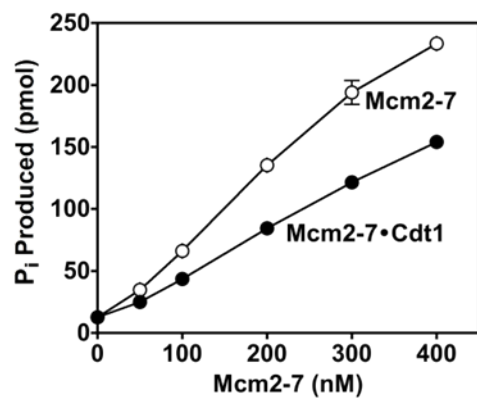
B

C

D

**Figure 3.2: Cdt1 inhibits ATPase activity of Mcm2-7**

ATP hydrolysis by Mcm2-7 or Mcm2-7•Cdt1 was measured by thin layer chromatography as described in Materials and Methods. **(A)** ATPase activity of various amounts of Mcm2-7 (empty circles) and Mcm2-7•Cdt1 (filled circles). **(B)** ATP hydrolysis of Mcm2-7 complexes (200 nM) was determined in a time course experiment and is shown on the left. The rate of hydrolysis is shown on the right. There is a significant difference between the means (P < 0.0001) **(C)** The rate of ATP hydrolysis by Mcm2-7 complexes (200 nM) with and without Cdt1 added in solution was determined in a time course. Cdt1 was purified as described in Materials and Methods, except a portion was further purified by size exclusion chromatography. Reactions in panels A and B were performed at least twice with the mean +/- standard error plotted. Some of the error bars are occluded by the symbols. **(D)** ATP hydrolysis by a sample lacking protein and Cdt1 alone (400 nM) was determined.

3.3.3   Cdt1 inhibits DNA unwinding by Mcm2-7

Since Mcm2-7 requires energy to carry out its helicase function (reviewed in 20), we predicted that the reduction in ATPase activity by Cdt1 would result in a concomitant reduction in DNA unwinding activity. To this end, we compared the DNA unwinding activity of Mcm2-7 and Mcm2-7•Cdt1 using a radiolabelled synthetic dsDNA fork substrate [14]. The DNA substrate contains a duplex region of 31 base pairs, one single-strand with a biotin-streptavidin moiety and one single-stranded extension or tail composed of 60 deoxythymidylates (dT60) [14]. Consistent with ATPase activity, DNA unwinding by equal amounts of complexes was approximately two-fold lower with Mcm2-7•Cdt1 than with Mcm2-7 (Figures 3.3A, B). We next attempted to examine the effect on activity of Mcm2-7 complexes when Cdt1 was added separately. As shown in Figure 3.3C, the dsDNA band that typically migrates just below the fork substrate was more pronounced following the addition of ≥ 100 nM Cdt1. This was indicative of high

single-strand exonuclease activity that degraded the poly dT60 tail on the fork substrate. As such, we could not assess the effect on DNA unwinding by Mcm2-7 when Cdt1 was added separately.
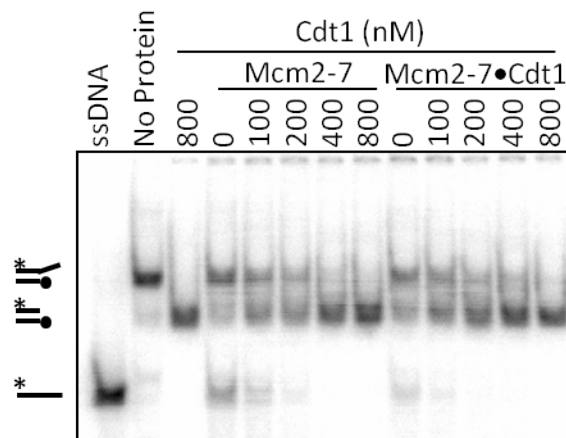
A
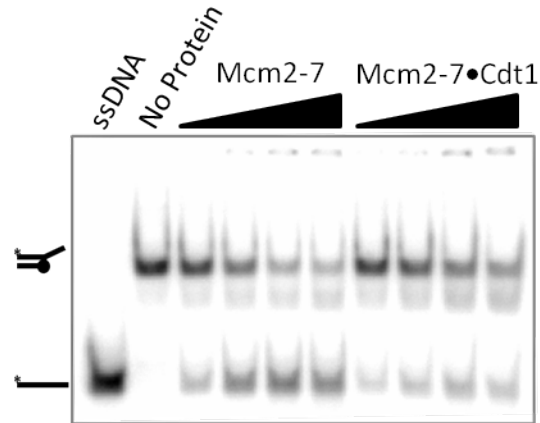
B
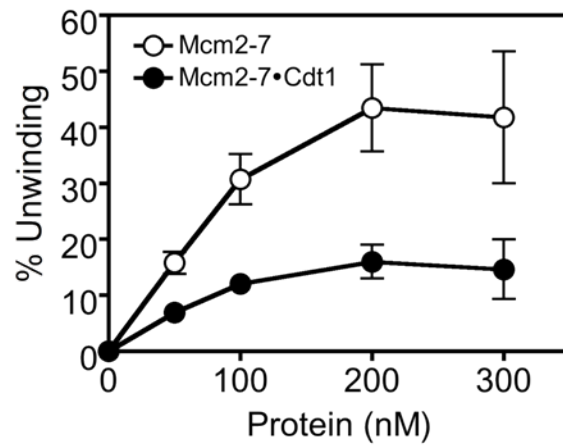
C

Figure 3.3: Cdt1 inhibits DNA unwinding by Mcm2-7

DNA unwinding activity by Mcm2-7 and Mcm2-7•Cdt1 was measured using a dsDNA fork substrate (1 nM) as outlined in Materials and Methods. **(A)** Shown is a representative gel of a DNA unwinding assay. The upper band corresponds to the double stranded DNA substrate. The lower band is single stranded DNA product. **(B)** Reactions in panel A were performed in triplicate with the mean +/- standard error plotted. Some of the error bars are occluded by the symbols. Quantification was performed by densitometry using ImageQuant 5.2 (Molecular Dynamics). **(C)** DNA unwinding by Mcm2-7 and Mcm2-7•Cdt1 complexes with and without Cdt1 added in solution. Cdt1 was purified as described in Materials and Methods, except a portion was further purified by size exclusion chromatography.

3.3.4   DNA binding activity of Mcm2-7•Cdt1

Mcm2-7 requires ATP to bind ssDNA, yet shows little to no affinity for dsDNA [13, 21]. As such, we next examined whether DNA binding by Mcm2-7 was altered by the presence of Cdt1 using gel filtration. In this case, DNA binding of radiolabelled Mcm2-7 or Mcm2-7•Cdt1 is detected by co-elution with DNA. Protein bound to DNA elutes early from the column (fractions 10-12), whereas free protein elutes later (fractions 16-31). First, increasing amounts of ssDNA were titrated into a constant amount of Mcm2-7 (Figure 3.4A) or Mcm2-7•Cdt1 (Figure 3.4B). While binding increased in a DNA-dependent manner, little to no difference in the ability of the two complexes to bind ssDNA was observed (Figure 3.4C).

Since Cdt1 is required to load Mcm2-7 onto origins of DNA, we thought to also investigate dsDNA binding activity of the two complexes. In a similar fashion as described above for ssDNA, dsDNA was titrated into a fixed amount of Mcm2-7 (Figure 3.5A) or Mcm2-7•Cdt1 (Figure 3.5B). Except at the lowest concentration of dsDNA tested, Mcm2-7•Cdt1 showed slightly lower binding compared to Mcm2-7 alone (Figure

3.5C). However, the overall amount of binding to dsDNA by either complex is considerably lower than that for ssDNA (compare Figures 3.4C and 3.5C), consistent with the fact that Mcm2-7 binds dsDNA poorly [13, 21].

Taken together, Cdt1 has little to no effect on the ability of Mcm2-7 to bind DNA. These results also suggest that the inhibitory effect conferred by Cdt1 on DNA unwinding by Mcm2-7 is not due to a defect in DNA binding.
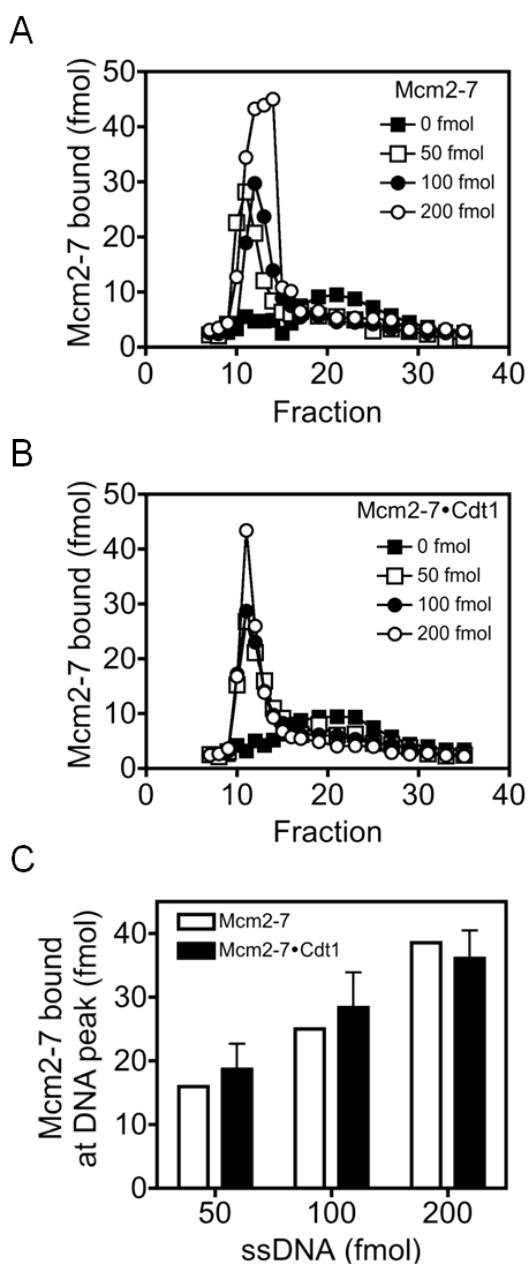
Figure 3.4: ssDNA binding activity of Mcm2-7 and Mcm2-7•Cdt1

DNA binding of Mcm2-7 complexes was measured using gel filtration as described in Materials and Methods. Shown are representative DNA binding assays for **(A)** Mcm2-7 and **(B)** Mcm2-7•Cdt1. **(C)** The amount of Mcm2-7 bound in the DNA peak at ssDNA concentrations of 50, 100 and 200 fmol, less the amount of protein bound in the absence of DNA. Shown is the mean +/- standard error for three replicates where indicated.
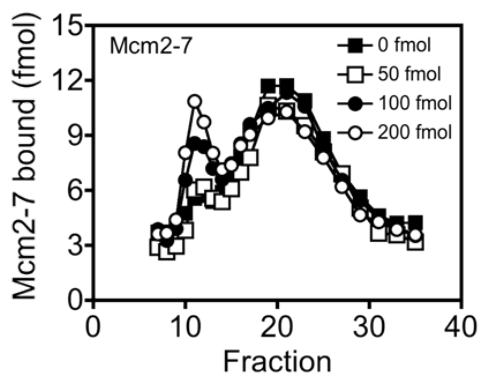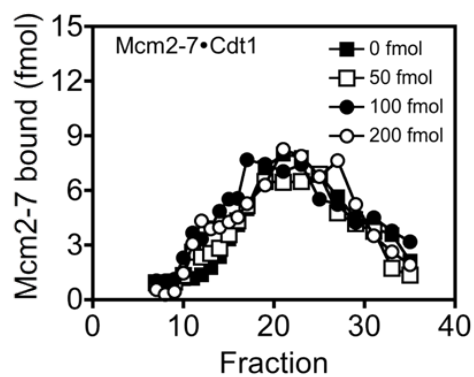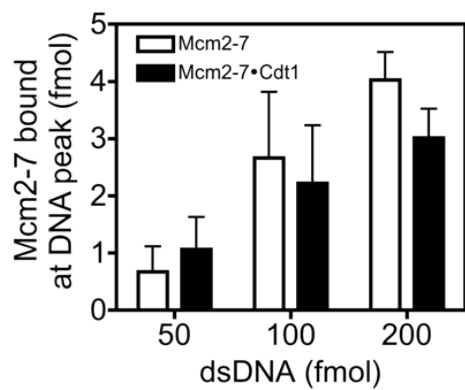
A

B

C

Figure 3.5: dsDNA binding activity of Mcm2-7 and Mcm2-7•Cdt1

Binding of Mcm2-7 complexes to dsDNA was measured via gel filtration as described in Materials and Methods. Shown are representative DNA binding assays for **(A)** Mcm2-7 and **(B)** Mcm2-7•Cdt1. **(C)** The amount of Mcm2-7 bound in the DNA peak at dsDNA concentrations of 50, 100 and 200 fmol, less the amount of protein bound in the absence of DNA. Shown is the mean +/- standard error for three replicates.

3.3.5   *In vitro* assembly of the pre-RC

In addition, we thought it was important to assemble the pre-RC on origins of replication from pure proteins because we wanted to control the modification state of the components. In this case, Mcm2-7 with or without Cdt1 was added to origin DNA coupled to magnetic beads in the presence of ORC, Cdc6 and ATP. Previous studies have used salt extraction to distinguish between two types of Mcm2-7 interactions with DNA: (i) salt sensitive, whereby Mcm2-7 complexes "associate" with DNA via protein-protein interactions with origin-bound pre-RC components; and (ii) salt resistant, in which Mcm2-7 complexes have been "loaded" onto origin DNA. To this end, beads were washed twice with buffer containing 0.3 M potassium glutamate (low salt) or once with low salt and once with buffer containing 0.5 M sodium chloride (high salt). In order to specifically isolate proteins bound to DNA rather than those interacting non-specifically with the magnetic beads, samples were treated with DNase I. Regardless of whether Mcm2-7 was purified from G1-arrested yeast extracts (Figure 3.6A) or reconstituted from individual subunits purified from bacterial-expression systems (Figure 3.7), loading was dependent on ORC, Cdc6 and Cdt1, consistent with published reports [2, 5, 6, 9]. We also found that the loading of Mcm2-7 using ORC and Mcm2-7 purified from yeast extracts was greater than that observed using pure proteins (compare Figure 3.6A, lane 4 and Figure 3.7, lane 7). Frigola and colleagues [9] reported that Mcm2-7 reconstituted from
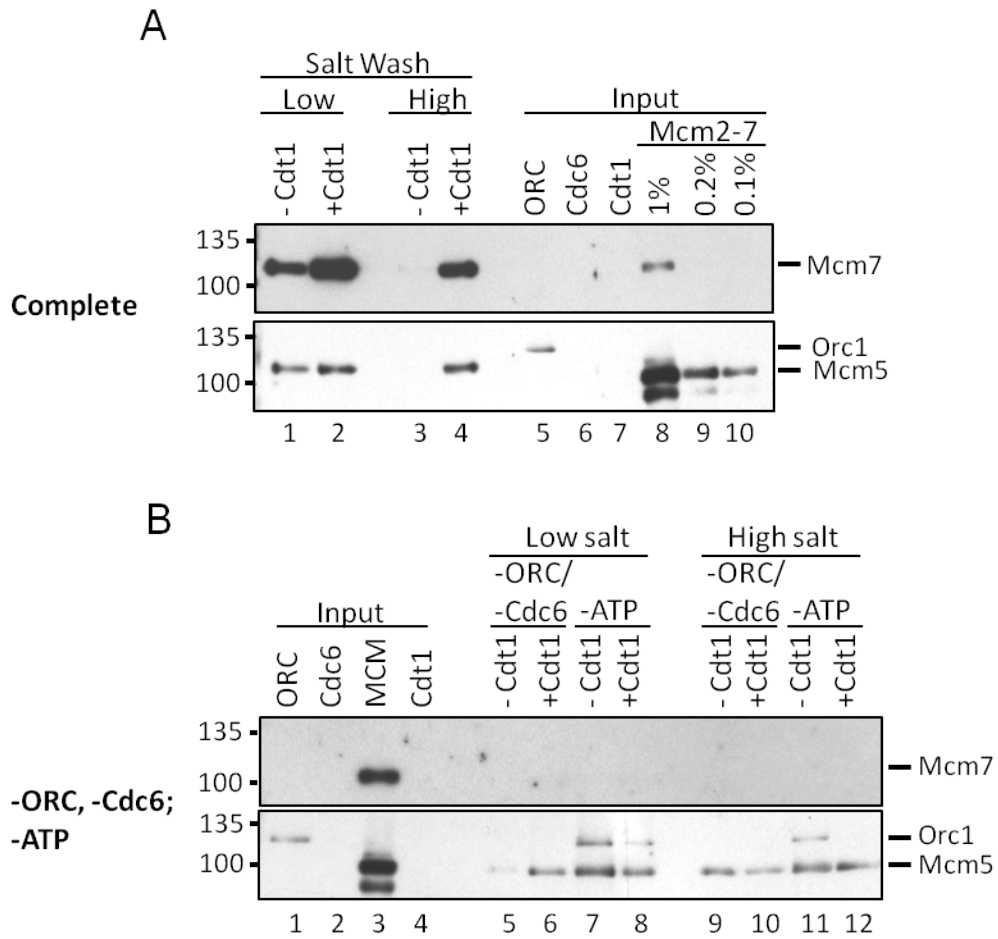
Figure 3.6: *In vitro* reconstitution of Mcm2-7 loading

(A) Western blot analysis of complete pre-RC formation using yeast-purified Mcm2-7 and ORC. Reactions contained 25 nM ARS1-coated beads, 5 mM ATP, 25 nM ORC, 50 nM Cdc6, 100 nM Mcm2-7 and where indicated, 100 nM Cdt1. Beads were washed twice with low-salt buffer (0.3 M K-glutamate; lanes 1 and 2) or once with low-salt and once with high-salt buffer (0.5 M NaCl; lanes 3 and 4). **(B)** Control reactions in the absence of ORC and Cdc6 (lanes 5 and 6, and 9 and 10) or in the absence of ATP (lanes 7 and 8, and 11 and 12). Beads were washed as in A. Input, 1% unless indicated; Elution, 50%. Migration of proteins is shown on the left and those analyzed are indicated on the right.

E. coli-expressed proteins was able to load onto origins as efficiently as Mcm2-7 purified from yeast. However, these authors used yeast-purified ORC in both loading reactions.

In order to determine the reason for the difference in Mcm2-7 loading efficiency, we next examined the ORC and Mcm2-7 complexes in more detail. It was conceivable that there was a difference in the subunit assemblies between yeast- and bacterial-expressed complexes. However, regardless of the source, the stoichiometry of ORC and Mcm2-7 subunits within each complex was approximately 1:1 (Figures 3.8A, B). The hydrolysis of ATP by ORC and Cdc6 is required for the stable association of Mcm2-7 with origins [6, 9, 22-24]. As such, we examined the ATPase activity of the pre-RC components on their own or in combination with each other (Figure 3.8C). Preliminary results demonstrated that while the ATPase activity of bacterial-expressed ORC was approximately two-fold lower than that of ORC purified from G1-arrested yeast extracts (yORC), the ATPase activity of ORC and Cdc6 together was augmented, but comparable between the two sources of ORC. Whereas the hydrolysis of ATP by yeast-purified Mcm2-7 (yMCM) was slightly lower than that of reconstituted Mcm2-7, there was little to no difference in ATPase activity between the two sources of protein when combined with other pre-RC components.
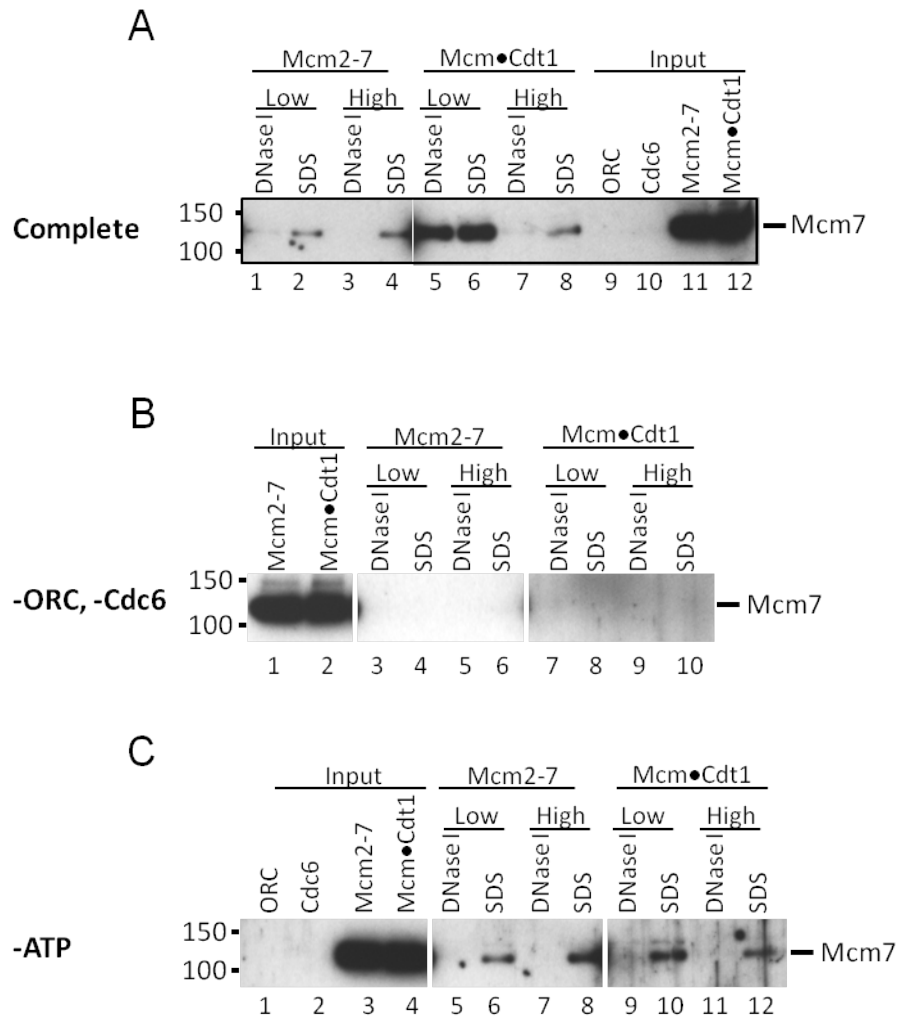
Figure 3.7: *In vitro* loading reactions using pure proteins

(A) Western blot analysis of complete pre-RC formation using proteins purified from bacterial-expression systems. Reactions contained 25 nM ARS1-coated beads, 5 mM ATP, 25 nM ORC, 50 nM Cdc6, 100 nM Mcm2-7 or 100 nM Mcm2-7•Cdt1. Beads were washed with low salt buffer (lanes 1 and 2, and 5 and 6) or high salt buffer (lanes 3 and 4, and 7 and 8). Beads were treated with DNase I, and then boiled in 1x SDS sample loading buffer (SDS). Control reactions in the **(B)** absence of ORC and Cdc6 (lanes 3-10) or **(C)** absence of ATP (lanes 5-12) are also shown. Beads were washed and treated as in A. Input, 10%; DNase I or SDS elution, 50%. Migration of proteins is shown on the left and those analyzed are indicated on the right.
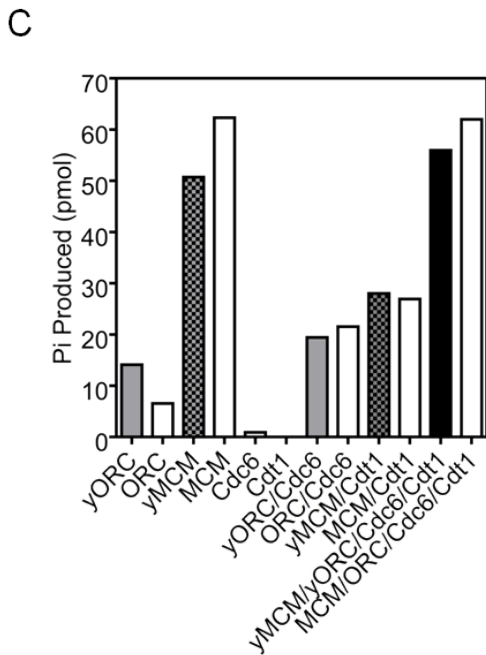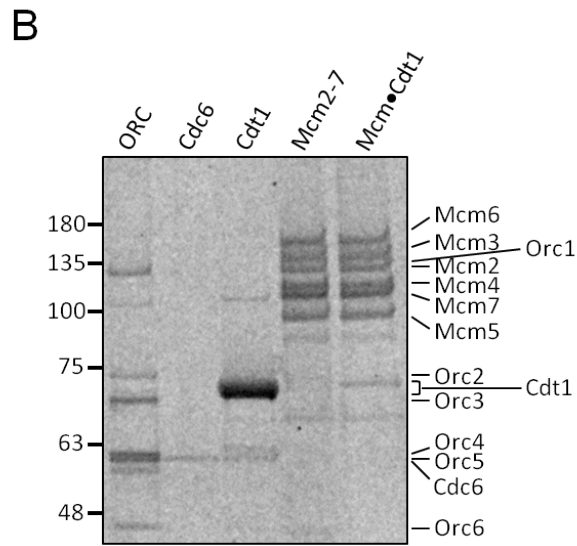
A

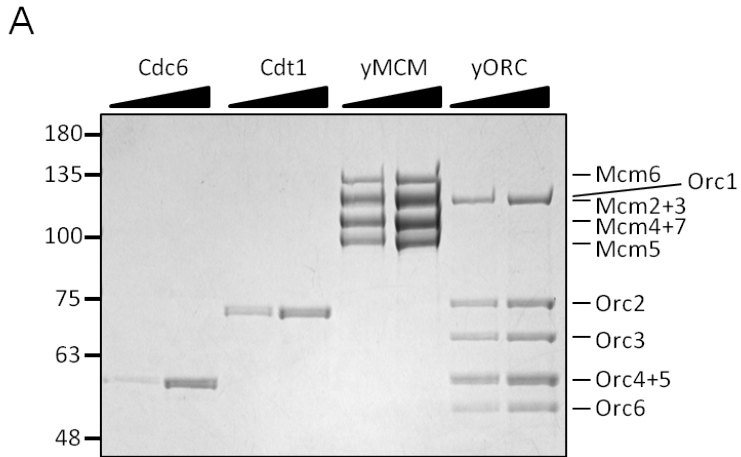

B

C

Figure 3.8: Biochemical analysis of pre-RC components

(A) Aliquots of each of the protein component were run on an 8% SDS-PAGE gel and stained with Coomassie brilliant blue. yMCM and yORC (kindly provided by Mike O'Donnell) were purified from G1-arrested yeast extracts; Cdc6 and Cdt1 were purified from *E. coli*. **(B)** Individual proteins were purified from bacterial-expression systems as described in Materials and Methods. An aliquot of each component was run on an 8% SDS-PAGE gel and stained with SYPRO Ruby protein gel stain (Life Technologies). Cdt1, 500 ng. Protein amounts represent 50% of the input used in the loading reactions shown in Figure 3.7. **(C)** ATP hydrolysis was measured by thin layer chromatography as described in Materials and Methods. Reactions contained 200 nM of each component and were incubated at 30°C for 30 minutes. yORC (grey bars), yMCM (checkered grey bars), complexes purified from G1-arrested yeast extracts.

3.3.6 Cdt1 stabilizes Mcm2-7

We observed in our initial Mcm2-7 reconstitutions (Figure 3.1) that Cdt1 appeared to "rationalize" Mcm2-7. That is, in the presence of Cdt1, stoichiometric amounts of Mcm2-7 were observed, whereas in the absence of Cdt1, multimers and/or subcomplexes of Mcm subunits were more pronounced. Reconstitutions of Mcm2-7•Cdt1 complexes in the O'Donnell lab have also shown similar results (L. Langston, pers. comm.). From these data, we hypothesized that Cdt1 may play a role in stabilizing Mcm2-7 and took several approaches to explore this in greater detail. Using pure proteins, we investigated the formation of Mcm2-7 subcomplexes in the presence or absence of Cdt1 (Figure 3.9). Similar to that observed for Mcm2-7, in the presence of Cdt1, stoichiometric amounts of Mcm2, 4 and 6 (Mcm evens) were observed (compare Figures 3.9A and B). Surprisingly, while a subcomplex consisting of Mcm odds formed in the absence of Cdt1 (Figure 3.9C), a subcomplex consisting of stoichiometric amounts of all four proteins appeared to form (Figure 3.9D). We also found that in the absence of Cdt1, Mcm odds eluted from gel filtration as both trimers and hexamers (Figure 3.9D, fractions 30-32 and 24-26).
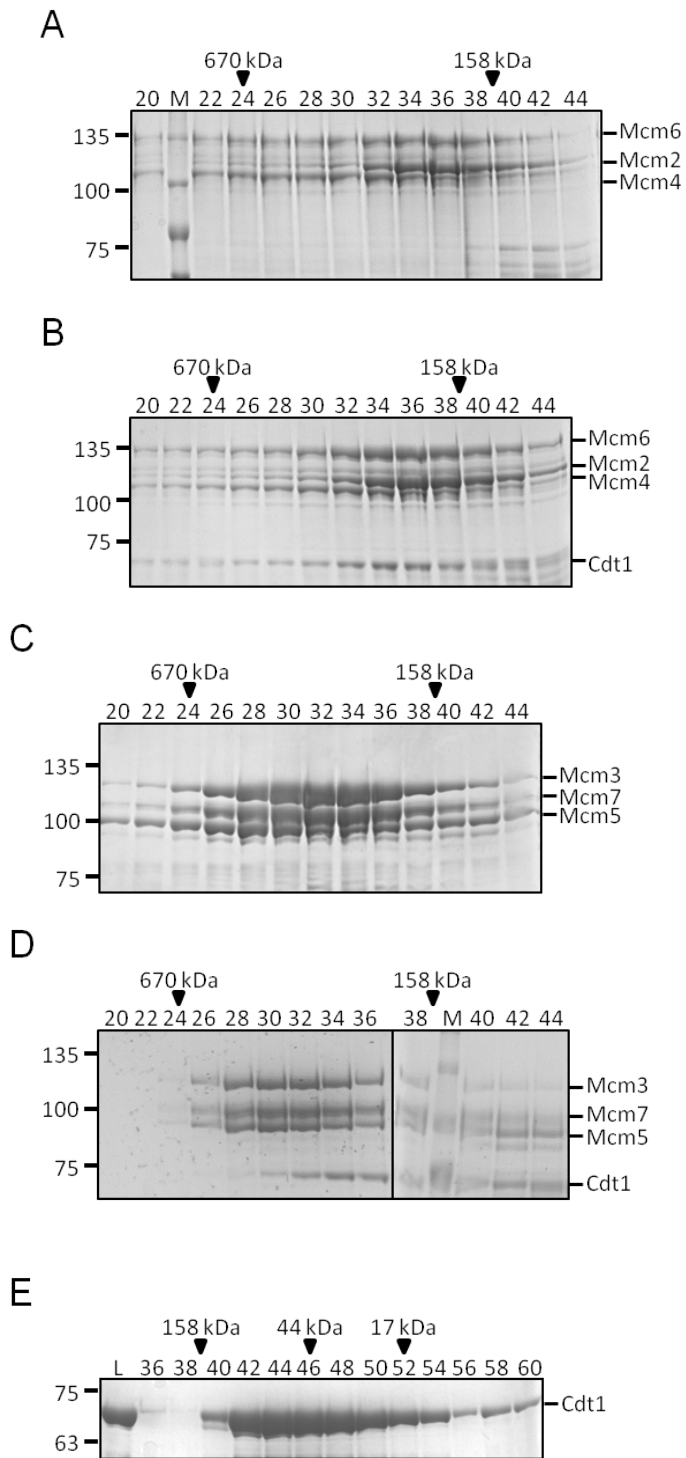
Figure 3.9: Reconstitution of Mcm2-7 subcomplexes

Individual proteins were combined and purified over a Superose 6 gel filtration column as described in Materials and Methods. Shown are reconstitutions for **(A)** Mcm246, **(B)** Mcm246 in the presence of Cdt1, **(C)** Mcm357 and **(D)** Mcm357 with Cdt1. **(E)** Size exclusion chromatography of Cdt1 alone under the same conditions. The migration of size standards is shown on the left and the proteins stained are shown on the left of each panel. The elution of molecular weight standards run separately under the same conditions is shown at the top of each panel.

It is of note that Mcm2-7 complexes and subcomplexes reconstituted from subunits purified from *E. coli* were done in the absence of ATP. Serendipitously, we discovered that when all six Mcm subunits are expressed in yeast, purification over anti-FLAG M2 resin (via FLAG-Mcm5) in the absence of ATP only pulls out the Mcm3, 5 and 7. Conversely, the addition of ATP to the purification recovers all six Mcm subunits (Figure 3.10).

The Diffley lab recently showed that after a low salt wash, only Mcm3, 5 and 7 (Mcm odds) are retained on origin DNA in ATPγS upon mixing Mcm2-7 in a pre-RC loading reaction lacking Cdt1 [9]. As such, we next investigated the recruitment of Mcm odds to ORC-Cdc6 in the absence of Mcm evens and Cdt1 using silver staining (Figure 3.11). We found that the Mcm357 subcomplex was associated (low salt) with origin DNA in the absence of both Mcm246 and Cdt1 (Figure 3.11, lanes 1 and 2). In addition, this association was enhanced in the presence of the poorly hydrolysable ATP analog, ATPγS (Figure 3.11, compare lanes 1 and 2). Consistent with published results [5, 9], and regardless of the ATP analog used, none of the pre-RC components bound to origin DNA in the absence of ORC and Cdc6 (Figure 3.11, lanes 3 and 4). While we observed binding of ORC and Cdc6 in the absence of ATP, the association of the Mcm odds complex was dependent on ATP (Figure 3.11, lane 5).
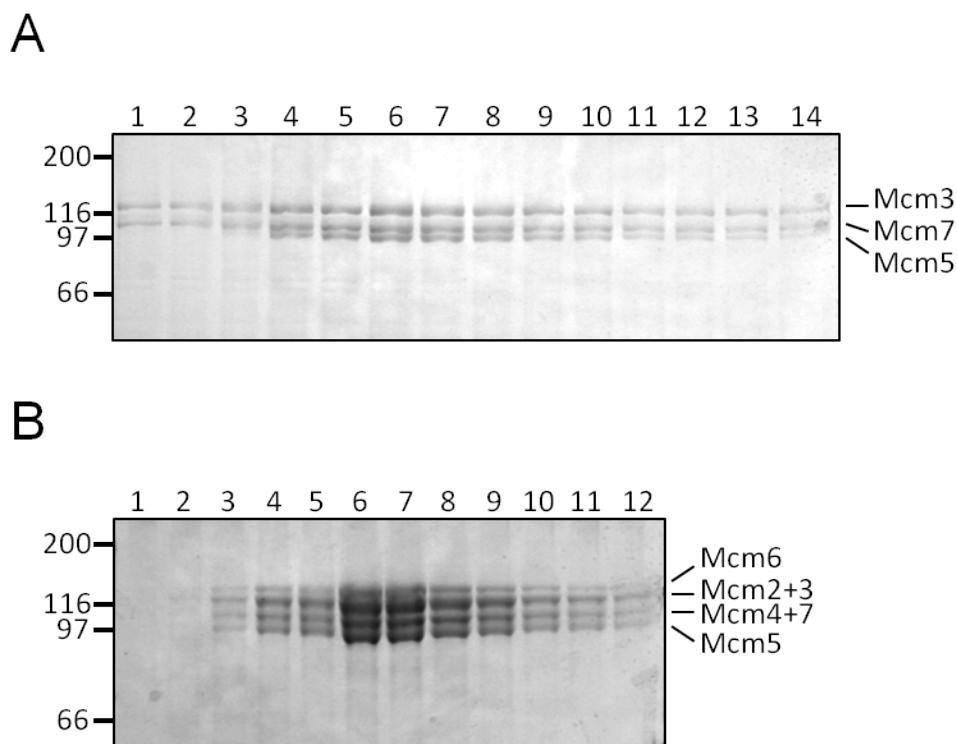
Figure 3.10: Mcm2-7 dissociates into subcomplexes in the absence of ATP

Yeast Mcm2-7 was isolated from G1-arrested yeast extracts and purified by anti-FLAG M2 resin via a FLAG tag on Mcm5. **(A)** Purification in the absence of ATP recovers only Mcm3, 5 and 7. Shown is a Coomassie brilliant blue-stained SDS-PAGE gel (8%) of the indicated fractions. **(B)** All six Mcm subunits are recovered when Flag-Mcm2-7 is purified in the presence of ATP. Individual fractions were separated on an 8% SDS-PAGE gel and stained with Coomassie brilliant blue. The migration size of protein standards is shown on the left and of the Mcm subunits isolated on the right.
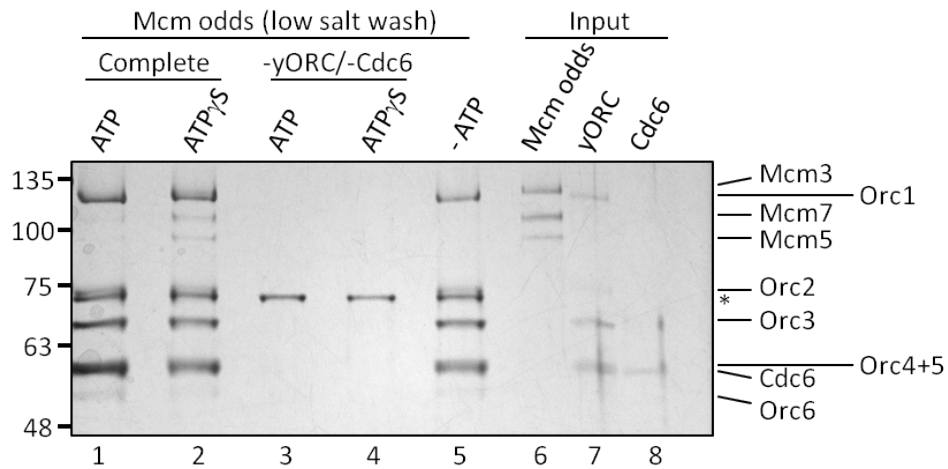
Figure 3.11: Mcm357 associates with origins in the absence of Cdt1

Mcm357 subcomplexes were tested for the association with ARS1 origin DNA in the absence of Cdt1. Complete reactions contained 400 nM Mcm357, 100 nM yORC, 200 nM Cdc6 and 62.5 nM ARS1-coated magnetic beads in the presence of 5 mM ATP (lane 1) or ATPγS (lane 2). Control reactions in the absence of ORC and Cdc6 (lanes 3 and 4) and in the absence of ATP (lane 5) are also shown. Samples were incubated at 30°C for 30 minutes, the beads were then washed once with low salt buffer and DNA-bound proteins eluted with DNase I. Samples were separated on an 8% SDS-PAGE gel and silver stained. The asterix (*) denotes DNase I in reaction lanes 1-5. Elution (lanes 1-5), 100%; Input (lanes 6-8), 0.2 pmol each protein component.

3.4 Discussion

We have shown here, using yeast proteins purified from bacterial-expression systems, that Cdt1 can form a stable complex with Mcm2-7. It is noteworthy that this interaction did not require any other replication factors or post-translational modification. This is consistent with a recent report demonstrating that Mcm2-7•Cdt1 complexes could be reconstituted from pure proteins [9]. We also demonstrated that Cdt1 inhibits the ATPase activity of Mcm2-7, either when reconstituted with Mcm2-7 (Mcm2-7•Cdt1) or when added separately to Mcm2-7. There was an approximate two-fold reduction in ATPase activity compared to Mcm2-7 alone. Fernández-Cid and colleagues [6] recently observed that in the presence of ARS1 origin DNA, the binding of Cdt1 to Mcm2-7 caused a 35% reduction in the rate of ATPase activity. In addition, we discovered a two-fold reduction in DNA unwinding by Mcm2-7•Cdt1 relative to Mcm2-7. We also observed that Mcm2-7 and Mcm2-7•Cdt1 complexes bound DNA with equal affinity. Since the hydrolysis of ATP by Mcm2-7 is neither augmented by nor dependent on DNA and the fact that ATP hydrolysis by Mcm2-7 is required for the complex to translocate along and unwind DNA [20], our results suggest that the defect in helicase activity by Mcm2-7•Cdt1 is not due to a reduced ability to bind DNA, but rather the result of the inhibitory effect on Mcm2-7 ATPase activity conferred by Cdt1 binding.

Consistent with published results, we further demonstrated that recombinant Cdt1 is both required and competent to load Mcm2-7 complexes onto replication origins in a high salt-stable manner. The loading efficiency was greater in the presence of Mcm2-7 and ORC purified from G1-arrested yeast extracts than pure proteins. We found little to no difference in the stoichiometry of the two ORC complexes or the hydrolysis of ATP by ORC-Cdc6 that would account for this difference. ORC is a target for CDK to prevent re-replication during S phase (reviewed in 25) and it has been shown that phosphorylated ORC reduces the association of Mcm2-7•Cdt1 with ORC-Cdc6 and inhibits Mcm2-7 loading [26]. In addition, a complex consisting of ORC-Cdc6-Mcm2-7 (OCM) that is essential for Mcm2-7 double hexamer formation at origins was severely reduced by CDK-phosphorylated ORC [6]. These findings rule out post-translational modification as a determining factor. Attempts to determine the DNA binding efficiency

of bacterial-expressed ORC failed and as such we cannot preclude that subtle structural differences between yeast- and bacterial-expressed ORC confer upon the former a more stable interaction with DNA and/or other pre-RC components.

Furthermore, we observed that the stability of Mcm2-7 is enhanced in the presence of Cdt1. Interestingly, we found that when ATP was present during the purification of Mcm proteins from G1-arrested yeast extracts, all six Mcm subunits formed hexamers with equal stoichiometry. Conversely, Mcm2-7 dissociated into a stable Mcm357 complex when ATP was absent during purification. Previous results from our lab suggest that the binding of ATP by Mcm467 stabilizes the formation of hexamers. Moreover, the Mcm odds appeared to migrate as a hexamer in the absence of Cdt1, indicating intermolecular contacts. This is not without precedence as several Mcm subunits can form homodimers [27]. Consistent with data from the Diffley lab [9], a subcomplex consisting of Mcm357 can associate with origin DNA in the absence of Mcm2, 4, and 6 and Cdt1. This association was greater in the presence of ATPγS. Furthermore, the association of Mcm357 with ORC-Cdc6 at origins, via Mcm3 [9], was severely reduced in the presence of ATP. Consistent with published results [9], this suggests that ATP hydrolysis can cause the release of Mcm subunits when attempts to load an incomplete Mcm2-7•Cdt1 complex are made.

We do not yet know how Cdt1 inhibits the ATPase activity of Mcm2-7, but it is likely mediated through Mcm6. Several reports have shown that Cdt1 interacts with the C-terminus of Mcm6 to load Mcm2-7 onto origins [7, 8, 15, 16, 18]. Since ATPase active sites are located at the interface between Mcm subunits [12, 20, 28], it is also possible that Cdt1 binds to and disrupts the ATPase sites formed between Mcm6 and its neighboring subunits, namely Mcm2 and Mcm4. The Mcm6/2 active site represents one of the three major sites of ATP hydrolysis within Mcm2-7 [12]. Binding of Cdt1 to Mcm2-7 may also induce subtle structural changes in the Mcm2-7 complex that disrupt one or more of the three major ATPase active sites. Indeed, the ATPase rate of AAA+ ATPases is altered upon subtle structural changes, such as due to interaction with another protein [29]. Furthermore, structural changes in Mcm2-7 have been suggested, such as due to the

binding of Cdc45 and GINS which causes a 300-fold increase in ATPase activity by Mcm2-7 [30, 31].

As further evidence to support the essential role of Cdt1, the Speck lab [6] recently showed that in the absence of Cdt1, recruitment of Mcm2-7 to origins by ORC-Cdc6 is abrogated. On the other hand, the binding of Cdt1 to Mcm2-7 alleviates an autoinhibitory property within the C-terminal tail of Mcm6 to promote helicase loading. The hydrolysis of ATP by Orc1 and Cdc6 causes the release of Cdt1 and formation of a complex consisting of ORC, Cdc6 and Mcm2-7 (OCM) which functions in Mcm2-7 double hexamer assembly [6]. Of note, the inhibitory effect conferred upon Mcm2-7 by Cdt1 was independent of origin DNA and other pre-RC factors. It is also intriguing that we and others [6] have observed a partial, rather than a complete, inhibition of Mcm2-7 activity in the presence of Cdt1. Any amount of untimely helicase activity by Mcm2-7 would be detrimental to the fidelity of DNA replication. As such, it is possible that another mechanism exists to fully downregulate Mcm2-7 function during G1 phase. Taken together, our results further support the essential role Cdt1 plays in modulating Mcm2-7 activity. Moreover, the interaction of Cdt1 with Mcm2-7 may represent a quality control mechanism during G1 phase to prevent wanton DNA unwinding until all pre-RC components are recruited and post-translational modification states are met.

3.5 References

1. Tanaka,S. & Diffley,J.F. Interdependent nuclear accumulation of budding yeast Cdt1 and Mcm2-7 during G1 phase. *Nat. Cell Biol.* **4**, 198-207 (2002).

2. Evrin,C., Clarke,P., Zech,J., Lurz,R., Sun,J. *et al.* A double-hexameric MCM2-7 complex is loaded onto origin DNA during licensing of eukaryotic DNA replication. *Proc. Natl. Acad. Sci. U. S. A* **106**, 20240-20245 (2009).

3. Chen,S., de Vries,M.A., & Bell,S.P. Orc6 is required for dynamic recruitment of Cdt1 during repeated Mcm2 7 loading. *Genes Dev* **21**, 2897-2907 (2007).

4. Gambus,A., Khoudoli,G.A., Jones,R.C., & Blow,J.J. MCM2-7 form double hexamers at licensed origins in Xenopus egg extract. *J. Biol. Chem.* **286**, 11855-11864 (2011).

5. Remus,D., Beuron,F., Tolun,G., Griffith,J.D., Morris,E.P. *et al.* Concerted loading of Mcm2-7 double hexamers around DNA during DNA replication origin licensing. *Cell* **139**, 719-730 (2009).

6. Fernandez-Cid,A., Riera,A., Tognetti,S., Herrera,M.C., Samel,S. *et al.* An ORC/Cdc6/MCM2-7 complex is formed in a multistep reaction to serve as a platform for MCM double-hexamer assembly. *Mol. Cell* **50**, 577-588 (2013).

7. Zhang,J., Yu,L., Wu,X., Zou,L., Sou,K.K. *et al.* The interacting domains of hCdt1 and hMcm6 involved in the chromatin loading of the MCM complex in human cells. *Cell Cycle* **9**, 4848-4857 (2010).

8. Wu,R., Wang,J., & Liang,C. Cdt1p, through its interaction with Mcm6p, is required for the formation, nuclear accumulation and chromatin loading of the MCM complex. *J. Cell Sci.* **125**, 209-219 (2012).

9. Frigola,J., Remus,D., Mehanna,A., & Diffley,J.F. ATPase-dependent quality control of DNA replication origin licensing. *Nature* **495**, 339-343 (2013).

10. Takara,T.J. & Bell,S.P. Multiple Cdt1 molecules act at each origin to load replication-competent Mcm2-7 helicases. *EMBO J.* **30**, 4885-4896 (2011).

11. Ferenbach,A., Li,A., Brito-Martins,M., & Blow,J.J. Functional domains of the Xenopus replication licensing factor Cdt1. *Nucleic Acids Res.* **33**, 316-324 (2005).

12. Davey,M.J., Indiani,C., & O'Donnell,M. Reconstitution of the Mcm2-7p heterohexamer, subunit arrangement, and ATP site architecture. *J. Biol. Chem.* **278**, 4491-4499 (2003).

13. Stead,B.E., Sorbara,C.D., Brandl,C.J., & Davey,M.J. ATP binding and hydrolysis by Mcm2 regulate DNA binding by Mcm complexes. *J. Mol. Biol.* **391**, 301-313 (2009).

14. Kaplan,D.L., Davey,M.J., & O'Donnell,M. Mcm4,6,7 uses a "pump in ring" mechanism to unwind DNA by steric exclusion and actively translocate along a duplex. *J Biol. Chem.* **278**, 49171-49182 (2003).

15. Jee,J., Mizuno,T., Kamada,K., Tochio,H., Chiba,Y. *et al.* Structure and mutagenesis studies of the C-terminal region of licensing factor Cdt1 enable the identification of key residues for binding to replicative helicase Mcm proteins. *J. Biol. Chem.* **285**, 15931-15940 (2010).

16. Wei,Z., Liu,C., Wu,X., Xu,N., Zhou,B. *et al.* Characterization and structure determination of the Cdt1 binding domain of human minichromosome maintenance (Mcm) 6. *J. Biol. Chem.* **285**, 12469-12473 (2010).

17. Cook,J.G., Chasse,D.A., & Nevins,J.R. The regulated association of Cdt1 with minichromosome maintenance proteins and Cdc6 in mammalian cells. *J. Biol. Chem.* **279**, 9625-9633 (2004).

18. Yanagi,K., Mizuno,T., You,Z., & Hanaoka,F. Mouse geminin inhibits not only Cdt1-MCM6 interactions but also a novel intrinsic Cdt1 DNA binding activity. *J. Biol. Chem.* **277**, 40871-40880 (2002).

19. Kawasaki,Y., Kim,H.D., Kojima,A., Seki,T., & Sugino,A. Reconstitution of Saccharomyces cerevisiae prereplicative complex assembly in vitro. *Genes Cells* **11**, 745-756 (2006).

20. Iyer,L.M., Leipe,D.D., Koonin,E.V., & Aravind,L. Evolutionary history and higher order classification of AAA+ ATPases. *J. Struct. Biol.* **146**, 11-31 (2004).

21. Bochman,M.L. & Schwacha,A. Differences in the single-stranded DNA binding activities of MCM2-7 and MCM467: MCM2 and MCM5 define a slow ATP-dependent step. *J. Biol. Chem.* **282**, 33795-33804 (2007).

22. Bowers,J.L., Randell,J.C., Chen,S., & Bell,S.P. ATP hydrolysis by ORC catalyzes reiterative Mcm2-7 assembly at a defined origin of replication. *Mol Cell* **16**, 967-978 (2004).

23. Randell,J.C., Bowers,J.L., Rodriguez,H.K., & Bell,S.P. Sequential ATP hydrolysis by Cdc6 and ORC directs loading of the Mcm2-7 helicase. *Mol Cell* **21**, 29-39 (2006).

24. Evrin,C., Fernandez-Cid,A., Zech,J., Herrera,M.C., Riera,A. *et al.* In the absence of ATPase activity, pre-RC formation is blocked prior to MCM2-7 hexamer dimerization. *Nucleic Acids Res.* **41**, 3162-3172 (2013).

25. Bell,S.P. & Dutta,A. DNA replication in eukaryotic cells. *Annu. Rev. Biochem* **71**, 333-374 (2002).

26.   Chen,S. & Bell,S.P. CDK prevents Mcm2-7 helicase loading by inhibiting Cdt1 interaction with Orc6. *Genes Dev.* **25**, 363-372 (2011).

27.   Davey,M.J. & O'Donnell,M. Replicative helicase loaders: ring breakers and ring makers. *Curr. Biol.* **13**, R594-R596 (2003).

28.   Erzberger,J.P. & Berger,J.M. Evolutionary relationships and structural mechanisms of AAA+ proteins. *Annu. Rev. Biophys. Biomol. Struct.* **35**, 93-114 (2006).

29.   Hanson,P.I. & Whiteheart,S.W. AAA+ proteins: have engine, will work. *Nat. Rev. Mol. Cell Biol.* **6**, 519-529 (2005).

30.   Costa,A., Ilves,I., Tamberg,N., Petojevic,T., Nogales,E. *et al.* The structural basis for MCM2-7 helicase activation by GINS and Cdc45. *Nat. Struct. Mol. Biol.* **18**, 471-477 (2011).

31.   Ilves,I., Petojevic,T., Pesavento,J.J., & Botchan,M.R. Activation of the MCM2-7 helicase by association with Cdc45 and GINS proteins. *Mol. Cell* **37**, 247-258 (2010).

Chapter 4

4   Investigating the role of phosphorylation on Mcm2-7 activity

4.1   Introduction

Faithful duplication of the genome is essential to the maintenance of the genetic integrity of all organisms. Errors during this process can lead to diseases arising from genomic instability, such as cancer [1]. Eukaryotes have developed highly conserved and tightly controlled mechanisms to ensure this occurs once and only once per cell division cycle. Primary to this control is the strict temporal separation of helicase loading during late M and G1 phase and helicase activation during S phase of the cell cycle [2-4]. Mcm2-7 is loaded into the pre-RC in an inactive state. During S phase, a series of events are thought to occur in order to activate Mcm2-7 to unwind DNA. The prevailing view suggests that one of these events involves DDK-dependent hyperphosphorylation of the N-terminal domains of Mcm4 and Mcm6 within Mcm2-7 [5-8]. There exist conflicting results surrounding the activation of Mcm2-7 to unwind DNA. While some studies demonstrated that DDK-dependent hyperphosphorylation of Mcm4 and Mcm6 was required for Mcm2-7 activation [5-8], another study showed no effect on Mcm2-7 activity after phosphatase treatment [9]. A recent report [8] demonstrated that the N-terminus of Mcm4 contains an inhibitory activity that is alleviated by DDK. Indeed, mutations in N-terminal domains of Mcm subunits that can be phosphorylated are able to bypass the requirement for DDK *in vivo* [8, 10]. Recently, the Stillman lab identified a phosphomimetic (PM) form of Mcm4 deleted for the inhibitory domain (Figure 4.1A) that when incorporated into Mcm2-7 is able to bypass the requirement for DDK [8]. In contrast, the Schwacha lab demonstrated that the activity of yeast Mcm2-7 purified from baculovirus-expression systems was unaltered after phosphatase treatment [9]. In an effort to clarify the ambiguity between Mcm2-7 phosphorylation and activation, I incorporated the phosphomimetic Mcm4 mutant into Mcm2-7 complexes. Here I show that wildtype and phosphomimetic Mcm2-7 complexes reconstituted from individual subunits purified from bacterial-expression

systems exhibit activity. I also show that the activity of phosphomimetic Mcm2-7 is comparable to that of wildtype.

4.2   Materials and Methods

4.2.1   Cloning of Mcm2-7 genes

For bacterial expression of Mcm proteins, each of the MCM genes was amplified from *Saccharomyces cerevisiae* genomic DNA and cloned into pET plasmids as described in Davey *et al*. [11]. A PKA recognition motif was fused to *MCM3* as described in Stead *et al*. [12]. For *mcm4pm*, a mutant version of the *MCM4* gene containing glutamic acid substitutions at the previously characterized DDK targets sites [5] was generated by gene synthesis. To do so, a portion of the *MCM4* coding sequence was synthesized with substitutions of the codons coding for threonine 163 and serines 164 to 167, 171 and 174 to codons coding for glutamic acids generating a fragment spanning nucleotides 302 and 923 of the MCM4 coding sequence (Bio Basic Inc). A silent *Hpa*I cut site was introduced to facilitate cloning by making the following base substitutions: G474T and T477C. The fragment was then digested with *Xba*I and *Stu*I and inserted into the same sites of a Leu-selectable *CEN/ARS* plasmid containing *MCM4* (pMD379), generating YCplac111-*mcm4pm* (pMD390). pMD390 was then used to PCR amplify the *mcm4pm* deletion fragment (residues 146-933) with primer MD456, 5'-d(CGATTACATATGCCAAGAA-GAATTGTGGATTTTG)-3', which inserts a *Nde*I site at the *mcm4pm* start codon, and primer MD274, 5'-d(TGATTGTAGAGATCTTCAGACACGGTTATTCAG)-3', which inserts a *Bgl*II site immediately downstream of the *mcm4pm* stop codon. The resultant PCR product was digested with *Nde*I and *Bgl*II and cloned into the same sites of pET24a (Novagen) to generate pMD418 and the construct confirmed by sequencing.

For yeast expression of *mcm4pm*, pMD390 was used to PCR amplify the *mcm4pm* deletion fragment (amino acids 146-933) with primer MD456, 5'-d(CGATTACATATGCCAAGAAGAATTGTGGATTTTG)-3', which inserts a *Nde*I site at the *mcm4pm* start codon, and primer MD420, 5'-d(ATCGACGCTCAGCGAATGAA-TGTAGTAGACAGC)-3', which inserts a *Blp*I site immediately downstream of the *mcm4pm* stop codon. This PCR fragment was digested with NdeI and BlpI and cloned

into the same sites of *Nde*I-*Blp*I of YCplac111 containing the *MCM4* 5' UTR in-frame with the ATG start site to generate pMD421 and the construct confirmed by sequencing.

4.2.2   *mcm4pm* yeast strain

For yeast expression of *mcm4pm*, pMD421 was transformed into a heterozygous diploid yeast strain (MATa/α *his3Δ1*/*his3Δ1 leu2Δ0*/*leu2Δ0 lys2Δ0*/LYS2 MET15/*met15Δ0 ura3Δ0*/*ura3Δ0* MCM4/*mcm4*::KanMX DBF4/*dbf4*::NatMX).   Transformants were grown on synthetic complete (SC) media lacking leucine and containing G418 (200 µg/ml) and clonNAT (100 µg/ml). The diploid strain was sporulated, the tetrads dissected and Leu+, G418[R] and clonNAT[R] haploid spore colonies selected. A single spore colony was isolated and the strain (YMD230) was confirmed by sequencing of pMD421 and the NatMX and KanMX cassettes, at the *DBF4* and *MCM4* loci, respectively.

4.2.3   Purification of Mcm subunits

Mcm subunits were purified as previously described [11], with the following modifications. Mcm2 and Mcm3pk were purified as described in Stead *et al*. [12]. Cell lysis was performed using an Avestin Emulsiflex C3 homogenizer.

Mcm4wt-containing cells were lysed in 800 ml Tris/sucrose (50 mM Tris-HCl, pH 7.5; 10% (w/v) sucrose) containing 0.5 M NaCl and 2 mM DTT. Insoluble material was removed by centrifugation at 27, 000 x g for 30 minutes at 4°C. The resulting supernatant was treated with 0.3 g/ml ammonium sulfate and then centrifuged again. The pellet was resuspended in 200 ml Buffer H (20 mM HEPES-NaOH, pH 7.5; 10% (v/v) glycerol; 1 mM EDTA; 2 mM DTT) and dialyzed against Buffer H overnight. The protein was diluted to a conductivity equal to 60 mM NaCl in Buffer H and then applied to a 200 ml SP Sepharose column equilibrated in Buffer H containing 100 mM NaCl. The column was washed with 1 L Buffer H before eluting the protein with a 1400 ml, 100-350 mM NaCl gradient in Buffer H. Fractions containing Mcm4wt, as determined by Coomassie-stained gels, were pooled (280 ml, 0.2 mg/ml) and dialyzed against Buffer H for 2 h at 4°C. The protein was then applied to a 40 ml heparin agarose column equilibrated in Buffer H containing 100 mM NaCl. The column was washed with 200 ml

Buffer H containing 100 mM NaCl and the protein eluted with a 400 ml, 100-500 mM NaCl gradient in Buffer H. Fractions containing Mcm4wt were pooled (90 ml, 0.2 mg/ml) and dialyzed against Buffer H overnight at 4°C. The protein was applied to a 20 ml ssDNA-Sepharose column equilibrated in Buffer H. The column was washed with 200 ml Buffer H and the protein eluted with a 200 ml, 0-500 mM NaCl gradient in Buffer H. Fractions containing Mcm4wt were pooled (17 ml, 1 mg/ml) and dialyzed against Buffer H containing 100 mM NaCl for 2 h at 4°C. The protein was then applied to a 1 ml MonoS 5/50 column equilibrated in Buffer H containing 100 mM NaCl. The column was washed with 10 ml Buffer H containing 100 mM NaCl before eluting the protein with a 20 ml, 100-500 mM NaCl gradient in Buffer H. Fractions containing Mcm4wt were pooled and then stored at -80°C.

Cells containing Mcm4PM were lysed in 400 ml Tris/sucrose containing 0.5 M NaCl and the insoluble material was removed by centrifugation at 27, 000 x g for 30 minutes at 4°C. The lysate was treated with 0.2 g/ml ammonium sulfate and re-pelleted. The resulting supernatant was removed and the pellet resuspended in Buffer A (20 mM Tris-HCl, pH 7.5; 10% (v/v) glycerol; 1 mM EDTA; 2 mM DTT) containing 0.15 g/ml ammonium sulfate and re-pelleted. The supernatant was removed and the pellet resuspended in Buffer A containing 0.1 g/ml ammonium sulfate and re-pelleted. The pellet was resuspended in 50 ml Buffer A and dialyzed against Buffer A for 3 h. The protein was diluted to a conductivity equal to 60 mM NaCl in Buffer A before being applied to a 70 ml Fast Flow Q Sepharose column equilibrated in Buffer A containing 100 ml NaCl. The column was washed with 700 ml Buffer A containing 100 mM NaCl and the protein eluted with a 700 ml, 100-500 mM NaCl gradient in Buffer A. Fractions containing Mcm4PM were pooled (44 ml, 1.1 mg/ml) and dialyzed against Buffer A containing 50 mM NaCl overnight. The supernatant was centrifuged at 27, 000 x g for 10 minutes at 4°C and then applied to an 8 ml MonoQ 10/100 column equilibrated in Buffer A containing 100 mM NaCl. The column was washed with 80 ml Buffer A containing 100 mM NaCl before eluting the protein with an 80 ml, 100-500 ml NaCl gradient in Buffer A. Fractions containing Mcm4PM were pooled and then stored at -80°C.

4.2.4   Reconstitution of Mcm2-7 complexes

Mcm2-7 complexes were reconstituted as described in Davey *et al*. [11] with the following exceptions. An equimolar amount (2 nmol) of each MCM subunit (Mcm4PM was substituted for Mcm4wt in the case of Mcm2-7^{4PM}) was mixed and concentrated using an Amicon Ultra 50 kDa cutoff device (Millipore) at 4°C to a final volume of 0.2 ml. High molecular weight fractions containing all six MCM proteins from the MonoQ column were pooled and concentrated using an Amicon Ultra 50 kDa cutoff device at 4°C to a final volume of 0.2 ml. The protein was then applied to a Superose 6 10/300 gel filtration column (GE Healthcare) equilibrated in Buffer H containing 100 mM NaCl. After the first 5.9 ml, fractions of 250 µl were collected at 4°C. Peak fractions were analyzed by SDS-PAGE (6%) and confirmation of equal stoichiometry determined by densitometry using ImageQuant 5.2 software (Molecular Dynamics). Peak fractions were also examined for ATPase and DNA unwinding activity as described below.

4.2.5   ATP hydrolysis

ATP hydrolysis was measured by thin layer chromatography (TLC). Each 12 µl reaction contained 1 mM [γ-^{32}P]ATP (10 Ci/mmol; PerkinElmer Life Sciences), 20 mM Tris acetate, pH 7.5, 10 mM magnesium acetate, and 2 mM DTT as well as 0.5 µM of each MCM protein or 200 nM Mcm2-7, unless otherwise indicated. For end point assays, reactions were incubated for 60 minutes at 30°C and then quenched with 12 µl of ATPase stop solution (50 mM EDTA, pH 8; 1% SDS). For time course experiments, 2 µl of each reaction was removed at 0, 15, 30, 45 and 60 minute intervals and quenched with 2 µl of ATPase stop solution. A portion (1 µl) of each reaction was spotted onto a polyethyleneimine cellulose TLC sheet (EM Science) and then developed in 0.6 M potassium phosphate, pH 3.4 for 15 minutes. The dried TLC sheets were exposed to a PhosphorStorage screen (GE Healthcare) and then scanned on a Storm 860 scanner (HE Healthcare). Densitometry analysis using ImageQuant 5.2 (Molecular Dynamics) was used to determine the volume of the spots corresponding to P_i and ATP. The amount of Pi produced (in pmol) was determined by: [(volume Pi)/(volume Pi+volume ATP)] x 500 µM.

4.2.6   DNA unwinding

DNA unwinding assays were performed using a DNA substrate containing 30 base pairs of duplex with 60 nucleotides of single stranded DNA on one strand and a 5' biotin on the other as previously described [13]. Primer 2T, 5'-d(ATGTCCTAGCAAGCCAGAAT-TCGGCAGCGTC-(T)60)-3' was labelled with ^{32}P at the 5' end and annealed to 1B, 5'-biotin-d(GACGCTGCCGAATTCTGGCTTGCTAGGACAT)-3' by boiling 2 minutes in 10 mM Tris-HCl, pH 8.5, 30 mM sodium citrate and 300 mM NaCl, and then cooled slowly to room temperature. Each 6 µl reaction contained 20 mM Tris-acetate, pH 7.5, 10 mM magnesium acetate, 100 µM EDTA, 5 mM DTT, 5 mM ATP, 67 nM streptavidin, 5% PEG 3350, 100 mM sodium glutamate, 5 mM creatine phosphate, 20 µg/ml creatine kinase, 1 nM DNA substrate (concentration of labelled strand) and the indicated concentrations of Mcm2-7. DNA unwinding assays involving PEG titrations lacked sodium glutamate. If necessary, proteins were diluted in 20 mM Tris-acetate, pH 7.5, 100 µM EDTA, 2 mM DTT, 10% glycerol, 40 µg/ml BSA. Reactions were incubated at 37°C for 10 minutes and then quenched by adding 0.7 µl of unlabelled 2T (1 µM) and 1.5 µl of Proteinase K (10 mg/ml) and incubated at 37°C for an additional 2 minutes. Samples were then treated with 2 µl of 5% SDS, 100 mM EDTA, 25% (v/v) glycerol, 0.1% bromophenol blue and 0.1% xylene cyanol FF. DNA products were resolved on 8% native polyacrylamide gels using 1x TBE (100 mM Tris, 90 mM borate, 1 mM EDTA) at 150 V for 40 minutes at room temperature. The gels were dried, exposed to PhosphorStorage screens and scanned on a Storm 860 scanner (GE Healthcare). The volume of bands corresponding to ssDNA and dsDNA as well as a background volume were determined by densitometry using ImageQuant 5.2 (Molecular Dynamics). The percentage of ssDNA product in an unreacted sample (no protein) was ≤ 5%. To normalize for the variability in these values, the percentage of unwinding was calculated by: % unwinding = (% ssDNA$_S$-% ssDNA$_U$)/(1-% ssDNA$_U$), where % ssDNA$_S$ represents the percentage of ssDNA in the sample lane and % ssDNA$_U$ represents the percentage of ssDNA in the unreacted sample lane.

4.2.7　DNA binding

DNA binding was measured by electrophoretic mobility shift assay (EMSA) using a 5'-end ^{32}P-labelled poly dT60 DNA substrate. Each 6μl reaction contained 20 mM Tris-acetate, pH 7.5, 10 mM magnesium acetate, 100 μM EDTA, 5 mM DTT, 5 mM ATP, 5 mM creatine phosphate, 20 μg/ml creatine kinase and 1 nM DNA substrate and the indicated concentrations of Mcm2-7 complexes. Reactions were incubated for 10 minutes at 37°C and glycerol added to a final concentration of 5% (v/v). Samples were resolved on a 5% native (Tris-borate-EDTA) polyacrylamide gel (19:1 acrylamide:Bis-acrylamide) containing 5% glycerol, 0.1% NP-40 and 10 mM magnesium acetate at 30 mA for 3 hours. The gel was dried and exposed to a PhosphorStorage screen and imaged on a Storm 860 scanner (GE Healthcare).

4.3　Results

4.3.1　Creation of phosphomimetic Mcm4

To explore the role of phosphorylation on Mcm2-7 activity, we first cloned the phosphomimetic mutant of Mcm4 [8] (Figure 4.1A) into a centromere-based (CEN) plasmid with a single replication origin as described in Materials and Methods. In order to confirm that this mutant supported viability in the absence of DDK, the *mcm4pm*-containing plasmid (CEN-*mcm4pm*) was initially transformed into a heterozygous diploid yeast strain deleted for *MCM4* and *DBF4*. The use of a heterozygous diploid was required since *MCM4* and *DBF4* are essential genes. Upon sporulation, tetrads were dissected and screened for Leu+ (CEN-*mcm4pm*), G418 (*mcm4Δ*) and clonNAT (*dbf4Δ*) resistances. Figure 4.1B shows growth of the isolated *mcm4pm*-containing haploid spore that fulfilled the function of Mcm4 and bypassed the requirement for DDK efficiently. Of note, yeast cells bearing the Mcm4 phosphomimetic mutation exhibit robust cell cycle progression in the absence of DDK similar to wildtype cells [8].
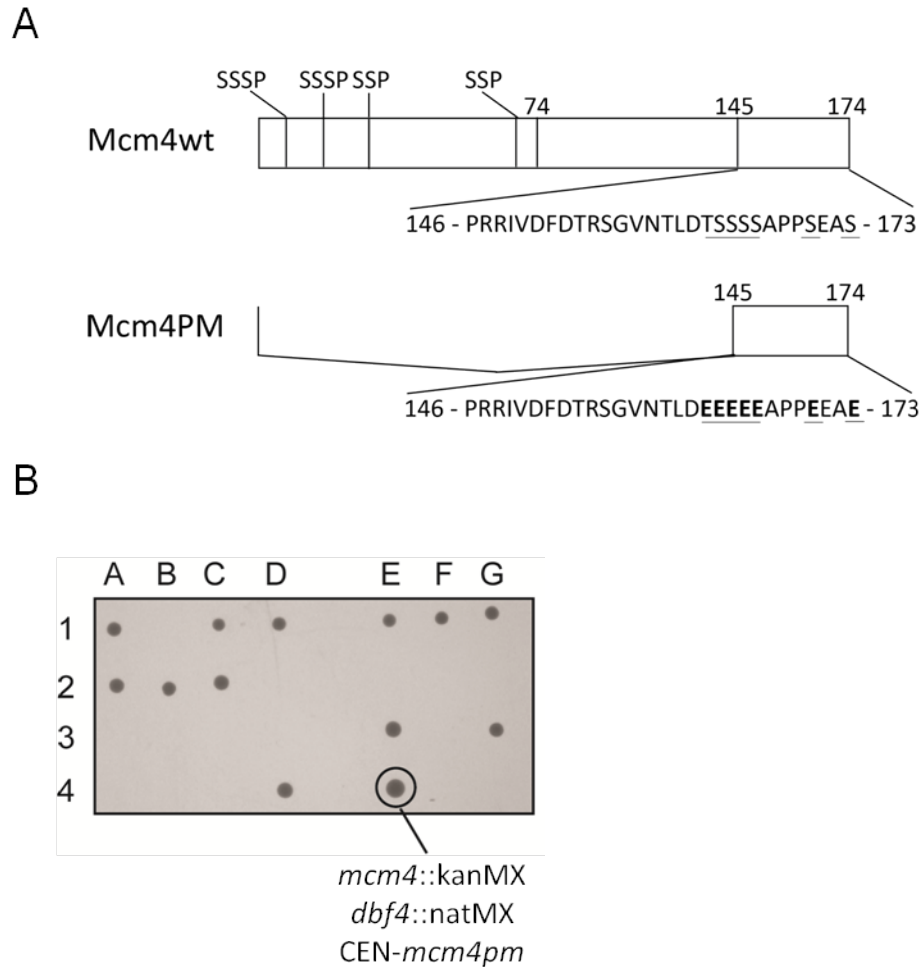
Figure 4.1: Phosphomimetic Mcm4

(A) Shown are schematic diagrams for the N-terminal regions of wildtype Mcm4 and phosphomimetic Mcm4 (Mcm4PM). *mcm4pm* was created by deleting the first 435 nucleotides of MCM4, corresponding to residues 1-145, and mutating one proximal threonine (T163) and six serine residues (S164-167, S171, S174) (underlined) to glutamic acid (E, bold and underlined). Adapted from 8. **(B)** DDK bypass by the *mcm4pm* allele (CEN-*mcm4pm*) was confirmed in a haploid yeast strain deleted for *MCM4* and *DBF4* (indicated by a circle). Haploid spores were grown on synthetic complete (SC) media lacking leucine and containing G418 (200 µg/ml) and clonNAT (100 µg/ml). Columns denoted by letters represent tetrads. Rows denoted by numbers represent haploid spores dissected from the same tetrad.

4.3.2   Characterization of the Mcm4PM subunit

After confirming that the *mcm4pm* mutant allele was able to bypass the requirement for DDK, we thought to characterize the mutant subunit using *in vitro* biochemical analyses. To this end, yeast Mcm subunits, including the Mcm4PM mutant, were purified separately from bacterial-expression systems. Figure 4.2 depicts an SDS-PAGE gel of each of the Mcm subunits after the final purification step. Consistent with the deletion of 145 N-terminal residues, or approximately 15 kDa, the Mcm4PM subunit migrated faster than Mcm4wt (105 kDa) on SDS-PAGE with an apparent size of approximately 90 kDa.

The Mcm2-7 complex contains six unique ATPase sites located at subunit interfaces that play important roles for function of the complex [14]. Within Mcm2-7, Mcm4 forms dimer interfaces with Mcm7 and Mcm6. Mcm3/7, Mcm7/4 and Mcm6/2 (Figure 1.2D) have been shown to be functionally important to the ATPase activity of the complex and cell viability [11, 15]. In order to investigate the role of phosphorylation on Mcm2-7 ATPase activity, I set out to examine the hydrolysis of ATP by Mcm4PM pairwise combinations. For this, Mcm4 was mixed separately with each of its neighboring subunits, Mcm6 or Mcm7, and incubated at 30°C. As shown in Figure 4.3A, the rate of ATP hydrolysis for the Mcm7/4 dimer was two-fold lower for the phosphomimetic protein relative to wildtype Mcm4. On the other hand, the Mcm4/6 dimer showed little to no difference in the rate of ATP hydrolysis between the phosphomimetic and the wildtype Mcm4 (Figure 4.3B). Consistent with Mcm7/4 being one of the functional ATPase active sites, this pairwise combination showed considerably higher ATPase activity relative to Mcm4/6, regardless of the form of Mcm4 used (compare Figures 4.3A and B).

Next, the ATPase activity of multimers of Mcm subunits with and without phosphomimetic Mcm4 was investigated. To this end, various derivations of Mcm subunits with Mcm4wt or Mcm4PM were incubated with radiolabelled ATP. In general, and consistent with the time course experiment above, there was a two-fold reduction in ATPase activity of Mcm7/4PM compared to Mcm7/4wt (Figure 4.3C). Interestingly, the addition of Mcm6 or Mcm3 to Mcm7/4 stimulated ATPase activity for both wildtype and

phosphomimetic Mcm4. On the other hand, the addition of Mcm2 and/or Mcm5 to Mcm7/4-containing multimers reduced ATPase activity relative to a Mcm7/4 dimer. When the phosphomimetic Mcm4 subunit was included with combinations of the other five subunits, a slightly lower ATPase activity was observed relative to that when wildtype was included.
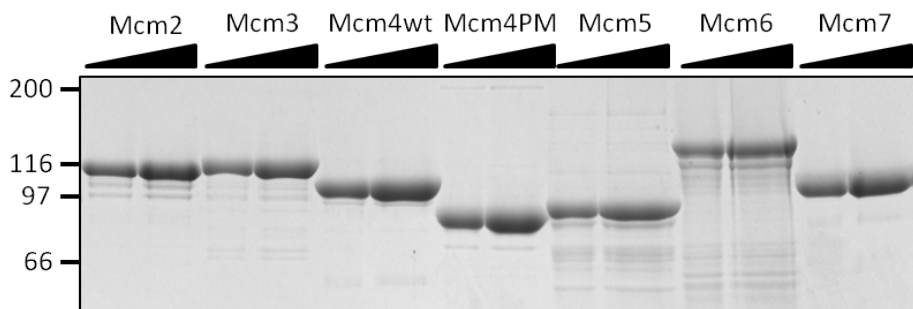
Figure 4.2: Purification of Mcm2-7 subunits

Individual Mcm subunits were expressed and purified separately from *E. coli* as described in Materials and Methods. Aliquots of each of the purified Mcm subunits were run on an 8% SDS-PAGE gel and stained with Coomassie brilliant blue. The migration of size standards is depicted on the left.
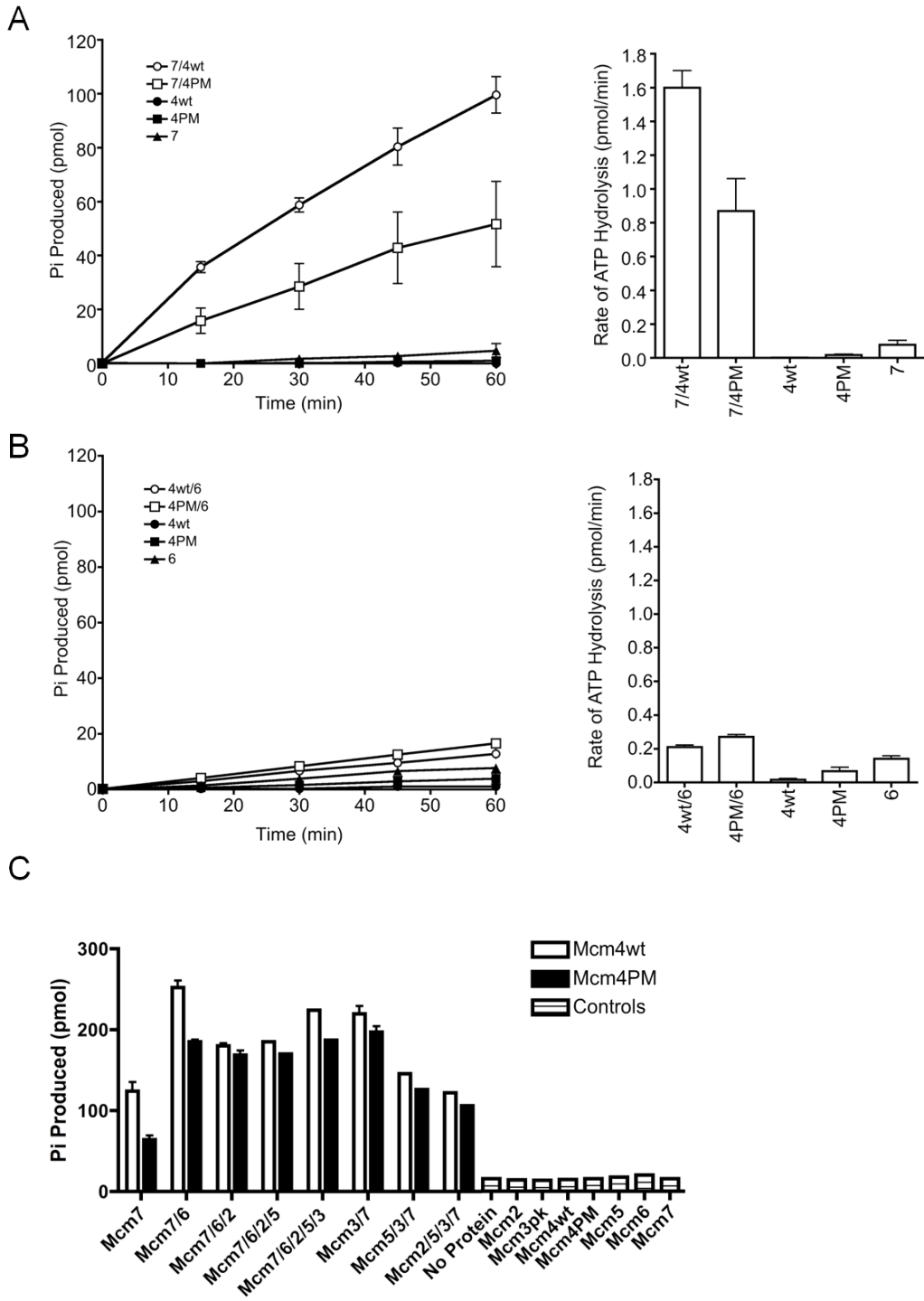
Figure 4.3: ATPase activity of Mcm4PM

ATP hydrolysis was determined by combining Mcm subunits and incubating at 30°C in the presence of radiolabelled ATP. **(A)** Mcm7/4wt and Mcm7/4PM and **(B)** Mcm4wt/6 and Mcm4PM/6 as determined in a time course experiment. Shown are the time course (left) and the rate of hydrolysis from part B (right). **(C)** ATPase activity of Mcm multimers with or without phosphomimetic Mcm4. ATPase activity of individual Mcm subunits is also shown. Protein combinations were incubated at 30°C for one hour in the presence of radiolabelled ATP. Reactions were performed in triplicate with the mean and standard error plotted where indicated.

4.3.3   Reconstitution of Mcm2-7 complexes

Mcm2-7 complexes were assembled from individual subunits as described in Materials and Methods. Peak fractions of wildtype and phosphomimetic Mcm2-7 from size exclusion chromatography are shown in Figures 4.4A and C, respectively. Both Mcm2-7wt and Mcm2-7^{4PM} displayed a peak of elution corresponding to a size of ~670 kDa. This elution profile is consistent with the predicted molecular weight of the ~600 kDa toroidal Mcm2-7 complex [15]. Densitometry analysis of fractions 20-24 demonstrated that both wildtype and phosphomimetic Mcm2-7 formed hexameric complexes assembled from six Mcm subunits in equal stoichiometry (ie. 1:1 ratio).

4.3.4   Biochemical activities of Mcm2-7 complexes

Following reconstitution of wildtype and phosphomimetic Mcm2-7 (Figure 4.4A, C), I set out to confirm that the complexes exhibited activity. To this end, Mcm2-7wt and Mcm2-7^{4PM} were assayed for ATPase and DNA unwinding activity as described in Materials and Methods. In contrast to MtMCM, SsoMCM and other DNA helicases, the ATPase activity of eukaryotic Mcm2-7 is not stimulated by DNA [16, 17]. First, to test ATPase activity, peak fractions from size exclusion chromatography were mixed with

[32]P-radiolabelled ATP, incubated at 30°C for 60 minutes, and the products from hydrolysis were separated by thin layer chromatography (TLC). The peak in ATPase activity co-eluted with peak protein from size exclusion chromatography for both the wildtype and the phosphomimetic Mcm2-7 complexes (Figure 4.4). These results confirmed that both complexes were competent to hydrolyze ATP.

To test the ability of Mcm2-7 to unwind DNA, an established helicase assay was employed utilizing a radiolabelled synthetic fork substrate [13]. The DNA substrate contains a duplex region of 31 base pairs, one strand with a biotin-streptavidin moiety and one single-stranded extension or tail composed of 60 deoxythymidylates (dT60) [13]. The Schwacha lab observed that the *in vitro* helicase activity of baculovirus-expressed yeast Mcm2-7 was inhibited by chloride ions, yet stimulated by acetate or glutamate [9]. In contrast to this, the addition of ≤ 200 mM acetate or glutamate to the assay had no discernible effect on helicase activity.

A

670 kDa
▼

18 20 22 24 26 28 30 32

— 6
— 3
— 2
116 —   — 4wt
                             — 7
97 —   — 5

B

C

670 kDa
▼

18 20 22 24 26 28 30 32

— 6
— 3
— 2
116 —   — 7
                             — 5
97 —   — 4PM

D
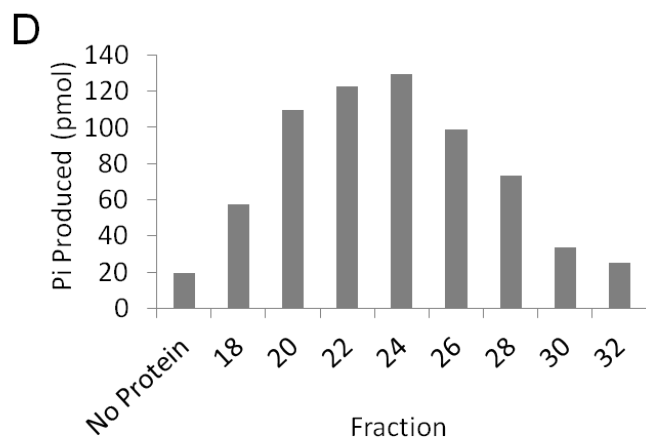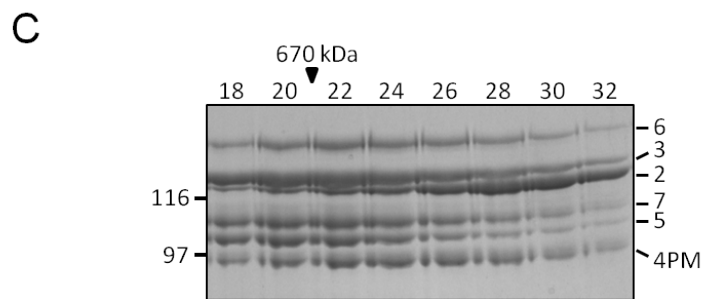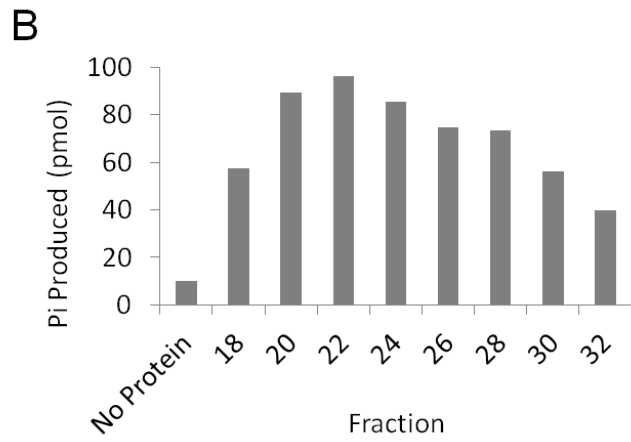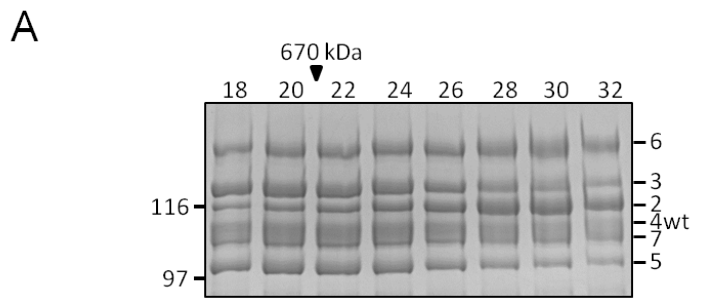
Figure 4.4: Reconstitution of Mcm2-7 complexes

Mcm2-7 complexes were reconstituted from individual subunits shown in Figure 4.2 and as described in Materials and Methods. **(A)** Size exclusion chromatography and **(B)** ATPase activity of Mcm2-7wt complexes. **(C)** Size exclusion chromatography and **(D)** ATPase activity of Mcm2-7^{4PM} complexes. (A, C) For size exclusion chromatography, shown are representative 6% SDS-PAGE gels of peak fractions stained with Coomassie brilliant blue. The migration of size standards and individual Mcm subunits is depicted on the left and right of each panel, respectively. The elution of molecular size standards run separately under the same conditions is indicated above the respective panels. (B, D) ATP hydrolysis was measured across the peak fractions of Mcm2-7 complexes. Mcm2-7 fractions were incubated with radiolabelled ATP for 60 minutes and processed as described in Materials and Methods. Shown are representative assays of the amount of Pi produced as determined by densitometry using ImageQuant 5.2 (Molecular Dynamics).

After observing no anion-dependent stimulation of Mcm2-7 activity, I tested volume excluders. In contrast to Bochman and Schwacha [9], the addition of polyethylene glycol (PEG) to the assay greatly enhanced helicase activity of Mcm2-7wt (Figure 4.5). This stimulation was concentration-dependent with maximum DNA unwinding activity achieved with 5% PEG. Sodium glutamate and PEG were added to the standard helicase buffer in subsequent assays.

To assay for DNA unwinding activity of wildtype (Figure 4.6A) and phosphomimetic Mcm2-7 (Figure 4.6B), peak fractions from gel filtration chromatography were incubated with radiolabelled synthetic fork substrate and processed as described in Materials and Methods. Consistent with ATPase activity (Figure 4.4), there was a good correlation between peak DNA unwinding activity (Figure 4.6) and elution profile (Figure 4.4) of both Mcm2-7 complexes. Together with the ATPase activity, these data demonstrated that both Mcm2-7wt and Mcm2-7[4PM] formed active hexameric complexes.
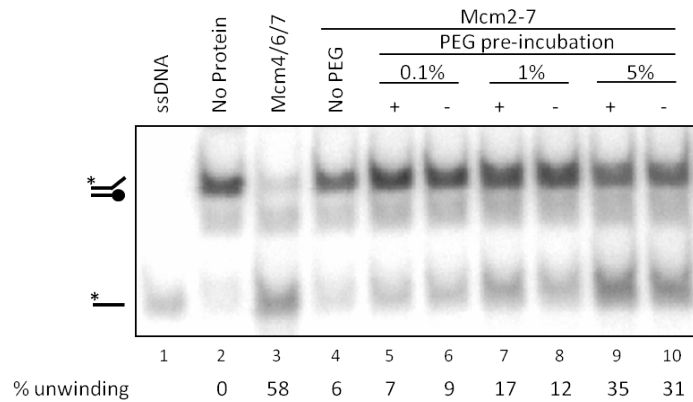
Figure 4.5: PEG stimulates Mcm2-7 helicase activity

Mcm2-7wt was first incubated with or without the indicated amounts of PEG 3350 for 15 minutes on ice. Reactions contained standard helicase buffer and included ssDNA (lane 1), no Mcm (lane 2), 200 nM Mcm467 (lane 3) or 200 nM Mcm2-7wt (lanes 4-10) and were supplemented with the indicated amounts of PEG 3350. Reactions were separated on an 8% native polyacrylamide gel, exposed to a phosphorstorage screen and scanned on a Storm Phosphorimager (GE Healthcare Life Sciences). The relative amount of DNA unwinding (% unwinding) was determined by subtracting the amount of ssDNA in the No Protein control.
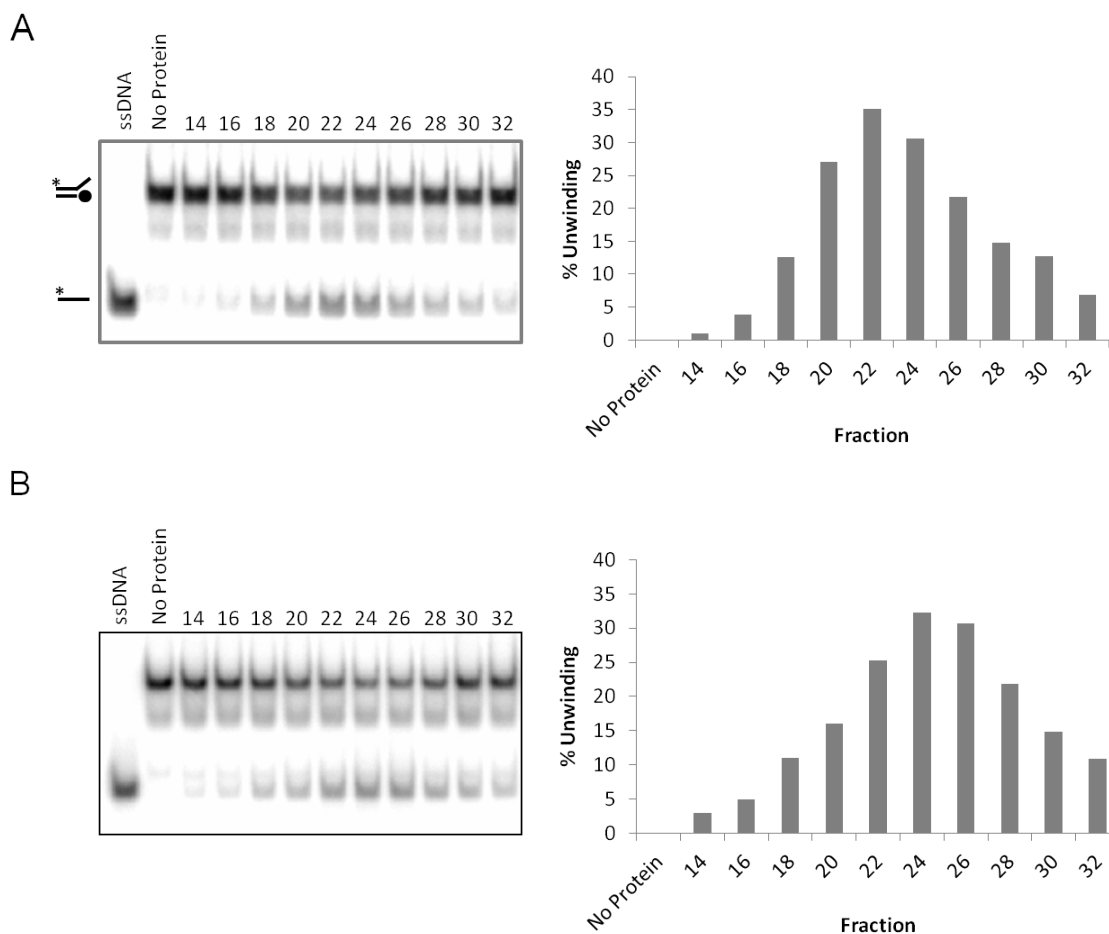
Figure 4.6: Mcm2-7 complexes exhibit DNA unwinding activity

DNA unwinding activity of **(A)** wildtype and **(B)** phosphomimetic Mcm2-7 complexes. Peak fractions from size exclusion chromatography of Mcm2-7 complexes were incubated with 1 nM ^{32}P-radiolabelled synthetic fork substrate in the presence of ATP. Reactions were separated on an 8% native polyacrylamide gel, exposed to a phosphorstorage screen and analyzed by a Storm Phosphorimager (GE Healthcare Life Sciences). Densitometry analysis of the gel image was done using ImageQuant 5.2 (Molecular Dynamics) and is shown on the right.

4.3.5   Comparison of Mcm2-7wt and Mcm2-7^{4PM} Activity

While we observed lower ATPase activity in majority of the Mcm multimers containing Mcm4PM compared to Mcm4wt (Figure 4.3), we thought it best to evaluate the activities of wildtype and phosphomimetic Mcm2-7 complexes in a side-by-side comparison. First, the ability of phosphomimetic Mcm2-7 to hydrolyze ATP relative to Mcm2-7 wildtype was examined. As shown in Figure 4.7A, the ATPase activity of phosphomimetic Mcm2-7 was comparable to that of wildtype, and remained linear over several protein concentrations. Next, using the radiolabelled synthetic fork substrate described above, the helicase activity of Mcm2-7^{4PM} relative to Mcm2-7wt was investigated. Consistent with ATPase activity, phosphomimetic Mcm2-7 displayed wildtype DNA unwinding activity at all concentrations tested (Figure 4.7B). We also sought to investigate any subtle differences between these complexes in ssDNA binding. Preliminary data showed that the ability of phosphomimetic Mcm2-7 to bind ssDNA was comparable to that of wildtype (Figure 4.7C). Taken together, the data presented here suggest that phosphomimetic Mcm4 has little to no effect on the activity of the Mcm2-7 complex.

A

Figure 4.7: Phosphomimetic Mcm2-7 exhibits wildtype activity
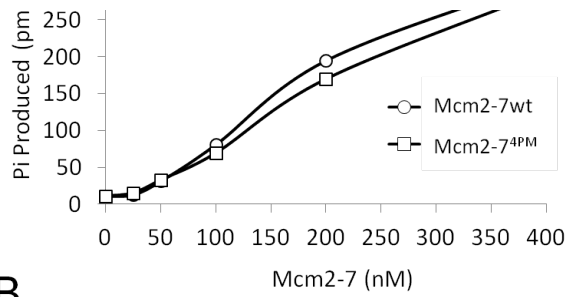
B
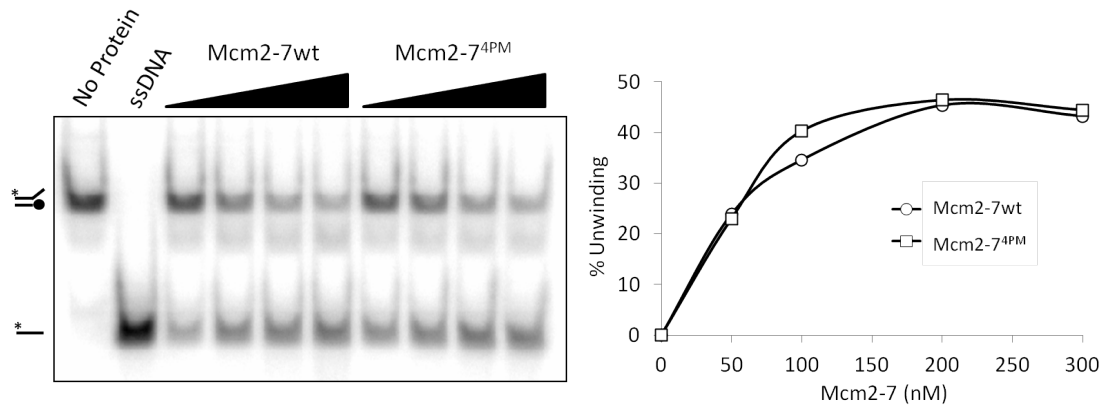
C
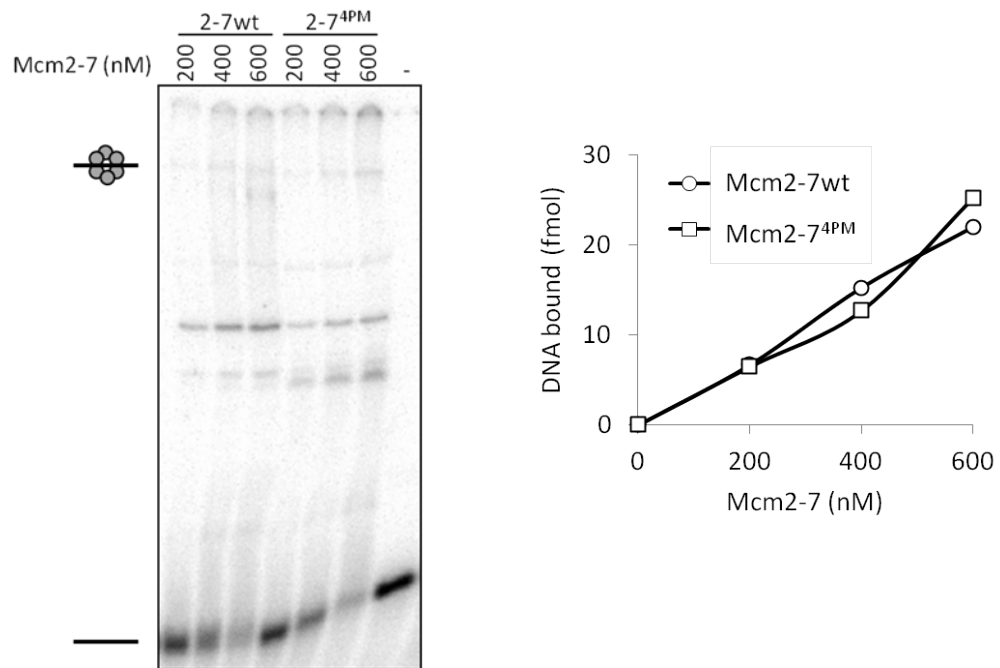
(A) ATPase activity of wildtype and phosphomimetic Mcm2-7 complexes. Shown is a representative assay. Increasing amounts of Mcm2-7 were incubated with radiolabelled ATP and processed as described in Materials and Methods. **(B)** DNA unwinding activity of wildtype and phosphomimetic Mcm2-7. Shown is a gel image of a representative assay (left panel) and the amount of DNA unwinding activity less background determined by densitometry analysis (right panel). **(C)** The effect on ssDNA binding by phosphomimetic Mcm2-7 was determined in an EMSA. Shown on the left is a gel image and on the right is the relative amount of DNA binding less background determined by densitometry.

4.4 Discussion

Mcm2-7 is the replicative DNA helicase in eukaryotes. In this study, we have shown that both wildtype and phosphomimetic Mcm2-7 complexes can be reconstituted from individual subunits purified from bacterial expression systems. Gel filtration chromatography demonstrated that both complexes eluted as hexamers consisting of Mcm subunits in equal stoichiometry. In addition, these complexes were competent to hydrolyze ATP and unwind DNA. Of note, the amount of DNA unwinding observed was comparable to that seen with yeast Mcm2-7 purified from baculovirus [9]. Unlike baculovirus-expressed Mcm2-7 [9], however, the addition of glutamate or acetate did not stimulate DNA unwinding activity by Mcm2-7 in this study. Surprisingly, helicase activity of Mcm2-7 was stimulated by the addition of PEG in a concentration-dependent manner. Notably, the results presented in this report demonstrate that Mcm2-7 can unwind DNA in the absence of DDK-dependent phosphorylation and that this activity occurs in the absence of other factors.

DDK-dependent phosphorylation of Mcm2-7 is thought to be required to activate Mcm2-7 to unwind DNA [5-8]. In yeast, DDK is proposed to be essential to relieve an inhibitory activity in the NSD of Mcm4 [8]. The combined deletion of the inhibitory

domain in the initial 145 amino acids of the N-terminus and the mutation of 7 proximal serine or threonine residues to aspartic acid [8] or glutamic acid (this study) in the NSD allows growth of yeast cells in the absence of DDK. In the present study, since Mcm2-7 was reconstituted from individual subunits expressed in bacteria, the wildtype complex represents an unmodified state. Comparison of the biochemical activities of wildtype and phosphomimetic Mcm2-7 suggest that phosphorylation is not required for *in vitro* helicase activity, a finding consistent with published results [9]. The results presented here do not exclude the possibility that DDK-dependent phosphorylation of Mcm2-7 and/or association with other factors (discussed below) is essential to regulate Mcm2-7 under the more stringent conditions of a cycling cell.

Unlike in cells, the DNA substrate used in this study contains DNA ends which facilitate helicase loading. Under the experimental conditions presented here, the Mcm2-7 complex can load onto ssDNA regardless of an open or closed conformation. The large biotin-streptavidin moiety would further assist in DNA unwinding by steric exclusion as Mcm2-7 translocates along DNA in a 3' to 5' direction. *In vivo*, since there are no DNA ends, Mcm2-7 must first load onto dsDNA and somehow switch to a ssDNA binding mode in order to unwind DNA. Indeed, Mcm2-7 is first loaded onto origins as a double hexamer [18]. Conceivably, phosphorylation of Mcm2-7 by DDK may facilitate a conformational change to permit this switch in binding modes and/or stabilize the association of Mcm2-7 with DNA. Studies of *Methanothermobacter thermautotrophicus* MCM suggest that a single point mutation analogous to the *bob1* mutation in yeast Mcm5 that can bypass the requirement for DDK causes a structural change in the complex [19].

DDK-dependent phosphorylation of Mcm2-7 is also thought to be required for the stable formation of a large helicase complex consisting of Cdc45/Mcm2-7/GINS (CMG complex) [20]. Additionally, reconstitution of *Drosophila* Mcm2-7 and CMG complexes purified from baculovirus showed that Cdc45 and GINS stimulated the ATPase, helicase and DNA binding activity of Mcm2-7 *in vitro* [21]. As well, Costa *et al.* [22] used single-particle electron microscopy to show that while Mcm2-7 alone exists as an open ring, CMG adopts a closed conformation with two distinct small pores. These authors propose a model in which the CMG complex induces melting of the DNA duplex and then

separates the single strands between the two pores. Interestingly, unlike Mcm2-7, CMG cannot bind dsDNA [18, 21, 23]. As well, Ilves *et al.* [21] found that the N-termini of Mcm2 and Mcm4 were not hyperphosphorylated in the CMG complex and that the modified residues mapped were the same in the free pool of MCMs and in CMG.

The data presented here do not completely address the role phosphorylation plays in activating Mcm2-7 to unwind DNA. Confounding the link between DDK phosphorylation and Mcm2-7 activation is the fact that under certain conditions, Mcm2 within Mcm2-7 is the primary target for DDK phosphorylation. For instance, studies with yeast and human proteins have shown that DDK can phosphorylate Mcm2 *in vitro* [24, 25]. Furthermore, previous studies from our lab showed that, in yeast, phosphorylation of Mcm2 regulates Mcm2-7 activity and affects the cell's response to DNA damage [26] and replicative stress [27]. The reconstitution of large macromolecular complexes from individual components is a powerful tool in which to easily manipulate, such as by order of addition or phosphorylation, and examine complexes as a whole and the contribution made by each protein involved.

4.5 References

1. Aguilera,A. & Gomez-Gonzalez,B. Genome instability: a mechanistic view of its causes and consequences. *Nat. Rev. Genet.* **9**, 204-217 (2008).

2. Boos,D., Frigola,J., & Diffley,J.F. Activation of the replicative DNA helicase: breaking up is hard to do. *Curr. Opin. Cell Biol.* **24**, 423-430 (2012).

3. Bell,S.P. & Dutta,A. DNA replication in eukaryotic cells. *Annu. Rev. Biochem* **71**, 333-374 (2002).

4. Chen,K.C., Csikasz-Nagy,A., Gyorffy,B., Val,J., Novak,B. *et al.* Kinetic analysis of a molecular model of the budding yeast cell cycle. *Mol Biol. Cell* **11**, 369-391 (2000).

5. Sheu,Y.J. & Stillman,B. Cdc7-Dbf4 phosphorylates MCM proteins via a docking site-mediated mechanism to promote S phase progression. *Mol Cell* **24**, 101-113 (2006).

6. Randell,J.C., Fan,A., Chan,C., Francis,L.I., Heller,R.C. *et al.* Mec1 is one of multiple kinases that prime the Mcm2-7 helicase for phosphorylation by Cdc7. *Mol. Cell* **40**, 353-363 (2010).

7. Francis,L.I., Randell,J.C., Takara,T.J., Uchima,L., & Bell,S.P. Incorporation into the prereplicative complex activates the Mcm2-7 helicase for Cdc7-Dbf4 phosphorylation. *Genes Dev.* **23**, 643-654 (2009).

8. Sheu,Y.J. & Stillman,B. The Dbf4-Cdc7 kinase promotes S phase by alleviating an inhibitory activity in Mcm4. *Nature* **463**, 113-117 (2010).

9. Bochman,M.L. & Schwacha,A. The Mcm2-7 complex has in vitro helicase activity. *Mol. Cell* **31**, 287-293 (2008).

10. Hardy,C.F., Dryga,O., Seematter,S., Pahl,P.M., & Sclafani,R.A. mcm5/cdc46-bob1 bypasses the requirement for the S phase activator Cdc7p. *Proc. Natl. Acad. Sci. U. S. A* **94**, 3151-3155 (1997).

11. Davey,M.J., Indiani,C., & O'Donnell,M. Reconstitution of the Mcm2-7p heterohexamer, subunit arrangement, and ATP site architecture. *J. Biol. Chem.* **278**, 4491-4499 (2003).

12. Stead,B.E., Sorbara,C.D., Brandl,C.J., & Davey,M.J. ATP binding and hydrolysis by Mcm2 regulate DNA binding by Mcm complexes. *J. Mol. Biol.* **391**, 301-313 (2009).

13. Kaplan,D.L., Davey,M.J., & O'Donnell,M. Mcm4,6,7 uses a "pump in ring" mechanism to unwind DNA by steric exclusion and actively translocate along a duplex. *J Biol. Chem.* **278**, 49171-49182 (2003).

14. Forsburg,S.L. Eukaryotic MCM proteins: beyond replication initiation. *Microbiol. Mol Biol. Rev.* **68**, 109-131 (2004).

15. Bochman,M.L., Bell,S.P., & Schwacha,A. Subunit organization of Mcm2-7 and the unequal role of active sites in ATP hydrolysis and viability. *Mol. Cell Biol.* **28**, 5865-5873 (2008).

16. McGeoch,A.T., Trakselis,M.A., Laskey,R.A., & Bell,S.D. Organization of the archaeal MCM complex on DNA and implications for the helicase mechanism. *Nat. Struct. Mol. Biol.* **12**, 756-762 (2005).

17. Kasiviswanathan,R., Shin,J.H., Melamud,E., & Kelman,Z. Biochemical characterization of the Methanothermobacter thermautotrophicus minichromosome maintenance (MCM) helicase N-terminal domains. *J. Biol. Chem.* **279**, 28358-28366 (2004).

18. Remus,D., Beuron,F., Tolun,G., Griffith,J.D., Morris,E.P. *et al.* Concerted loading of Mcm2-7 double hexamers around DNA during DNA replication origin licensing. *Cell* **139**, 719-730 (2009).

19. Fletcher,R.J., Bishop,B.E., Leon,R.P., Sclafani,R.A., Ogata,C.M. *et al.* The structure and function of MCM from archaeal M. Thermoautotrophicum. *Nat. Struct. Biol.* **10**, 160-167 (2003).

20. Moyer,S.E., Lewis,P.W., & Botchan,M.R. Isolation of the Cdc45/Mcm2-7/GINS (CMG) complex, a candidate for the eukaryotic DNA replication fork helicase. *Proc. Natl. Acad. Sci. U. S. A* **103**, 10236-10241 (2006).

21. Ilves,I., Petojevic,T., Pesavento,J.J., & Botchan,M.R. Activation of the MCM2-7 helicase by association with Cdc45 and GINS proteins. *Mol. Cell* **37**, 247-258 (2010).

22. Costa,A., Ilves,I., Tamberg,N., Petojevic,T., Nogales,E. *et al.* The structural basis for MCM2-7 helicase activation by GINS and Cdc45. *Nat. Struct. Mol. Biol.* **18**, 471-477 (2011).

23. Evrin,C., Clarke,P., Zech,J., Lurz,R., Sun,J. *et al.* A double-hexameric MCM2-7 complex is loaded onto origin DNA during licensing of eukaryotic DNA replication. *Proc. Natl. Acad. Sci. U. S. A* **106**, 20240-20245 (2009).

24. Lei,M., Kawasaki,Y., Young,M.R., Kihara,M., Sugino,A. *et al.* Mcm2 is a target of regulation by Cdc7-Dbf4 during the initiation of DNA synthesis. *Genes Dev* **11**, 3365-3374 (1997).

25. Montagnoli,A., Valsasina,B., Brotherton,D., Troiani,S., Rainoldi,S. *et al.* Identification of Mcm2 phosphorylation sites by S-phase-regulating kinases. *J. Biol. Chem.* **281**, 10281-10290 (2006).

26.   Stead,B.E., Brandl,C.J., & Davey,M.J. Phosphorylation of Mcm2 modulates Mcm2-7 activity and affects the cell's response to DNA damage. *Nucleic Acids Res.* **39**, 6998-7008 (2011).

27.   Stead,B.E., Brandl,C.J., Sandre,M.K., & Davey,M.J. Mcm2 phosphorylation and the response to replicative stress. *BMC. Genet.* **13**, 36 (2012).

Chapter 5

5 Discussion

5.1 Why study the regulation of Mcm2-7?

The regulation of DNA replication in eukaryotes is a fundamental process that ensures the faithful duplication of genetic material from one cell division cycle to the next (reviewed in 1). The study of the regulation DNA replication is crucial for understanding how perturbations during this process can lead to disease states caused by an unregulated cell cycle, such as cancer. Replicative DNA helicases are tasked with unwinding the double helix ahead of the replication fork in order to facilitate DNA synthesis by DNA polymerases [1-4]. These complexes can exist in various oligomeric states, ranging from monomers to dodecamers. Archaeal MCMs, for example, form a hexameric complex comprised of six identical subunits that are proposed to be functionally equal. In contrast, the eukaryotic Mcm2-7 complex is a heterohexamer formed from six paralogous subunits. This assembly is unique among hexameric helicases and creates six distinct ATPase active sites at subunit interfaces that vary in their ability to hydrolyze ATP [5-7]. Intriguingly, Mcm2-7 is loaded onto origins of replication as a head-to-head double hexamer, yet unwinds DNA as a single hexamer [8-10]. Additionally, outside of their helicase function, the Mcm subunits can exist as trimers, dimers and monomers [6, 11, 12]. Studies of the Mcm2-7 complex as a whole or the parts of which are essential to understanding the mechanism of DNA unwinding by this helicase.

Of further interest are the processes involved during Mcm2-7 helicase loading and helicase activation that ensure origins are fired once per cell cycle. In this context, Mcm2-7 is assembled into the pre-RC during G1 phase of the cell cycle. This process requires the collective effort of ORC, Cdc6 and Cdt1 to load the double hexamer around dsDNA [1]. While replication origins are licensed for DNA replication, no DNA unwinding occurs until the Mcm2-7 helicase is activated throughout S phase to unwind DNA by mechanisms that have yet to be fully elucidated. What is known is that the conversion from an inactive to an active helicase is dependent on the combined action of CDK and

DDK. These activities lead to an association between Mcm2-7 and two other replication factors, Cdc45 and GINS [13-15]. While several studies have explored this interaction, little is known about how Cdc45 and GINS stimulate Mcm2-7 to unwind DNA. Furthermore, Mcm2-7 is also phosphorylated by additional kinases, the consequences of which are not fully understood.

The importance of studying the regulation of Mcm2-7 is further exemplified by the plethora of studies demonstrating the potential for using the factors involved as biomarkers and/or targets for pharmacological inhibition in anti-cancer therapeutics. For example, a study evaluating the ability of proteins to be used as biomarkers to detect cancer cells in a wide variety of tissue samples found that the Mcm proteins were consistently better biomarkers for cell proliferation compared to traditional biomarkers such as Ki-67 and proliferating cell nuclear antigen (PCNA). Moreover, in cervical carcinoma samples, antibodies raised against human Cdc6 were found to detect a greater percentage of abnormal cells compared to anti-Ki-67 or anti-PCNA (reviewed in 16). Anti-cancer agents that target the degradation of Cdt1 may also be of value since Cdt1 is overexpressed in colon and non-small-cell lung carcinomas [17-19]. In addition, a synergistic effect between human Cdt1 and mutant p53 or human Cdc6 and mutant p53 overexpression resulted in augmented tumor growth and chromosomal instability in non-small-cell lung carcinomas [17]. Furthermore, many cancers with proliferative mutations typically have aberrant checkpoint responses which allow tumor cells to survive. In this regard, Cdc7, which is involved in the checkpoint response, has shown promise as a pharmacological target to inhibit in pre-clinical anti-cancer trials and indeed, small molecule inhibitors have been developed and are being optimized for this purpose [20, 21]. Additionally, Cdc7 overexpression was found in 91% of oral squamous cell carcinoma patient samples. The authors of this study further suggest that, since Cdc7 inhibits genotoxin-induced apoptosis, which in turn increases cancer cell survival during the DNA damage response, upregulation of Cdc7 increases the resistance to chemotherapy [22]. Cdc7 also phosphorylates TDP-43, a protein implicated in a number of neurodegenerative diseases, including amyotrophic lateral sclerosis (ALS) and Alzheimer's. A recent study suggests repurposing a small molecule inhibitor of Cdc7 (PHA767491), originally

developed as an anti-cancer agent, for use in preventing neurodegeneration caused by TDP-43 phosphorylation [23].

5.2 Summary of results

5.2.1 The C-terminal residues of *Saccharomyces cerevisiae* Mec1 are required for its localization, stability and function

To determine if the FATC domain has a general role in the stability of PIKK family members, we altered the C-terminus of *S. cerevisiae* Mec1 and integrated these into the yeast genome. Haploid yeast cells harboring a *mec1 W2368A* mutation, either untagged or epitope tagged, showed slower growth at the elevated temperature of 37°C compared to the physiological temperature of 30°C (Figure 2.1B). This change in the terminal tryptophan to alanine also caused sensitivity to hydroxyurea, an inhibitor of ribonucleotide reductase (Figure 2.1B).

Continuing from this, we explored the expression levels of C-terminal mutant Mec1 proteins in diploid yeast strains (Figure 2.2B). Western blotting using anti-Flag antibodies showed that all Flag-tagged *mec1* mutant alleles (Δ1, Δ2, Δ3 and 2369G) were expressed when yeast cells were grown at 30°C. While Flag-Mec1-W2368A and Flag-Mec1-2369G were expressed at near wild-type levels, the deletion proteins showed reduced expression, which was exacerbated by the extent of the deletion. As an interaction between Lcd1 and Mec1 is required for the checkpoint functions of Mec1, we investigated whether the mutant Mec1 proteins interacted with Lcd1 (Figure 2.2C). Co-immunoprecipitations of Flag-Mec1-W2368A, -Δ1 and -2369G revealed that each of these derivatives interacted with Lcd1 as efficiently as wild-type Mec1.

After discovering that the phenotypes of the Mec1 mutants were not due to their lack of expression or impaired interaction with Lcd1 we explored the kinase activity of the Mec1 derivatives (Figure 2.3B). Flag-tagged Mec1wt and derivatives were immunoprecipitated from diploid yeast cells and incubated with the substrate 4E-BP1. While phosphorylation of 4E-BP1 was considerably higher than background with the wildtype protein, the phosphorylation by Flag-Mec1-W2368A was 10-fold less than that

observed for Flag-Mec1wt. This result suggests that only low levels of kinase activity are required for cell viability since strains harboring the Mec1-W2368A mutation are viable at both 30°C and 37°C (Figure 2.1B). The lack of kinase activity demonstrated by the Mec1-2369G protein (Figure 2.2B) was most likely the cause of inviability of yeast strains carrying this mutation. Finally, the kinase activity was not above background for the Mec1 deletion mutants (Figure 2.2B). We cannot however, preclude the fact that the abrogation in kinase activity was a consequence of the lower protein levels of these mutants relative to Mec1wt (Figures 2.2B and 2.3A).

To investigate the lack of kinase activity demonstrated by the Mec1 mutants, we explored protein stability by various methods. First, examination of protein extracts revealed that the Mec1 mutants were susceptible to proteolysis in the absence of protease inhibitors after incubating at 30°C for 10 minutes compared to Mec1wt which remained stable up to two hours (Figure 2.4). Size exclusion chromatography of Flag-tagged Mec1 yeast extracts showed that each of the Mec1 mutants eluted in significantly higher molecular weight fractions relative to wildtype Mec1 (Figure 2.5). We suggest that the aberrant elution profiles by the Mec1 mutants may be due to improper folding of the proteins or extended interaction with chaperone complexes that are required for assembly of functional PIKK family members [24, 25]. In addition, we investigated the localization of Mec1 derivatives by confocal microscopy. Whereas eGFP-Mec1wt was predominantly localized to the nucleus, each of Mec1-W2368A, Mec1-2369G, Mec1-Δ1 and Mec1-Δ2 were found dispersed between the nucleus and cytoplasm (Figure 3.6).

Taken together, the above results indicated that the C-terminus of Mec1 was critical for proper folding and/or stability of the protein. Consequently, we predicted that it should be possible to discover second site suppressor mutations that restored protein levels and permitted growth of the *mec1-W2368A* strain at 37°C. We identified four unique mutations in three genes: Rfx1, Sml1 and Rpn3. We chose to investigate the *rpn3-L140P* mutation in more detail for two reasons. First, loss of function of Sml1 and Rfx1 are known to suppress nonfunctional alleles of *mec1* [26-28]. Second, Rpn3 encodes a component of the 19S proteasomal regulatory particle [29], thus possibly linking it to the stability of Mec1. Growth of a yeast strain carrying the *mec1-W2368A rpn3-L140P*

mutations was comparable to that of a wildtype strain at 37°C. In addition, the suppressor mutation was partially dominant (Figure 2.7B). Of note, the *rpn3-L140P* allele did not suppress the inviability of *mec1-Δ1*, *mec1-Δ2* or *mec1-2369G*. Moreover, we observed that this mutation caused a further reduction in growth on HU-containing plates (Figure 2.7C). We then confirmed the suppression of *mec1-W2368A* was due to *rpn3-L140P* by two independent methods. First, we compared the partially dominant effect of the *rpn3-L140P/RPN3* heterozygous diploid strain to the phenotype of a *mec1-W2368A* strain in which *rpn3-L140P* was genomically integrated (Figure 2.7D). Similar to the heterozygous diploid, integration of *rpn3-L140P* partially reversed the slow growth defect at 37C due to *mec1-W2368A*. Second, we screened the *RPN3* allele, via PCR and sequencing analysis, of independent spore colonies from a cross between *rpn3-L140P mec1-W2368A* and *RPN3 mec1-W2368A*. For 14 alleles (7 fast growing strains and 7 slow growing strains), the fast growth predicted the presence of the *rpn3-L140P* allele.

We next looked at the *rpn3-L140P* mutation alone in more detail since Rpn3 is an essential protein and L140 is located in a hydrophobic region conserved in fungal species (Figure 2.8A) and more broadly in eukaryotes Figure 2.8B). The protein levels of myc-Rpn3-L140P were comparable to that of myc-Rpn3 (Figure 2.8C). In addition, the growth of a *rpn3-L140P* strain was comparable to that of a wildtype strain at 30°C in rich media (Figure 2.8D). A very minimal reduction in growth was shown for cells grown at 37°C and in media containing the arginine analog canavanine.

To investigate whether rpn3-L140P would suppress a mutation similar to mec1-W2368A in a related PIKK family member, we introduced *rpn3-L140P* into a *tra1-F3744A* strain. We found that the rpn3-L140P mutation did not suppress the slow growth at 37°C or in media containing 6% ethanol (Figure 2.8E).

As Mec1-W2368A showed reduced protein stability (Figure 2.4), we explored the protein levels in the context of the *rpn3-L140P* mutation. For this, protein extracts were prepared in the absence of protease inhibitors from a *Flag⁵-mec1-W2368A/MEC1 rpn3-L140P/rpn3-L140P* yeast strain grown at either 30°C or 37°C. Western blot analysis revealed that the level of Mec1-W2368A in cells grown at 30°C was lower than that of

wildtype Mec1 (Figure 2.9A). The *rpn3-L140P* mutation augmented the level of Mec1-2368A relative to that from a *RPN3 mec1-W2368A* strain. While the level of Mec1-W2368A from extracts prepared from cells grown at 37C was considerably reduced relative to the wildtype, the *rpn3-L140P* mutation caused a striking increase in the level of Mec1-W2368A. From these results we suggest that *rpn3-L140P* helps to stabilize Mec1-W2368A, thereby permitting growth at elevated temperature. We also discovered that the *rpn3-L140P* mutation acts more broadly as it dramatically increased the level of Mec1-2369G in cells grown at 37C (Figure 2.9B).

We were intrigued by the suppression of *mec1-W2368A* by *rpn3-L140P* and thus explored Mec1 turnover mediated by proteasomal degradation. To this end, cells expressing Flag-tagged Mec1 or Mec1-W2368A were grown at 37°C and treated with MG-132, a proteasome inhibitor. Whereas wildtype Mec1 was unaltered by MG-132 treatment, there was an approximate two-fold increase in Mec1-W2368A levels following treatment (Figure 2.9D). These results suggest that the proteasome plays some part in Mec1 turnover. We did not observe evidence of ubiquitylation in either the wildtype or Mec1-W2368A proteins.

5.2.2   Modulation of Mcm2-7 activity by Cdt1

In budding yeast, Cdt1 is required for nuclear import and loading of Mcm2-7 onto chromatin in early G1 phase of the cell cycle. To investigate the interaction between Mcm2-7 and Cdt1 in isolation, individual components purified separately from bacterial-expression systems were combined and the complexes purified by size exclusion chromatography (Figure 3.1). Cdt1 co-eluted with each of the six Mcm subunits with the peak of elution equivalent to ~670 kDa and with equal stoichiometry (Figure 3.1A).

We next addressed whether the Mcm2-7•Cdt1 complex behaved differently from Mcm2-7 alone. Initially, the ability of the two complexes to hydrolyze ATP was compared. During both the titration of protein (Figure 3.2A) and time course experiments (Figure 3.2B), we consistently observed a lower ATPase activity with the Mcm2-7•Cdt1 complex compared to the Mcm2-7 complex. Overall, there was a two-fold reduction in the hydrolysis of ATP by Mcm2-7•Cdt1 relative to that of Mcm2-7 alone.

The two-fold reduction, rather than a complete inhibition, in ATPase activity by Mcm2-7•Cdt1 suggested that this reconstitution comprised a mixture of Mcm2-7 complexes with and without Cdt1. To this end, we asked whether the hydrolysis of ATP by the Mcm2-7•Cdt1 complex would be further inhibited if recombinant Cdt1 were added in solution (Figure 3.2C). While the rate of ATP hydrolysis by Mcm2-7 and Mcm2-7•Cdt1 was comparable after adding two-fold excess Cdt1, a maximum reduction in Mcm2-7•Cdt1 ATPase activity was reached with an equimolar amount of Cdt1 added. These data indicated that most, if not all, of the Cdt1 was associated with Mcm2-7 in the Mcm2-7•Cdt1 reconstitution.

We further compared the activity of Mcm2-7 and Mcm2-7•Cdt1 complexes in an established helicase assay [30]. In this regard, complexes were incubated with radiolabelled synthetic dsDNA fork substrate containing a biotin-streptavidin moiety and the ssDNA generated by unwinding were separated from duplex DNA by native polyacrylamide gel electrophoresis. Similar to ATPase activity, the DNA unwinding activity by Mcm2-7•Cdt1 was approximately two-fold lower than by Mcm2-7 alone (Figure 3.3). Unfortunately, the presence of nuclease contamination in the Cdt1 preparation nullified our ability to assess the effect on DNA unwinding by adding Cdt1 in solution to the Mcm2-7•Cdt1 complex.

We next addressed whether the DNA binding activity of Mcm2-7•Cdt1 was different from that of Mcm2-7. For this, radiolabelled Mcm2-7 or Mcm2-7•Cdt1 was incubated with either single-stranded M13 DNA (Figure 3.4) or double-stranded plasmid DNA (Figure 3.5). Whereas ssDNA binding increased in a DNA-dependent fashion, little to no difference in the ability of the two complexes to bind ssDNA was found. For dsDNA binding, Mcm2-7•Cdt1 demonstrated slightly lower binding relative to Mcm2-7 at all except the lowest concentration of dsDNA tested. Consistent with the poor ability of Mcm2-7 to bind dsDNA [31, 32], the overall amount of binding to dsDNA by either complex was much lower than that to ssDNA. Taken together, these results indicate that Cdt1 has little to no effect on the DNA binding activity of Mcm2-7. In addition and

consequently, the ability for Cdt1 to inhibit the DNA unwinding activity of Mcm2-7 was not due to a defect in DNA binding by this helicase complex.

To further investigate the individual roles of Mcm2-7 and Cdt1, we set out to assemble the pre-RC on replication origins from pure proteins and proteins purified from G1-arrested yeast extracts. To this end, Mcm2-7 was added to biotinylated ARS1 origin DNA coupled to streptavidin-coated magnetic beads in the presence of ORC, Cdc6 and ATP. Beads were washed with either low salt or high salt buffer to differentiate between Mcm2-7 complexes that were associated with versus loaded onto origin DNA, respectively. Consistent with published results [8, 10, 33, 34], we found that origin loading of Mcm2-7 was dependent on ORC, Cdc6 and Cdt1 (Figures 3.6 and 3.7). We also observed a greater extent of loading using Mcm2-7 and ORC purified from G1-arrested yeast extracts compared to pure proteins. To determine the cause for this discrepancy, we examined these complexes in more detail. Analysis of complexes run on SDS-PAGE gels (Figures 3.8A and B) revealed that there was approximately equal stoichiometry of subunits in the respective complexes. Since the hydrolysis of ATP by ORC and Cdc6 is required for the stable association of Mcm2-7 with replication origins, we determined the ATPase activity of the pre-RC factors in isolation or in combination with each other (Figure 3.8C). While low, the hydrolysis of ATP by bacterial-expressed ORC was two-fold lower than that of ORC purified from G1-arrested yeast extracts. In contrast, and regardless of the source of ORC, the ATPase activity of ORC and Cdc6 combined was similar.

Intriguingly, we found that in the presence of Cdt1, the Mcm2-7 complex was comprised of subunits at or near equal stoichiometry. In contrast, in the absence of Cdt1, subcomplexes of Mcm subunits were more pronounced (Figure 3.1; M. O'Donnell and L. Langston, unpublished). In light of this, we predicted that Cdt1 plays a role in stabilizing Mcm2-7. To this end, we evaluated by gel filtration the formation of Mcm2-7 subcomplexes in the presence or absence of Cdt1 using purified proteins (Figure 3.9). Similar to that observed for Mcm2-7, a subcomplex containing Mcm2, 4 and 6 neared stoichiometry in the presence as opposed to the absence of Cdt1 (Figures 3.9A and B). Whereas the addition of Cdt1 had no discernible effect on the stoichiometry of a Mcm357

(Mcm odds) complex, the formation of both trimers and hexamers of Mcm357 was observed in the absence of Cdt1 (Figures 3.9C and D). Furthermore, we observed that when all six Mcm subunits were expressed in yeast, and when ATP was omitted from affinity chromatography purification, only the Mcm odds were recovered (Figure 3.10).

Encouraged by the above results and the recent finding that, in the presence of the poorly hydrolysable ATP analog ATPγS, only Mcm3, 5 and 7 were associated with origin DNA upon mixing Mcm2-7 in a pre-RC loading reaction lacking Cdt1 [33], we performed a loading assay in the absence of Mcm2, 4, 6 and Cdt1 (Figure 3.11). Consequently, after treating loading reactions with low salt buffer, we observed that the Mcm357 subcomplex could associate with ARS1 in the absence of Mcm2, 4, 6 and Cdt1. While the association of the Mcm odds complex was dependent on nucleotide, there was a greater amount of origin recruitment in the presence of ATPγS relative to ATP. Additionally and consistent with published data [10, 33], none of the pre-RC factors bound to origin DNA in the absence of ORC and Cdc6. Finally, we also observed non-specific binding of ORC and Cdc6 in the absence of ATP.

5.2.3   Investigating the role of phosphorylation on Mcm2-7 activity

To determine what role DDK-dependent phosphorylation of Mcm2-7 plays in modulating helicase activity, we utilized a phosphomimetic mutant of Mcm4 (Mcm4PM) deleted for the first 145 N-terminal residues and containing glutamic acid substitutions for seven proximal serine or threonine DDK target sites (Figure 4.1A) [35]. To confirm this mutant was able to bypass the requirement for DDK, we first cloned the *mcm4pm* allele into a CEN plasmid and transformed the construct into a *dbf4Δ/DBF4 mcm4Δ/MCM4* heterozygous diploid yeast strain. After sporulation and screening of tetrads, I isolated a haploid spore harboring the *mcm4pm* allele and that was viable upon the simultaneous loss of *MCM4* and *DBF4* (Figure 4.1B).

After confirming that the *mcm4pm* allele was able to bypass the requirement for DDK *in vivo*, we set out to analyze the Mcm4PM protein *in vitro*. For this, we utilized a bacterial-expression system to separately purify yeast Mcm subunits including the Mcm4PM mutant (Figure 4.2). As ATPase active sites are located at dimer interfaces

within the Mcm2-7 hexamer, I next investigated the effect of the Mcm4 phosphomimetic mutation on the hydrolysis of ATP over time by Mcm pairwise combinations (Figure 4.3). The rate of ATPase activity for the Mcm7/4 dimer was two-fold lower when Mcm4PM was used instead of the wildtype protein (Figure 4.3A). Although not statistically significant, combining the phosphomimetic Mcm4 mutant with Mcm6 resulted in a marginally higher rate of ATPase activity compared to when wildtype Mcm4 was used (Figure 4.3B). Overall and regardless of the version of Mcm4 used, the Mcm7/4 pairwise combination demonstrated a much higher level of ATPase activity relative to Mcm4/6.

We next evaluated the effect of the phosphomimetic Mcm4 mutant on ATPase activity by multimers of Mcm subunits in an end-point assay (Figure 4.3C). As with the time course experiment, there was an approximately two-fold reduction in ATPase activity by Mcm7/4PM relative to Mcm7/4wt. Regardless of the derivative of Mcm4 used, combining Mcm6 or Mcm3pk with Mcm7 and Mcm4 stimulated ATPase activity. In contrast, the addition of Mcm2 and/or Mcm5 to Mcm7/4-containing multimers reduced the hydrolysis of ATP relative to Mcm7/4 dimers. When Mcm4PM was combined with the other five Mcm subunits, a somewhat reduced ATPase activity was shown compared to that when wildtype Mcm4 was used.

To further investigate the role of phosphorylation by DDK on Mcm2-7 activity, we reconstituted Mcm2-7 complexes with wildtype (Figure 4.4A) or phosphomimetic Mcm4 (Figure 4.4C) from individual proteins purified from bacterial-expression systems. Since these complexes were assembled from pure proteins, the wildtype Mcm2-7 complex represents a non-phosphorylated state, whereas the phosphomimetic Mcm2-7 complex corresponds to a DDK-phosphorylated (on Mcm4) state. Individual subunits were mixed, concentrated and complexes purified by size exclusion chromatography. Consistent with the predicted molecular weight of a ~600 kDa toroidal complex, both Mcm2-7wt and Mcm2-7^{4PM} demonstrated a peak of elution of ~670 kDa. In addition, each of these hexamers was comprised of six Mcm subunits in equal stoichiometry.

Following the reconstitution of these complexes, we investigated their respective activities via *in vitro* biochemical methods. First, the ATPase activity across the peak fractions from size exclusion chromatography was assessed (Figures 4.4B and D). For this, protein complexes were mixed with ^{32}P-radiolabelled ATP, incubated at 30°C and samples spotted onto TLC sheets to separate ATP and Pi. The peak in ATPase activity co-eluted with peak protein for both the wildtype and the phosphomimetic Mcm2-7 complexes. Since the essential function of Mcm2-7 is to unwind duplex DNA, we performed a helicase assay using a radiolabelled synthetic fork substrate (Figure 4.5) [30]. Experimental conditions to achieve efficient DNA unwinding activity were initially performed with wildtype Mcm2-7. As a previous report found that the *in vitro* helicase activity of yeast Mcm2-7 purified from baculovirus was stimulated by anions, acetate or glutamate was added to the standard helicase conditions. Interestingly, while there was little to no anion-dependent effect on Mcm2-7 DNA unwinding activity, the addition of 5% PEG augmented helicase activity nearly six-fold. After determining the appropriate buffer conditions to achieve helicase activity, peak gel filtration fractions of wildtype and phosphomimetic Mcm2-7 were assayed for their ability to unwind DNA (Figure 4.6). As with ATPase activity, the peak in DNA unwinding activity co-eluted with peak protein for both complexes. Together, these data indicated that both wildtype and phosphomimetic Mcm2-7 formed active hexameric complexes.

As lower ATPase activity was demonstrated in majority of the Mcm multimers containing the Mcm4PM mutant subunit (Figure 4.3C), we next performed *in vitro* biochemical analyses to compare activities of the wildtype and the phosphomimetic Mcm2-7 complexes. Surprisingly, the ATPase (Figure 4.7A) and DNA unwinding (Figure 4.7B) activities of phosphomimetic Mcm2-7 were comparable to those of the wildtype complex. In addition, we investigated the DNA binding activity of these complexes using a radiolabelled poly dT60 substrate. Similarly to the ATPase and helicase activities, preliminary data demonstrated that the ability of phosphomimetic Mcm2-7 to bind ssDNA was comparable to that of wildtype Mcm2-7 (Figure 4.7C). Whereas the Mcm4PM subunit showed lower ATPase activity in subunit combinations,

the above comparative results suggest that the phosphomimetic Mcm4 subunit has little to no effect on the activity of the Mcm2-7 helicase.

5.3   Phosphoregulation of Mcm2-7 to unwind DNA

It is interesting that in eukaryotes Mcm2-7 is loaded onto replication origins in early G1 phase of the cell cycle in an inactive state. Throughout S phase, the events that trigger Mcm2-7 to unwind DNA are poorly understood. Several reports have shown that the amino termini of Mcm2, Mcm4 and Mcm6 are the major substrates for DDK [36, 37]. In particular, studies in budding yeast indicate that hyperphosphorylation of Mcm4 within Mcm2-7 is the essential function of DDK [35]. As the wildtype Mcm2-7 complex was reconstituted from pure proteins, my results suggest that *in vitro* helicase activity can occur in the absence of post-translational modification. In support of this, biochemical analyses of a phosphomimetic Mcm2-7 complex did not show augmented activity. While phosphomimetic Mcm4 can bypass the requirement for DDK *in vivo* ([35] and this study), it is possible that this mutant, when reconstituted into the Mcm2-7 hexamer, was not sufficient to observe enhanced activity. My results, however, are consistent with data from the Schwacha lab showing that yeast Mcm2-7 purified from baculovirus-expression systems exhibits robust *in vitro* helicase activity [38]. Their study also found that DNA unwinding is unaffected by phosphatase treatment of Mcm2-7.

Upon origin loading, Mcm2-7 double hexamers switch from a dsDNA binding mode to a ssDNA binding mode. The mechanisms involved in this process have yet to be elucidated. It is possible that throughout S phase, phosphorylation of Mcm2-7 is required to induce a conformational change to permit a switch in binding modes to facilitate DNA unwinding.   Structural changes have been proposed based on studies of an archaeal MCM complex harboring a mutation analogous to the *bob1* mutation in budding yeast [39]. In fact, Bochman and Schwacha [38] proposed that circularization of Mcm2-7 is required for DNA unwinding. This theory is further supported by studies of the bovine papillomavirus E1 helicase [40]. Interestingly, Mcm2-7 does not unwind DNA as a double hexamer, but rather as single hexamers to facilitate bidirectional replication fork progression. It is possible that DDK-dependent phosphorylation of Mcm2-7 may disrupt

the double hexamer and stabilize the association of single Mcm2-7 hexamers with ssDNA.

Phosphorylation of Mcm2-7 may create binding sites for the accessory factors Cdc45 and GINS. In budding yeast, Cdc45 is recruited to early origins during G1 phase, yet the stable interaction between Mcm2-7 and Cdc45 during S phase is dependent on the activities of CDK and DDK [41-43]. Furthermore, RNAi knock-down of GINS and Cdc45 revealed that these proteins are essential for S phase progression in *Drosophila* cells [44]. Mcm2-7 is thought to be the core of a larger CMG complex assembled at replication origins. To date, CMG complexes that associate with replicating DNA have been shown in *Xenopus* egg extracts [45], *Drosophila* embryos [44], budding yeast [46] and human cells (reviewed in 47). In fact, *Drosophila* Mcm2-7 CMG exhibited enhanced activity relative to Mcm2-7 alone [48]. These included an increase in the rate of ATP hydrolysis, robust helicase activity and augmented affinity for DNA. However, the role of Mcm2-7 phosphorylation is still unknown as the amino termini of Mcm2 and Mcm4 were not hyperphosphorylated in the CMG and the modified residues mapped were the same in the CMG and in Mcm2-7. Additionally, the disparity in *in vitro* helicase activity between budding yeast Mcm2-7 and *Drosophila* Mcm2-7 is not known. It may be due to differences in the modulation of Mcm2-7 activity between these organisms. Perhaps combining the phosphomimetic Mcm2-7 complex with Cdc45 and GINS would augment helicase activity beyond the level reported in this study. Future reconstitution studies of budding yeast CMG using pure proteins will help to address the role of phosphorylation in activating Mcm2-7 to unwind DNA.

While Mcm4 is the essential DDK target *in vivo,* phosphorylation of other Mcm subunits may also be necessary for Mcm2-7 activation. It was recently reported that Cdc7 associated with Mcm4 and Mcm5 in yeast two-hybrid and co-immunoprecipitation analyses [49]. The binding of Cdc7 to Mcm5 is intriguing as Mcm5 is the only Mcm subunit not phosphorylated by DDK in budding yeast or any other species [47]. Furthermore, DDK phosphorylation of Mcm4 and Mcm6 is highly influenced by pre-RC formation [50]. In an extensive study using *in vitro* assembled pre-RCs as a DDK substrate

and mass spectrometry, the Bell lab identified DDK phosphorylation sites on budding yeast Mcm4 and Mcm6 [36]. That study also found that phosphorylation of either subunit was sufficient for yeast cell proliferation. As such, it would be interesting to investigate the effect on *in vitro* helicase activity by a Mcm2-7 complex containing phosphomimetic mutations in either or both of Mcm4 and Mcm6.

DDK phosphorylation of Mcm2-7 is also stimulated by prior phosphorylation by one or more kinases. In fact, it was previously observed that DDK could not bind Mcm2-7 or phosphorylate Mcm4 or Mcm6 without prior phosphorylation [50]. Using *in vitro* assembled pre-RCs as a DDK substrate, the Bell lab demonstrated that DDK phosphorylation of Mcm4 and Mcm6 required prior phosphorylation of these subunits at either S/T-P or S/T-Q sites [36]. That same report strongly suggested that Mec1 directly targets the S/T-Q sites and that DNA replication is positively modulated by these modifications. The authors further propose that priming phosphorylation by Mec1 and other kinases enhances DDK phosphorylation of Mcm4 and Mcm6 in two ways. First, phosphorylation at S-S/T-P and S-S/T-Q sites generates an acidic phosphoserine/threonine that directs DDK to an adjacent serine residue upstream. In this regard, the number of possible DDK targets sites in Mcm4 and Mcm6 is increased by approximately two-fold. Second, it is possible that the processive phosphorylation of the N-terminal tail of Mcm4 by DDK [42] is due to phosphorylation of S/T stretches that precede several of these phosphogenerated DDK target sites [36].

The role of Mec1 has been most characterized for its function in checkpoint signaling. Data from the Bell lab has now extended that role to include requisite priming phosphorylation of Mcm2-7 for subsequent DDK targeting. From the current study, it appears that the terminal tryptophan of Mec1 is required for its function. As our results suggest that only low levels of kinase activity are essential for viability, it would be intriguing to determine the effect of Mec1wt and the Mec1-W2368A mutant on Mcm2-7 phosphorylation *in vitro*. It is possible that any effect on Mcm2-7 by Mec1 phosphorylation will only be evident in the context of the pre-RC. As such, it would also be beneficial to carry out *in vitro* studies, such as pre-RC loading experiments, to determine the effect of Mec1 and DDK phosphorylation on Mcm2-7 helicase activity

within the pre-RC. However, the involvement of priming Mcm2-7 by the metazoan Mec1 homolog ATR may not hold true in these organisms as S-S/T-Q sites are not found in the N-termini of metazoan Mcm2-7 [36]. As such, future studies examining the phosphorylation of and downstream effect on Mcm2-7 activity in metazoans is necessary.

5.4 Cdt1 acts as a negative regulator of Mcm2-7 activity

Cdt1 is an important eukaryotic replication licensing factor that is tasked with the nuclear import and origin loading of the Mcm2-7 replicative helicase during early G1 phase [51, 52]. Mcm2-7 remains inactive within the pre-RC until it is activated during S phase by mechanisms yet to be fully elucidated. Here, I propose a model in which Cdt1 acts to negatively regulate the helicase activity of Mcm2-7 (Figure 5.1) prior to the onset of S phase. In this model, Cdt1 induces a structural change in Mcm2-7 which alters its ATPase activity and ultimately the helicase function of Mcm2-7. It has been reported that AAA+ ATPases, such as Mcm2-7, exhibit altered ATPase rates upon subtle structural changes, such as caused by an interaction with another protein [53]. In the absence of Cdt1, Mcm2-7 exhibits fully functional ATPase activity. This ATPase activity is sufficient to facilitate DNA unwinding by Mcm2-7. In contrast, the association of Cdt1 with Mcm2-7 via the C-terminal region of Mcm6 [54-56] induces a conformational change such that it disrupts the ATPase sites within Mcm2-7. A recent report suggested that in addition to the C-terminus of Mcm6, there is at least one more binding site in a different region of Mcm2-7 [34]. In support of this model, the ATPase assays presented in the current study involving Mcm2-7•Cdt1 complexes or when Cdt1 is added in solution to Mcm2-7 showed that the hydrolysis of ATP is reduced by approximately two-fold relative to Mcm2-7 alone. To further corroborate this, a recent report demonstrated that the binding of Cdt1 to Mcm2-7 resulted in a 35% reduction in the ATPase rate [34]. The abrogation in ATPase activity, in turn, prevents DNA unwinding. The DNA unwinding assays presented in Chapter 3 revealed a two-fold reduction in helicase activity by Mcm2-7•Cdt1 complexes compared to Mcm2-7 alone. As the energy produced from ATP hydrolysis is required for helicase activity, the reduced DNA unwinding activity is due to the inhibition in ATPase activity by Mcm2-7. Mcm2-7 demonstrates an ATP-dependent DNA binding activity, with approximately 100-fold higher affinity for ssDNA (35 nM)

than dsDNA (25µM) [31]. As we observed little to no difference in ssDNA binding between Mcm2-7 alone and Mcm2-7•Cdt1 complexes, the reduction in ATPase activity is not likely due to a defect in ATP binding by Mcm2-7.
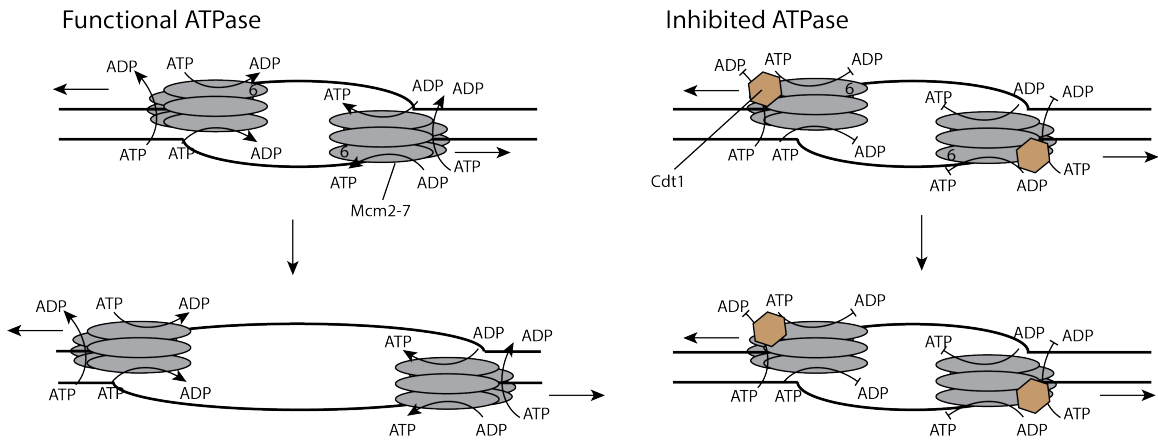
Figure 5.1: Model of inhibition of Mcm2-7 helicase activity by Cdt1

In the absence of Cdt1, Mcm2-7 is capable of ATP hydrolysis (Functional ATPase). This activity allows Mcm2-7 to unwind duplex DNA. Conversely, an interaction between Cdt1 and the C-terminus of Mcm6 induces a structural change that disrupts ATPase activity by Mcm2-7 (Inhibited ATPase). In addition to a Cdt1-Mcm6 interaction, Cdt1 may bind to other sites within Mcm2-7.

5.5   Cdt1 acts to stabilize Mcm2-7

In vivo, Cdt1 is required for the assembly of Mcm2-7 in both the cytoplasm and nucleoplasm prior to pre-RC formation [55]. *In vitro* reconstitution of the pre-RC using purified components from either *S. cerevisiae* or *Xenopus* egg extracts has demonstrated that Cdt1 is required to load Mcm2-7 onto origins of replication in a high salt-stable manner [8-10]. Consistent with this, using yeast pre-RC proteins purified from *E. coli*, we demonstrated that Cdt1 is required for origin loading of Mcm2-7. Recently, it was demonstrated that while Mcm3, 5 and 7, which are neighbours in the Mcm2-7 hexamer, associated (low salt) with origins independently of Cdt1 in the presence of the poorly hydrolysable analog of ATP, ATPγS, substoichiometric levels of Mcm2, 4 and 6 were present. In the presence of ATPγS and Cdt1, however, all six Mcm subunits associated with origin DNA with equimolar ratio[33]. Of note, Cdt1-independent association of Mcm2-7 was abolished in the presence of ATP [33]. The authors of that study propose a model in which Cdt1 plays a role in stabilizing Mcm2-7 during initial origin recruitment. We believe our data fit this model. In the presence of Cdt1, stoichiometric levels of Mcm2-7 subunits were observed, whereas in the absence of Cdt1, multimers and/or subcomplexes of Mcm subunits were more pronounced. Furthermore, indicative of Mcm release via ATP hydrolysis by ORC-Cdc6 when criteria for appropriate origin licensing are not met [33], we observed a reduction in origin association of a subcomplex of Mcm357 in the presence of ATP relative to ATPγS. Surprisingly, we observed that when ATP was added during the purification of Mcm2-7 proteins from G1-arrested yeast extracts, hexamers were formed from Mcm subunits in equimolar ratio. Conversely, only Mcm3, 5 and 7 were isolated in the absence of ATP. Significantly, reconstitutions of Mcm2-7 complexes from bacterial-expressed proteins were performed in the absence of ATP. The basis for the requirement for ATP during purification of Mcm2-7 complexes from yeast extracts is currently unknown. The ATP binding status at ATPase active sites within Mcm2-7 is thought to be communicated between subunits and cause conformational changes [6]. Predicated on this, we suggest that ATP substitutes for the lack of Cdt1 to stabilize the Mcm2-7 hexamer when purified from yeast extracts. By the same token,

conformational changes in Mcm2-7 from Cdt1 binding help to stabilize the Mcm2-7 hexamer.

5.6 Conclusions

Although much work has focused on the Mcm2-7 eukaryotic replicative DNA helicase, very little is known about how its activity is regulated during the early stages of the initiation of DNA replication. Taken together, the work presented in this thesis will aid in decoding the regulatory processes and protein factors involved in modulating Mcm2-7 activity. I have demonstrated that the C-terminus of budding yeast Mec1 plays a role in folding and stability of this kinase; a feature likely common to PIKK family members. My results also indicate that Mec1 turnover may be regulated by the proteasome. Moreover, I have demonstrated that Cdt1 negatively regulates Mcm2-7 activity. This provides a mechanism to prevent untimely DNA unwinding by Mcm2-7. My studies also demonstrate that a phosphomimetic mutant of Mcm4 does not augment enzymatic activity of Mcm2-7. This suggests that phosphorylation of Mcm4 by DDK alone is not sufficient to stimulate the activity of Mcm2-7 and which may involve prior phosphorylation by other kinases, such as Mec1.

5.7 References

1.   Bell,S.P. & Dutta,A. DNA replication in eukaryotic cells. *Annu. Rev. Biochem* **71**, 333-374 (2002).

2.   Boos,D., Frigola,J., & Diffley,J.F. Activation of the replicative DNA helicase: breaking up is hard to do. *Curr. Opin. Cell Biol.* **24**, 423-430 (2012).

3.   Singleton,M.R., Dillingham,M.S., & Wigley,D.B. Structure and mechanism of helicases and nucleic acid translocases. *Annu. Rev. Biochem.* **76**, 23-50 (2007).

4.   Chen,K.C., Csikasz-Nagy,A., Gyorffy,B., Val,J., Novak,B. *et al.* Kinetic analysis of a molecular model of the budding yeast cell cycle. *Mol Biol. Cell* **11**, 369-391 (2000).

5.   Patel,S.S. & Picha,K.M. Structure and function of hexameric helicases. *Annu. Rev. Biochem.* **69**, 651-697 (2000).

6.   Davey,M.J., Indiani,C., & O'Donnell,M. Reconstitution of the Mcm2-7p heterohexamer, subunit arrangement, and ATP site architecture. *J. Biol. Chem.* **278**, 4491-4499 (2003).

7.   Bochman,M.L., Bell,S.P., & Schwacha,A. Subunit organization of Mcm2-7 and the unequal role of active sites in ATP hydrolysis and viability. *Mol. Cell Biol.* **28**, 5865-5873 (2008).

8.   Evrin,C., Clarke,P., Zech,J., Lurz,R., Sun,J. *et al.* A double-hexameric MCM2-7 complex is loaded onto origin DNA during licensing of eukaryotic DNA replication. *Proc. Natl. Acad. Sci. U. S. A* **106**, 20240-20245 (2009).

9.   Gambus,A., Khoudoli,G.A., Jones,R.C., & Blow,J.J. MCM2-7 form double hexamers at licensed origins in Xenopus egg extract. *J. Biol. Chem.* **286**, 11855-11864 (2011).

10.   Remus,D., Beuron,F., Tolun,G., Griffith,J.D., Morris,E.P. *et al.* Concerted loading of Mcm2-7 double hexamers around DNA during DNA replication origin licensing. *Cell* **139**, 719-730 (2009).

11.   Ishimi,Y. A DNA helicase activity is associated with an MCM4, -6, and -7 protein complex. *J. Biol. Chem.* **272**, 24508-24513 (1997).

12.   Schwacha,A. & Bell,S.P. Interactions between two catalytically distinct MCM subgroups are essential for coordinated ATP hydrolysis and DNA replication. *Mol. Cell* **8**, 1093-1104 (2001).

13.   Araki,H. Regulatory mechanism of the initiation step of DNA replication by CDK in budding yeast. *Biochim. Biophys. Acta* **1804**, 520-523 (2010).

14. Heller,R.C., Kang,S., Lam,W.M., Chen,S., Chan,C.S. *et al.* Eukaryotic origin-dependent DNA replication in vitro reveals sequential action of DDK and S-CDK kinases. *Cell* **146**, 80-91 (2011).

15. Zou,L. & Stillman,B. Formation of a preinitiation complex by S-phase cyclin CDK-dependent loading of Cdc45p onto chromatin. *Science* **280**, 593-596 (1998).

16. Semple,J.W. & Duncker,B.P. ORC-associated replication factors as biomarkers for cancer. *Biotechnol. Adv.* **22**, 621-631 (2004).

17. Karakaidos,P., Taraviras,S., Vassiliou,L.V., Zacharatos,P., Kastrinakis,N.G. *et al.* Overexpression of the replication licensing regulators hCdt1 and hCdc6 characterizes a subset of non-small-cell lung carcinomas: synergistic effect with mutant p53 on tumor growth and chromosomal instability--evidence of E2F-1 transcriptional control over hCdt1. *Am. J Pathol.* **165**, 1351-1365 (2004).

18. Hofmann,J.F. & Beach,D. cdt1 is an essential target of the Cdc10/Sct1 transcription factor: requirement for DNA replication and inhibition of mitosis. *EMBO J.* **13**, 425-434 (1994).

19. Petropoulou,C., Kotantaki,P., Karamitros,D., & Taraviras,S. Cdt1 and Geminin in cancer: markers or triggers of malignant transformation? *Front Biosci.* **13**, 4485-4494 (2008).

20. Swords,R., Mahalingam,D., O'Dwyer,M., Santocanale,C., Kelly,K. *et al.* Cdc7 kinase - a new target for drug development. *Eur. J. Cancer* **46**, 33-40 (2010).

21. Kulkarni,A.A., Kingsbury,S.R., Tudzarova,S., Hong,H.K., Loddo,M. *et al.* Cdc7 kinase is a predictor of survival and a novel therapeutic target in epithelial ovarian carcinoma. *Clin. Cancer Res.* **15**, 2417-2425 (2009).

22. Cheng,A.N., Jiang,S.S., Fan,C.C., Lo,Y.K., Kuo,C.Y. *et al.* Increased Cdc7 expression is a marker of oral squamous cell carcinoma and overexpression of Cdc7 contributes to the resistance to DNA-damaging agents. *Cancer Lett.* **337**, 218-225 (2013).

23. Liachko,N.F., McMillan,P.J., Guthrie,C.R., Bird,T.D., Leverenz,J.B. *et al.* CDC7 inhibition blocks pathological TDP-43 phosphorylation and neurodegeneration. *Ann. Neurol.* **74**, 39-52 (2013).

24. Boulon,S., Bertrand,E., & Pradet-Balade,B. HSP90 and the R2TP co-chaperone complex: building multi-protein machineries essential for cell growth and gene expression. *RNA. Biol.* **9**, 148-154 (2012).

25. Makhnevych,T. & Houry,W.A. The role of Hsp90 in protein complex assembly. *Biochim. Biophys. Acta* **1823**, 674-682 (2012).

26. Desany,B.A., Alcasabas,A.A., Bachant,J.B., & Elledge,S.J. Recovery from DNA replicational stress is the essential function of the S-phase checkpoint pathway. *Genes Dev.* **12**, 2956-2970 (1998).

27. Huang,M., Zhou,Z., & Elledge,S.J. The DNA replication and damage checkpoint pathways induce transcription by inhibition of the Crt1 repressor. *Cell* **94**, 595-605 (1998).

28. Weinert,T.A., Kiser,G.L., & Hartwell,L.H. Mitotic checkpoint genes in budding yeast and the dependence of mitosis on DNA replication and repair. *Genes Dev.* **8**, 652-665 (1994).

29. Kominami,K., Okura,N., Kawamura,M., DeMartino,G.N., Slaughter,C.A. *et al.* Yeast counterparts of subunits S5a and p58 (S3) of the human 26S proteasome are encoded by two multicopy suppressors of nin1-1. *Mol. Biol. Cell* **8**, 171-187 (1997).

30. Kaplan,D.L., Davey,M.J., & O'Donnell,M. Mcm4,6,7 uses a "pump in ring" mechanism to unwind DNA by steric exclusion and actively translocate along a duplex. *J Biol. Chem.* **278**, 49171-49182 (2003).

31. Bochman,M.L. & Schwacha,A. Differences in the single-stranded DNA binding activities of MCM2-7 and MCM467: MCM2 and MCM5 define a slow ATP-dependent step. *J. Biol. Chem.* **282**, 33795-33804 (2007).

32. Stead,B.E., Sorbara,C.D., Brandl,C.J., & Davey,M.J. ATP binding and hydrolysis by Mcm2 regulate DNA binding by Mcm complexes. *J. Mol. Biol.* **391**, 301-313 (2009).

33. Frigola,J., Remus,D., Mehanna,A., & Diffley,J.F. ATPase-dependent quality control of DNA replication origin licensing. *Nature* **495**, 339-343 (2013).

34. Fernandez-Cid,A., Riera,A., Tognetti,S., Herrera,M.C., Samel,S. *et al.* An ORC/Cdc6/MCM2-7 complex is formed in a multistep reaction to serve as a platform for MCM double-hexamer assembly. *Mol. Cell* **50**, 577-588 (2013).

35. Sheu,Y.J. & Stillman,B. The Dbf4-Cdc7 kinase promotes S phase by alleviating an inhibitory activity in Mcm4. *Nature* **463**, 113-117 (2010).

36. Randell,J.C., Fan,A., Chan,C., Francis,L.I., Heller,R.C. *et al.* Mec1 is one of multiple kinases that prime the Mcm2-7 helicase for phosphorylation by Cdc7. *Mol. Cell* **40**, 353-363 (2010).

37. Montagnoli,A., Valsasina,B., Brotherton,D., Troiani,S., Rainoldi,S. *et al.* Identification of Mcm2 phosphorylation sites by S-phase-regulating kinases. *J. Biol. Chem.* **281**, 10281-10290 (2006).

38.   Bochman,M.L. & Schwacha,A. The Mcm2-7 complex has in vitro helicase activity. *Mol. Cell* **31**, 287-293 (2008).

39.   Fletcher,R.J., Bishop,B.E., Leon,R.P., Sclafani,R.A., Ogata,C.M. *et al.* The structure and function of MCM from archaeal M. Thermoautotrophicum. *Nat. Struct. Biol.* **10**, 160-167 (2003).

40.   Schuck,S. & Stenlund,A. Assembly of a double hexameric helicase. *Mol. Cell* **20**, 377-389 (2005).

41.   Zou,L. & Stillman,B. Assembly of a complex containing Cdc45p, replication protein A, and Mcm2p at replication origins controlled by S-phase cyclin-dependent kinases and Cdc7p-Dbf4p kinase. *Mol Cell Biol.* **20**, 3086-3096 (2000).

42.   Sheu,Y.J. & Stillman,B. Cdc7-Dbf4 phosphorylates MCM proteins via a docking site-mediated mechanism to promote S phase progression. *Mol Cell* **24**, 101-113 (2006).

43.   Masai,H., Taniyama,C., Ogino,K., Matsui,E., Kakusho,N. *et al.* Phosphorylation of MCM4 by Cdc7 kinase facilitates its interaction with Cdc45 on the chromatin. *J. Biol. Chem.* **281**, 39249-39261 (2006).

44.   Moyer,S.E., Lewis,P.W., & Botchan,M.R. Isolation of the Cdc45/Mcm2-7/GINS (CMG) complex, a candidate for the eukaryotic DNA replication fork helicase. *Proc. Natl. Acad. Sci. U. S. A* **103**, 10236-10241 (2006).

45.   Kubota,Y., Takase,Y., Komori,Y., Hashimoto,Y., Arata,T. *et al.* A novel ring-like complex of Xenopus proteins essential for the initiation of DNA replication. *Genes Dev.* **17**, 1141-1152 (2003).

46.   Gambus,A., Jones,R.C., Sanchez-Diaz,A., Kanemaki,M., van,D.F. *et al.* GINS maintains association of Cdc45 with MCM in replisome progression complexes at eukaryotic DNA replication forks. *Nat. Cell Biol.* **8**, 358-366 (2006).

47.   Labib,K. How do Cdc7 and cyclin-dependent kinases trigger the initiation of chromosome replication in eukaryotic cells? *Genes Dev.* **24**, 1208-1219 (2010).

48.   Ilves,I., Petojevic,T., Pesavento,J.J., & Botchan,M.R. Activation of the MCM2-7 helicase by association with Cdc45 and GINS proteins. *Mol. Cell* **37**, 247-258 (2010).

49.   Ramer,M.D., Suman,E.S., Richter,H., Stanger,K., Spranger,M. *et al.* Dbf4 and Cdc7 proteins promote DNA replication through interactions with distinct Mcm2-7 protein subunits. *J. Biol. Chem.* **288**, 14926-14935 (2013).

50.   Francis,L.I., Randell,J.C., Takara,T.J., Uchima,L., & Bell,S.P. Incorporation into the prereplicative complex activates the Mcm2-7 helicase for Cdc7-Dbf4 phosphorylation. *Genes Dev.* **23**, 643-654 (2009).

51. Tanaka,S. & Diffley,J.F. Interdependent nuclear accumulation of budding yeast Cdt1 and Mcm2-7 during G1 phase. *Nat. Cell Biol.* **4**, 198-207 (2002).

52. Randell,J.C., Bowers,J.L., Rodriguez,H.K., & Bell,S.P. Sequential ATP hydrolysis by Cdc6 and ORC directs loading of the Mcm2-7 helicase. *Mol Cell* **21**, 29-39 (2006).

53. Hanson,P.I. & Whiteheart,S.W. AAA+ proteins: have engine, will work. *Nat. Rev. Mol. Cell Biol.* **6**, 519-529 (2005).

54. Wei,Z., Liu,C., Wu,X., Xu,N., Zhou,B. *et al.* Characterization and structure determination of the Cdt1 binding domain of human minichromosome maintenance (Mcm) 6. *J. Biol. Chem.* **285**, 12469-12473 (2010).

55. Wu,R., Wang,J., & Liang,C. Cdt1p, through its interaction with Mcm6p, is required for the formation, nuclear accumulation and chromatin loading of the MCM complex. *J. Cell Sci.* **125**, 209-219 (2012).

56. Zhang,J., Yu,L., Wu,X., Zou,L., Sou,K.K. *et al.* The interacting domains of hCdt1 and hMcm6 involved in the chromatin loading of the MCM complex in human cells. *Cell Cycle* **9**, 4848-4857 (2010).

Curriculum Vitae

Name   Lance DaSilva

Education

2008-present Ph.D. Candidate   University of Western Ontario, London, Ontario, Canada
Department of Biochemistry
Supervisors: Dr. M. Davey and Dr. D. Edgell

2006-2008   M.Sc.   University of Waterloo, Waterloo, Ontario, Canada
Department of Biology
Supervisor: Dr. B. Duncker

1993-1998   B.Sc.   Carleton University, Ottawa, Ontario, Canada
Honours Biology

Honours and Awards

2013   ASBMB Graduate Student Travel Award
2011   Ontario Graduate Scholarship
2010   Graduate Thesis Research Award
2009   Ontario Graduate Scholarship
2008   Ontario Graduate Scholarship in Science & Technology
2007   University of Waterloo Graduate Scholarship Research Award
2006   University of Waterloo Graduate Scholarship Research Award

Related Work Experience

2003-2005   Research Assistant
University of Waterloo, Waterloo, Ontario, Canada
Department of Biology

1998-2003   Research Assistant
Ottawa Hospital Research Institute, Ottawa, Ontario, Canada
Neuroscience

Research Publications

1. **DaSilva LF**, Pillon S, Genereaux J, Davey MJ, Gloor GB, Karagiannis J and Brandl CJ (2013) The C-terminal residues of *Saccharomyces cerevisiae* Mec1 are required for its Localization, Stability and Function. *G3: Genes, Genomes, Genetics* **3**: 1661-1674.

2. Gidvani RD, Sudmant P, Li G, **DaSilva LF**, McConkey BJ, Duncker BP and Ingalls BP (2012) A Quantitative Model of the Initiation of DNA Replication in *Saccharomyces cerevisiae* Predicts the Effects of System Perturbations. *BMC Systems Biology* **6**:1-20.

3. **Da-Silva LF** and Duncker BP (2007) ORC function in late G1: maintaining the license for DNA replication. *Cell Cycle* **6**:128-130.

4. Semple JW, **Da-Silva LF**, Jervis EJ, Ah-Kee J, Al-Attar H, Kummer L, Heikkila JJ, Pasero P, Duncker BP (2006) An essential role for Orc6 in DNA replication through maintenance of pre-replicative complexes. *EMBO J* **25**:5150-5158.

5. Gougeon PY, Prosser DC, **Da-Silva LF**, Ngsee JK (2002) Disruption of Golgi morphology and trafficking in cells expressing mutant prenylated rab acceptor-1. *J Biol Chem* **277**:36408-36014.

6. Abdul-Ghani M, Gougeon PY, Prosser DC, **Da-Silva LF**, Ngsee JK (2001) PRA isoforms are targeted to distinct membrane compartments. *J Biol Chem* **276**:6225-6233.

7. Hutt DM, **Da-Silva LF**, Chang LH, Prosser DC, Ngsee JK (2000) PRA1 inhibits the extraction of membrane-bound rab GTPase by GDI1. *J Biol Chem* **275**:18511-18519

Abstracts and Presentations

1. **DaSilva LF**, Kolaczyk T, Ma X, Langston L, O'Donnell M, Davey MJ and Edgell DR. June 2013. Abstract, oral and poster presentation. Seventeenth Annual Buffalo DNA Replication and Repair Symposium. Buffalo, NY. "Modulation of Mcm2-7 Activity by Cdt1".

2. **DaSilva LF**, Kolaczyk T, Ma X and Davey MJ. April 2013. Abstract, oral and poster presentation. ASBMB/ Experimental Biology 2013 Meeting. Boston, MA. "Modulation of Mcm2-7 Activity by Cdt1".

3. **DaSilva LF** and Davey MJ. November 2011. Oral presentation. Department of Biochemistry Graduate Seminar Series. London, ON. "Modulation of Mcm2-7 Activation in the Early Regulation of DNA Replication".

4. **DaSilva LF** and Davey MJ. March 2011. Oral presentation. Department of Biochemistry Graduate Seminar Series. London, ON. "Modulation of Mcm2-7 Activation in the Early Regulation of DNA Replication".

5. **DaSilva LF** and Davey MJ. July 2011. Oral presentation. Replication, Repair, Recombination and Chromosome Segregation Symposium. London, ON. "Modulation of Mcm2-7 Activation in the Early Regulation of DNA Replication".

6. **DaSilva LF**, Kolaczyk T, Ma X and Davey MJ. June 2011. Abstract and poster presentation. 15th Annual Buffalo DNA Replication and Repair Symposium. Buffalo, NY. "Modulation of Mcm2-7 Activity by Cdt1".

7. **DaSilva LF** and Davey MJ. May 2010. Abstract and poster presentation. 14th Annual Buffalo DNA Replication and Repair Symposium. Buffalo, NY. "Modulation of Mcm2-7 Activation in the Early Regulation of DNA Replication".

8. **DaSilva LF** and Davey MJ. April 2009. Oral presentation. Department of Biochemistry Mini-Retreat. London, ON. "Modulation of Mcm2-7 Activation in the Early Regulation of DNA Replication".

9. **DaSilva LF** and Davey MJ. July 2008. Oral presentation. Replication, Repair, Recombination and Chromosome Segregation Symposium. London, ON. "Studies on the Activation of Mcm2-7 to Unwind DNA".

10. **DaSilva LF** and Davey MJ. March 2008. Poster presentation. Margaret Moffat Research Day. London, ON. "Studies on the Activation of Mcm2-7".

11. **DaSilva LF** and Duncker BP. April 2007. Oral presentation. Graduate Student Research Conference. Waterloo, ON. "Functional characterization of the Origin Recognition Complex (ORC) in *Saccharomyces cerevisiae*".

12. Semple JW, **Da-Silva LF**, Jervis EJ, Ah-Kee J, Al-Attar H, Kummer L, Heikkila JJ, Pasero P and Duncker BP. August 2006. Abstract and poster presentation. Salk/Caltech Meeting on DNA Replication and Genome Integrity. San Diego, CA. "An essential role for Orc6 in DNA replication through maintenance of pre-replicative complexes after MCM loading".

Teaching Experience

2011   Biochemistry and Molecular Biology 2280A, University of Western Ontario, London, ON.

2009-2011   Clinical Biochemistry 3386B, University of Western Ontario, London, ON.

Relevant Technical Experience

Bacterial expression and purification of recombinant proteins
AKTA chromatography system
FACS analysis
Mammalian cell culture
Confocal microscopy
Radioactive work certification
Co-immunoprecipitation
Chromatin immunoprecipitation (ChIP)
Chromatin fractionation
Yeast Two-Hybrid screening technology
Polyclonal antibody production and purification

Volunteer Experience

2009-2012   Society of Graduate Students Council Member and Representative for the
             Department of Biochemistry, University of Western Ontario

2006-2007   Graduate Student Advisor for the International Genetically Engineered
             Machine (iGEM), University of Waterloo

2006-2007   Social Representative for the Biology Department Graduate Student
             Association, University of Waterloo